



HAL
open science

Technique de gestion de ressources radios pour l'amélioration de l'efficacité énergétique dans les réseaux cellulaires hétérogènes

Antonio de Domenico de Domenico

► To cite this version:

Antonio de Domenico de Domenico. Technique de gestion de ressources radios pour l'amélioration de l'efficacité énergétique dans les réseaux cellulaires hétérogènes. Mathématiques générales [math.GM]. Université de Grenoble, 2012. Français. NNT : 2012GRENM012 . tel-00720622

HAL Id: tel-00720622

<https://theses.hal.science/tel-00720622>

Submitted on 25 Jul 2012

HAL is a multi-disciplinary open access archive for the deposit and dissemination of scientific research documents, whether they are published or not. The documents may come from teaching and research institutions in France or abroad, or from public or private research centers.

L'archive ouverte pluridisciplinaire **HAL**, est destinée au dépôt et à la diffusion de documents scientifiques de niveau recherche, publiés ou non, émanant des établissements d'enseignement et de recherche français ou étrangers, des laboratoires publics ou privés.

THÈSE

Pour obtenir le grade de

DOCTEUR DE L'UNIVERSITÉ DE GRENOBLE

Spécialité : **Informatique**

Arrêté ministériel : 7 août 2006

Présentée par

Antonio De Domenico

Thèse dirigée par **Andrzej Duda et Emilio Calvanese Strinati**

préparée au sein **UMR 5217 - LIG - Laboratoire d'Informatique de Grenoble**
et de **l'École doctorale Mathématiques, Sciences et Technologies de l'Information, Informatique**

Energy Efficient Mechanisms for Heterogeneous Cellular Networks

Thèse soutenue publiquement le **21 mars 2012**,
devant le jury composé de :

Prof. Jean-Marc Brossier

Grenoble-INP, Président

Prof. Josep Vidal

UPC Barcelone, Rapporteur

Prof. Mérouane Debbah

Supélec Paris, Rapporteur

Prof. Maria-Gabriella Di Benedetto

Université de Rome "La Sapienza", Examineur

Dr. Gunther Auer

DoCoMo Euro-Labs, Examineur

Prof. Andrzej Duda

Grenoble INP-Ensimag, Directeur de thèse

Dr. Emilio Calvanese Strinati

CEA-LETI Grenoble, Co-Encadrant de thèse



Abstract

Wireless communication proliferates into nearly each aspect of the human society, driving to the exponential growth in number of permanently connected devices. Powerful smart-phones and tablets, ubiquitous wireless broadband access, and machine-to-machine communications generate volumes of data traffic that were unpredictable few years back. In this novel paradigm, the telecommunication industry has to simultaneously guarantee the economical sustainability of broadband wireless communications and users' quality of experience. Additionally, there is a strong social incentive to reduce the carbon footprint due to mobile communications, which has notably increased in the last decade.

In this context, the integration of femtocells in cellular networks is a low-power, low-cost solution to offer high data rates to indoor customers and simultaneously offload the macrocell network. However, the massive and unplanned deployment of femtocell access points and their uncoordinated operations may result in harmful co-channel interference. Moreover, a high number of lightly loaded cells increases the network energy consumption.

In this thesis, we investigate the effects of femtocells deployment on the cellular network energy efficiency. Moreover, we look into adaptive mechanisms for femtocell networks as a means to pave the way towards agile and economically viable mobile communications. Our goal is to dynamically match resource demand and offered capacity in order to limit the average power consumption and co-channel interference while guaranteeing quality of service constraints. We take advantage of the unusual communication context of femtocells to propose resource allocation and network management schemes that coordinate the access points activity, power consumption, and coverage. Simulation results show that our proposals improve system energy efficiency and users' performance in both networked and stand-alone femtocell deployment scenarios.

Keywords

Femtocell networks; two-tier cellular networks; energy efficiency; interference mitigation; resource allocation; local access point; network management; agile wireless communications; quality of service; transmission reliability.

List of Publications

Book Chapters

- [B1] A. De Domenico, E. Calvanese Strinati, and M.G. Di Benedetto, "Cognitive Strategies for Green Two-Tier Cellular Networks: A Critical Overview," in Handbook on Green Information and Communication Systems, Wiley, 2012.

Journal Papers

- [J1] E. Calvanese Strinati, A. De Domenico, and L. Herault, "Green Communications: An Emerging Challenge for Mobile Broadband Communication Networks," Journal of Green Engineering, 267-301, vol.1, no.3, River Publishers, 2011.
- [J2] A. De Domenico, E. Calvanese Strinati, and M.G. Di Benedetto, "A Survey on MAC Strategies for Cognitive Radio Networks," IEEE Communications Surveys & Tutorials, vol.14, no.1, First Quarter 2012.

Conference Papers

- [C1] A. De Domenico, E. Calvanese Strinati, "A Radio Resource Management scheduling algorithm for self-organizing femtocells," IEEE 21st International Symposium on Personal, Indoor and Mobile Radio Communications Workshops (PIMRC Workshops 2010), pp.191-196, Istanbul, Turkey, 26-30 September 2010.
- [C2] E. Calvanese Strinati, A. De Domenico, and A. Duda, "Ghost femtocells: A novel radio resource management scheme for OFDMA based networks," IEEE Wireless Communications and Networking Conference (WCNC 2011), pp.108-113, Cancun, Mexico, 28-31 March 2011, 2011.
- [C3] M. Bennis, L. Giupponi, E.M. Diaz, M. Lalam, M. Maqbool, E. Calvanese Strinati, A. De Domenico, M. Latva-aho, "Interference management in self-organized femtocell networks: The BeFEMTO approach," 2nd International Conference on Wireless Communication, Vehicular Technology, Information Theory and Aerospace & Electronic Systems Technology (Wireless VITAE 2011), pp.1-6, Chennai, India, February 28-March 3 2011.
- [C4] A. De Domenico, E. Calvanese Strinati, and A. Duda, "Ghost Femtocells: an Energy-Efficient Radio Resource Management Scheme for Two-Tier Cellular Networks," 11th European Wireless Conference 2011 - Sustainable Wireless Technologies, pp.1-8, Vienna, Austria, 27-29 April 2011.

- [C5] A. De Domenico, R. Gupta, and E. Calvanese Strinati, "Dynamic Traffic Management for Green Open Access Femtocell Networks," The 74th IEEE Vehicular Technology Conference (VTC-Spring 2012), Yokohama, Japan, 6-9 May 2012.
- [C6] A. De Domenico, E. Calvanese Strinati, and A. Duda, "An Energy Efficient Cell Selection Scheme for Open Access Femtocell Networks," submitted to IEEE 23st International Symposium on Personal, Indoor and Mobile Radio Communications (PIMRC 2012), Sydney, Australia, 9-12 September 2012.

Patents

- [P1] A. De Domenico, E. Calvanese Strinati, "Radio Resource Management algorithm for femtocell networks," DD11965.
- [P2] A. De Domenico, E. Calvanese Strinati, "Dynamic Deployment Activation for Open Access Femtocell Networks" DD13177ST.
- [P3] A. De Domenico, R. Gupta, and E. Calvanese Strinati, "Cognitive architecture for dynamic traffic management in green small cells," DD13287.
- [P4] A. De Domenico, R. Gupta, and E. Calvanese Strinati, "Content and Context Aware Network Management," DD13347.

Contents

Abstract	i
List of Publications	iii
Contents	vii
List of Figures	x
List of Tables	xi
Abbreviations and Acronyms	xiii
Thesis Notations	xvii
1 Outline of the Thesis	1
Outline of the Thesis	1
1.1 Background and Main Contributions	1
1.2 Thesis Summary	2
2 Sustainable Broadband Cellular Networks	5
2.1 Introduction	6
2.1.1 Motivation	6
2.1.2 Fundamental Approaches for Ubiquitous Broadband Cellular Networks	7
2.1.3 Fundamental Approaches for Sustainable Cellular Networks	9
2.2 Femtocell Networks: an Overview	10
2.2.1 Notions, Concepts, and Definitions	10
2.2.2 Femtocell Reference Models and Scenarios	12
2.2.2.1 Deployment of Femtocells and Path loss Models	14
2.2.2.2 Femtocell Use Cases	15
2.2.2.3 EARTH Energy Efficiency Evaluation Framework	16
2.3 Medium Access Control Strategies for Cognitive Radio Ad-Hoc Networks	17
2.3.1 Classification of MAC Protocols for Cognitive Radio	19
2.3.2 Spectrum Sensing	24
2.3.3 Dynamic Spectrum Allocation	33
2.3.4 Dynamic Spectrum Sharing	38

2.3.5	Dynamic Spectrum Mobility	49
2.4	A Critical Overview on Agile Strategies for Two-Tier Cellular Networks	50
2.4.1	Spectrum Awareness and Victim Detection	50
2.4.2	Dynamic Radio Resource Management	53
2.4.3	Dynamic Spectrum Sharing	55
2.4.4	Green Agile Femtocell Networks	63
2.5	Conclusions	67
3	Green Ghost Femtocells	69
3.1	Introduction	70
3.1.1	Motivation	70
3.1.2	Related Work	70
3.1.3	Contribution	71
3.2	System Model	71
3.3	Energy per Bit versus Spectral Efficiency	73
3.4	Green Ghost Femtocells: the Proposed Interference Mitigation Paradigm	73
3.4.1	Problem Statement	73
3.4.2	The Proposed Ghost _{SAF} for Green Stand-Alone Femtocells	75
3.4.3	The Proposed Ghost _{NF} for Green Networked Femtocells	77
3.4.4	Complexity and Overhead of the RRM Ghost Algorithms	81
3.5	Simulation Results	83
3.6	Conclusion	88
4	Dynamic Activation for Open Access Femtocell Networks	89
4.1	Introduction	90
4.1.1	Motivation	90
4.1.2	Related Work	90
4.1.3	Contribution	91
4.2	System Model	91
4.3	Problem Statement	91
4.4	Proposed Advanced Open Access Algorithms	93
4.5	Simulation Results	96
4.6	Conclusions	100
5	Dynamic Traffic Management for Green Open Access Femtocell Networks	101
5.1	Introduction	102
5.1.1	Motivation	102
5.1.2	Related Work	102
5.1.3	Contribution	102
5.2	System Model	103
5.3	Classic DTX scheme and further improvements	103
5.4	Problem Statement	104
5.5	Multi-cell architecture for dynamic cell DTX and traffic management	105
5.6	Simulation Results	107
5.7	Conclusions	110

6	Conclusions and Future Work	111
6.1	Conclusions	111
6.2	Future Work	112
A	Complements to Chapter 3: Green Ghost Femtocells	117
	Bibliography	134

List of Figures

2.1	User experience challenges for uniform broadband wireless services in cellular networks.	6
2.2	Mobile traffic and operators revenue trends.	7
2.3	Solutions to achieve a uniform broadband wireless service.	8
2.4	Time-scale classification of energy-aware mechanisms for broadband heterogeneous cellular networks.	9
2.5	A generic femtocell architecture.	10
2.6	A two-tier cellular network.	11
2.7	Near-far scenarios in two-tier cellular networks.	12
2.8	Downlink interference scenarios in two-tier cellular networks.	13
2.9	The femtocell grid urban deployment model.	14
2.10	M-BS and FAP power consumption dependency on relative output power.	17
2.11	U.S. frequency allocation chart as of October 2003.	18
2.12	Cognitive radio MAC protocols chart.	20
2.13	Dealing with signalling and data transmission in multichannel CR networks.	22
2.14	The multichannel hidden terminal problem.	22
2.15	The IEEE 802.22 two stage sensing.	26
2.16	Simultaneous Sensing and Data Transmission in 802.22 DFH.	26
2.17	Double Hopping operating mode for three neighbouring cells.	27
2.18	The Markov model representing a network state transition.	28
2.19	The DC-MAC sequence of operations.	29
2.20	Channel superframe structure in C-MAC.	30
2.21	Sensing report and channel negotiation mechanism for CR networks.	32
2.22	A NCG representation of channel availability and interference constraints.	36
2.23	One point crossover operation in a genetic-based RRM algorithm.	38
2.24	The BT_i collision avoidance mechanism.	41
2.25	The BT_o collision avoidance mechanism.	41
2.26	Multi-hop cognitive network clusters connected by gateway nodes.	44
2.27	CogMesh MAC superframe.	45
2.28	Overlay interference model.	48
2.29	Two-hop cooperative transmission scheme for two-tier cellular networks.	54
2.30	Underlay transmission scheme.	56
2.31	Overlay transmission scheme in transmitter/receiver cooperation scenarios.	57
2.32	Interweave transmission approach in time/frequency/space domains.	58
2.33	Dynamic Spectrum Sharing according to SOCCER.	58
2.34	A Time Division Duplex transmission scheme for cross-tier interference mitigation.	59
2.35	A FFR scheme for two-tier cellular networks.	60

2.36	A two-tier network cooperation framework.	62
2.37	An overlay transmission scheme for two-tier cellular networks.	63
2.38	An energy-aware RRM for femtocell networks.	65
2.39	UE detection scheme in cell switch-off strategy.	66
3.1	Energy per bit versus Spectral Efficiency trade-off.	74
3.2	$Ghost_{SAF}$: proposed RRM algorithm for stand-alone femtocells.	80
3.3	Proposed architecture for networked Ghost femtocells.	81
3.4	$Ghost_{NF}$: proposed RRM algorithm for networked femtocells.	82
3.5	Average Energy Efficiency as a function of the power budget at each FAP in different traffic scenarios.	84
3.6	Average Energy Efficiency measured at M-UEs as a function of the power budget at each FAP in different traffic scenarios.	85
3.7	Average Energy Efficiency measured at macro cells as a function of the distance between the end-user and the M-BS.	86
3.8	Maximum number of cell edge M-UEs that can be contemporary served by the M-BS in different femtocell deployment scenarios	87
4.1	Classic approach vs. our Advanced Open Access scheme.	92
4.2	Proposed Advanced Open Access algorithms for networked and stand-alone femtocells.	93
4.3	Femtocell network Energy Consumption Gain with respect to the femtocell deployment ratio.	97
4.4	Aggregate Energy Consumption Gain with respect to the femtocell deployment ratio.	98
4.5	Performance experienced by cellular users with respect to the femtocell deployment ratio.	99
5.1	Classic DTX and E-DTX schemes.	104
5.2	Proposed algorithm to dynamically associate traffic and FAPs at femtocell networks.	107
5.3	Femtocell network Average Power Consumption with respect to the femtocell deployment ratio.	108
5.4	Femtocell network average aggregate Throughput with respect to the femtocell deployment ratio.	109
5.5	Macrocell average Power Consumption with respect to the femtocell deployment ratio.	110
6.1	Traffic dynamics both in the time and space domains.	113
6.2	Dynamic BS sleep control and its effects.	114
6.3	Capacity model of the proposed content/context aware framework.	115

List of Tables

2.1	BS Power model parameters.	16
2.2	DAB CR MAC protocols overview in this chapter.	23
2.3	Presented DSA CR MAC protocols/algorithms.	24
2.4	Characteristics of analysed CR-based RRM schemes.	63
3.1	Main system model parameters.	72
3.2	Packet Size and Spectral Efficiency for MCS.	76

Abbreviations and Acronyms

3GPP	Third Generation Partnership Project
AP	Access Point
ATIM	Ad-hoc Traffic Indication Message
BCH	Broadcast CHannel
BS	Base Station
BP	Beacon Period
CAPEX	CAPital Expenditure
CDMA	Code Division Multiple Access
CFR	Coalition Formation Request
CFSR	Channel Filtering Sender Receiver
CHWIN	Coordination window
CO ₂	Carbon Dioxide
CPC	Cognitive Pilot Channel
CQI	Channel Quality Indicator
CR	Cognitive Radio
CSG	Closed Subscriber Group
CSI	Channel State Information
CTS	Clear To Send
DAB	Direct Access Based
DCF	Distributed Coordination Function
DFH	Dynamic Frequency Hopping
DFHC	DFH Community
DCPC	Distributed Cognitive Pilot Channel
DSA	Dynamic Spectrum Allocation
DTP	Data Transfer Period
DTV	Digital Television
DTX	Discontinuous Transmission
EE	Energy Efficiency
EESM	Exponential Effective SINR Mapping
EMF	ElectroMagnetic Field
ETSI	European Telecommunications Standards Institute
FAP	Femtocell Access Point
FCS	Femto Coordination/Controller Server
FFR	Fractional Frequency Reuse
FR	Frequency Reuse
F-UE	Femto User
GB	Gigabyte

GSM	Global System for Mobile Communications
IEEE	Institute of Electrical and Electronics Engineers
ICIC	Inter-Cell Interference Coordination
IC	Interference Cancellation
ID	Identification
IP	Internet Protocol
ISD	Inter-Site Distance
ISM bands	Industrial, Scientific, and Medical bands
LAC	List of Available Channels
LCG	Link Contention Graph
LQM	Link Quality Metric
LTE	Long Term Evolution
LTRC	Long-Term Residency Channel
LUT	Look-Up-Table
M-BS	Macro Base Station
MAC	Medium Access Control
MC	Mesh Client
MCS	Modulation and Coding Scheme
MIESM	Mutual Information based Effective SINR Mapping
MIMO	Multiple Input Multiple Output
MOSS	Multi-Operator Spectrum Server
MR	Mesh Routers
MSP	Mobile Service Provider
M-UE	Macro Users
NACK	Negative Acknowledgement
NCG	Node Contention Graph
NE	Nash Equilibrium
NGMN	Next Generation Mobile Network
OFDM	Orthogonal Frequency Division Multiplexing
OFDMA	Orthogonal Frequency Division Multiple Access
OPEX	Operational Expenditure
OSG	Open Subscriber Group
OTA	Over-The-Air
PA	Power Amplifier
PER	Packet Error Rate
PF	Proportional Fair
QoE	Quality of Experience
QoS	Quality of Service
QP	Quiet Period
RAT	Radio Access Technology
RB	Resource Block
RF	Radio Frequency
RRM	Radio Resource Management
RSRP	Reference Signal Received Power
RTS	Request To Send
SE	Spectral Efficiency
SFC-C	Smart Femto Cell Controller
SINR	Signal to Interference and Noise Ratio

SIP	Spectral Image of primary users
SDO	Standard Development Organizations
SON	Self-Organizing Network
SRR	Short Range Radio
SUDU	Spectrum Usage Decision Unit
SUG	Secondary Users Group
TDD	Time Division Duplex
TDMA	Time Division Multiple Access
TTI	Transmission Time Interval
TVWS	TV White Space
UE	User Equipment
UMTS	Universal Mobile Telecommunications System
UWB	Ultra-WideBand
WCDMA	Wideband Code Division Multiple Access
WiFi	Wireless Fidelity
WiMAX	Worldwide Interoperability for Microwave Access
WRAN	Wireless Regional Area Network

Thesis Notations

The following list is not exhaustive and consists of the most relevant notations used in the dissertation. Matrices and vectors are denoted by boldface symbols, although calligraphic fonts are used to represent sets.

α	Channel fading instance
δ_M	Margin in the power control process of the Ghost algorithm
Δ_p	Coefficient that indicates the relation between BS power consumption and cell load
λ	Scheduling metric
η	Nominal spectral efficiency
ρ_d	Deployment ratio
σ^2	Noise variance
\mathbf{a}	Active FAPs vector
$cont$	Counter
\mathbf{D}	User degree vector
D_{th}	Delay threshold that distinguishes low/high priority traffic
\mathcal{E}	The edge set in the graph representation of the network
f	The fitness function in the BIOS algorithm
\mathcal{F}	The set of deployed FAPs
$\hat{\mathcal{F}}$	Subset of activated femtocells
\mathcal{F}^j	The subset of deployed FAPs, which composes the active set of the UE j
$\mathcal{F} \mathcal{UE}$	The set of femto UEs
$\mathcal{F} \mathcal{UE}^L$	The subset of femto UEs with low priority traffic
$\mathcal{F} \mathcal{UE}^H$	The subset of femto UEs with high priority traffic
\mathbf{g}	Channel gain Matrix
γ	SINR
γ_0	Normalized SINR
\mathcal{K}_j	The set of RBs allocated to the UE j
I	Mutual information
\mathcal{L}_A	Set of available channels at the cognitive node A
L	The learning factor in the BIOS algorithm

\mathcal{M}	The set of deployed M-BSs
\mathbf{M}^{Tx}	Scheduling matrix in the first step of the Ghost algorithm
\mathbf{M}^{Sp}	Scheduling matrix in the spreading process of the Ghost algorithm
\mathcal{M}^{UE}	The set of macro UEs
\mathcal{N}	The set players in the game theoretic models
n_i	Number of UEs associated to the i -th FAP
N_0	Noise variance
N_{F}	The number of deployed FAPs
N_{FUE}	The number of deployed F-UEs
N_{max}	Maximum number of UE served by a single FAP
N_{M}	The number of deployed MBSs
N_{MUE}	The number of deployed M-UEs
N_{RB}	Number of resource blocks in the bandwidth W
P^*	BS power consumption
P_0	BS power consumption at minimum load
P_L	The interference power limit in COMAC protocol
P_{max}	BS RF power budget
PQ_{jd}	Packet size for the user j and delay tolerance d
P^{RF}	BS irradiated power
P_r	Probability
$P_r(\text{out})$	Outage probability
\mathbf{PS}	Number of data bits that can be transmitted in a RB with a given MSC
\mathbf{R}	User throughput
R_{CT}	Coexistence region
r_{ctr}	Safe transmission range in COMAC control channel
S^{Ch}	The RB allocation matrix
S_i	The strategy space of player i in the game theoretic models
T	TTI length
\mathcal{T}	The set of observed TTIs
T_{tg}	Throughput target
u_i	The utility function of node i
\mathcal{V}	The vertex set in the graph representation of the network
\mathcal{V}_i	Set of strong interferer femtocells for the FAP i
W	Channel bandwidth
\mathbf{X}	UE/FAP Service matrix

Chapter 1

Outline of the Thesis

1.1 Background and Main Contributions

Nowadays, the number of mobile subscribers fairly equals the global population. Forecasts on telecommunication market assume an increase in subscribers and per subscriber data rate. Mobile operators will continue deploying additional Base Stations (BSs), which are required to fulfil data rate and coverage requirements of the next generation mobile networks.

To improve coverage and capacity, cellular networks can integrate Femtocell Access Points (FAPs) [1]. FAPs are low cost solutions to jointly offer high data rate to indoor users and offload the macrocell network. Market research indicates the success of this novel technology, which will lead to a dense and rapid femtocell deployment, especially in urban scenarios. However, interference mitigation issues arise due to the unplanned deployment of local Access Points (APs) in the same geographical region of the macrocell. Moreover, uncoordinated femtocell operations generate energy wastage; hence, adaptive mechanisms are required to efficiently configure, manage, and optimize activity of the femtocell network:

- First, in Chapter 2 of this dissertation, we discuss characteristics, advantages, and challenges of the femtocell network, and we overview main contributions proposed in the literature to enhance performance of femtocell networks.
- Second, in Chapter 3, we propose a novel paradigm for improving transmission robustness in femtocell deployment scenarios. This approach exploits the unusual characteristics of the femtocell deployment to lower the required irradiated power at femtocells to meet the users' data rate requirements. Then, we design two Radio Resource Management (RRM) algorithms that implement the proposed approach in both networked and stand-alone femtocells.
- Third, in Chapter 4, we investigate the impact of the femtocell access scheme on the network Energy Efficiency (EE). Moreover, we propose a novel access strategy that jointly coordinates the AP activity and the cell selection mechanism. This approach dynamically adjusts the number of activated FAPs according to the network deployment characteristics to limit the aggregate energy consumption.

- Finally, in Chapter 5, we investigate Discontinuous Transmissions (DTX) [2] and inter-cell coordination mechanisms in open access femtocell networks. We introduce a scheme that dynamically manages traffic, cell selection, and cell activation/deactivation to match required capacity with service demand. Our proposal exploits the latency-energy trade-off to enable great energy saving also at moderate load scenarios.

1.2 Thesis Summary

Chapter 2 - Sustainable Two-Tier Cellular Networks

Chapter 2 gives an insight of the technical context of this dissertation. In particular, we discuss the main challenges for telecommunication community in the light of the voice-to-data paradigm shift, which has unpredictably changed wireless communications. First, we present the main approaches proposed in the literature to increase the system Spectral Efficiency (SE); then, we give an overview on the mechanisms proposed to enhance the cellular network sustainability.

Amongst the presented approaches, in this thesis, we focus on both Cognitive Radio (CR) and femtocell networks as enabling technologies to deal with the challenges that characterize future cellular networks. Therefore, we present main functionalities of a cognitive network and we survey the cognitive MAC protocols proposed for wireless networks. In the last ten years, CR has been mainly investigated in the ad-hoc wireless network scenario [3], and only recently it has been proposed for enhancing cellular network performance [4].

Subsequently, we introduce the femtocell technology and critically discuss advantages, drawbacks, and challenges in the femtocell deployment. Finally, we overview some interesting solutions proposed in the literature to enable the cost-effective femtocell deployment and facilitate the coexistence of macrocells and femtocells in the same geographical region.

This background chapter summarizes the work presented in one book chapter [B1] and one journal paper [J2].

Chapter 3 - Green Ghost Femtocells

In Chapter 3, we deal with co-channel interference in two-tier cellular networks. Classic interference avoidance approaches propose to split the available time/frequency transmission resources such that resource partitioning results in limited interference. Actually, in interference-limited communications, the information theory suggests the usage of orthogonalization techniques whenever the perceived interference at the receiver can not be decoded and then cancelled [5]. Although interference cancellation techniques are limited by complexity and overhead, orthogonal spectrum sharing results in poor performance, especially implementing static allocation algorithms [6].

Hence, we take advantage of the characteristics of femtocell deployment, where few users are concomitantly served by a given AP and femtocells have fairly more transmission resources than required, to introduce a novel transmission paradigm (i.e., *the Ghost femtocell*) for cellular networks. We implement modulation and coding scaling techniques as well as power control in femtocell transmissions to trade-off frequency resources for irradiated power. The idea is to operate transmissions in the noisy regime [7] to limit the effect of concurrent wireless communications and increase the network Frequency Reuse (FR).

Most of the interference mitigation techniques proposed in the literature focuses either on femto-to-macro or femto-to-femto interferences (see Table 2.4); however, the proposed approach is effective on both types of interference. We implement the proposed Ghost paradigm in both stand-alone and networked femtocells; in the latter case cooperation further limits co-channel interference by coordinating the access of neighbouring FAPs.

Simulation results show that our proposals outperform classic RRM strategies, however, femtocell coordination results to be effective only in very dense femtocell deployment scenarios.

One patent [P1], one journal [J1], and four conference papers [C1], [C2], [C3], and [C4] contain the work presented in this chapter.

Chapter 4 - Dynamic Activation for Open Access Femtocell Networks

Network offloading due to femtocell deployment is a technical solution to reduce operational costs at mobile operators. However, the dense and unplanned deployment of femtocells can result in low EE, especially in lightly load scenarios. Moreover, uncoordinated femtocell transmissions generate interference in both data and control channels. Adapting mechanisms can adjust the femtocell activity with respect to the user presence and to the cell load, which leads to energy saving and improved communication robustness. Dynamic cell activation/deactivation mechanisms can improve the network performance enabling local APs to self switch off in absence of neighbouring end-users [8].

In this chapter, we investigate activation/deactivation strategies jointly with femtocell access schemes and cell selection mechanisms to optimize femtocell operations. The goal is threefold: first, we aim to understand the impact of femtocell deployment in the overall network energy consumption; second, we target at analysing how this energy consumption depends on the selected femtocell access scheme; third, we propose a novel cell selection scheme that exploits awareness about network deployment, user location, and link quality to effectively manage the femtocell network activity.

This algorithm, named as *Advanced Open Access*, is implemented in both networked and stand-alone femtocells; it allows to adapt the network capacity to traffic scenarios, dynamically reducing the number of simultaneously active APs and limiting the energy consumption. This network optimization comes at costs of higher overhead, which is, however, limited due to low mobility that characterizes indoor scenarios. Additionally, in the networked scenarios, the overhead and computational costs are shared at cooperative FAPs, although in the stand-alone case, end-users contribute to the optimization process to cope with the absence of inter-cell coordination.

Our investigations indicate that open access femtocells are characterized by a higher average power consumption with respect to closed access femtocells; nevertheless, they are more energy efficient from the overall cellular network perspective. Moreover, simulation results show that the proposed Advanced Open Access strategy strongly limits the system energy consumption while meeting data rate constraints.

The material of this chapter is reported in part in one patent [P2], and a conference paper [C6].

Chapter 5 - Dynamic Traffic Management for Green Open Access Femtocell Networks

In Chapter 4, we underline that energy-aware adaptive mechanisms are fundamental in femtocell networks to fulfil traffic constraints while minimizing the cellular network energy consumption. However, most of the work in the literature aims at managing femtocell activation/deactivation for improving the system EE at low load or in the absence of end-users. For instance, cell DTX allows BSs to completely switch off radio transmissions and associated processing when not involved in active transmissions [2].

Then, in Chapter 5, we propose a novel architecture that enables energy saving even at moderate load scenarios. We consider open access femtocells inter-connected by a high speed low latency backhaul, which allows the implementation of fast adaptation mechanisms without affecting communication reliability. Therefore, we introduce an algorithm for multi-cell traffic man-

agement that dynamically distributes user data amongst neighboring femtocells and adaptively controls their activity.

This algorithm is implemented at a local controller, which is aware of traffic characteristics, link qualities, APs deployments, and data rate constraints. However, we also discuss a distributed implementation of the proposed multi-cell transmission mechanism, and we compare the two solutions in terms of complexity and overhead.

Simulation results show that the dynamic management of FAP transmissions reduces the system power consumption while guaranteeing users' performance. This gain comes at the expense of cooperation costs and an increased packet delay, which is acceptable if it stays within the application Quality of Service (QoS) requirements.

The novelty of this chapter is based on a patent [P3] and a conference paper [C5].

Chapter 5 - Conclusion and Future Work

This chapter summarizes the thesis main contributions. Furthermore, we introduce three future research topics:

1. Interference Mitigation and DTX in Small Cell Networks,
2. Interference-Aware Heterogeneous Cellular Networks,
3. Content and Context Aware Network Management.

Note, that we have already started to investigate these problems and a patent [P4] has been proposed in the context of the third theme.

Chapter 2

Sustainable Broadband Cellular Networks

The telecommunication community faces with challenging issues to enable the economical sustainability of broadband wireless networks and enhance users' quality of experience. Femtocells have been proposed as a low cost solution to uniformly offer high data rate services in cellular networks; however, novel issues arise from the ad-hoc nature of femtocell access points. In our vision, femtocell technology and adaptive mechanisms inspired by the cognitive radio paradigm can jointly enable an agile and cost-effective broadband cellular network. This chapter presents the technical context of the thesis and provides a critical overview of work performed in the field by both industrial and academic research communities.

The chapter is organized as follows: In Section 2.1, we introduce the issues that characterize the future cellular networks and the main approaches proposed by industrial and research community to improve the network performance and sustainability. In Section 2.2, we discuss advantages, drawbacks, and main characteristics of femtocell networks. Then, in Section 2.3, we present the cognitive radio paradigm and its main functionalities and Section 2.4 gives an overview of state-of-the art solutions for mitigating interference and enhancing energy efficiency in femtocell networks. Finally, in Section 2.5, we conclude with related open issues.

2.1 Introduction

2.1.1 Motivation

The success of mobile cellular networks, has resulted in wide proliferation and demand for ubiquitous heterogeneous broadband mobile wireless services. Data traffic has surpassed voice and is growing rapidly. This trend is set to continue, with global traffic figures expected to double annually over the next five years [9]. A recent forecast indicates that the average smartphone will generate more than 1 Gigabyte (GB) of traffic per month in 2015 [10]. The mobile industry is, therefore, preparing to meet the requirement of GB traffic volumes and provide uniform broadband wireless services. Nowadays, indoor and cell edge users experience very poor performance (see Figure 2.1); therefore, such a rise in traffic rate demand and services requires cellular operators to further ameliorate and extend their infrastructure. Although this scenario may seem beneficial to the mobile communication market, it is leading to two undesired and harming consequences: first, combining the expenditure related to future infrastructure requirements with the revenue trend (see Figure 2.2), a negative cash-flow for United States and western European operators can be predicted by 2014 and 2015 [11], respectively; second, the growth of wireless network's energy consumption will cause an increase of the global carbon dioxide (CO_2) emissions, and impose more and more challenging operational cost for operators. Communication EE is indeed an alarming bottleneck in the telecommunication paradigm. In Sections 2.1.2 and 2.1.3, we give an overview on the approaches that are currently analysed by the telecommunication community to cope with data rate and EE constraints, respectively.

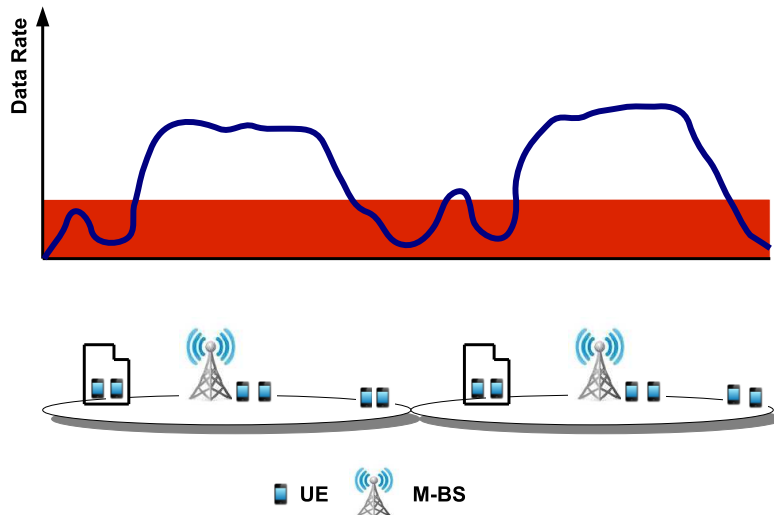


Figure 2.1: User experience challenges for uniform broadband wireless services in cellular networks.

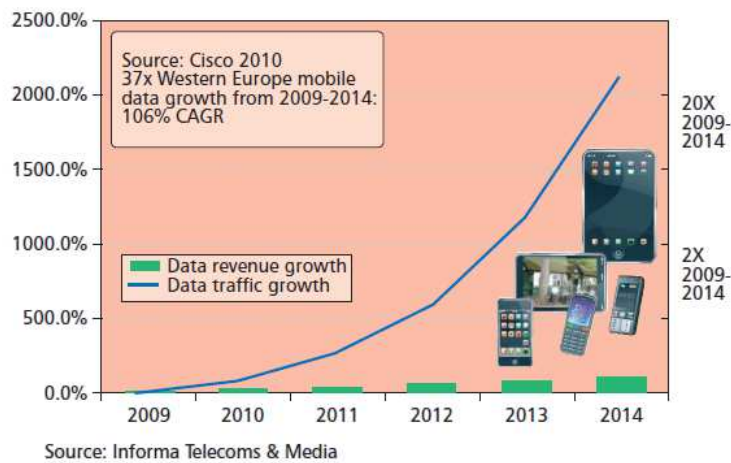


Figure 2.2: Mobile traffic and operators revenue trends [11].

2.1.2 Fundamental Approaches for Ubiquitous Broadband Cellular Networks

Three main approaches are investigated to improve the cellular network SE and satisfy the capacity demand driven by data traffic [12]:

1. Increasing the number of sites in the homogeneous cellular network;
2. Upgrading the radio access by implementing Inter-Cell Interference Coordination (ICIC), increasing bandwidth, number of antennas, and signal processing capabilities;
3. Deploying low-power low-cost nodes.

Current wireless cellular networks are typically deployed as homogeneous networks using a macro-centric planned process. A homogeneous cellular system is a network of BSs in a planned layout and a collection of User Equipments (UEs), in which all the BSs have similar transmit power levels, antenna patterns, receiver noise floors, and similar backhaul connectivity to the data network. Moreover, BSs offer unrestricted access to UEs in the network, and serve roughly the same number of devices. The locations of the Macro BSs (M-BSs) are carefully chosen by network planning, and their settings are properly configured to maximize the coverage and control the inter-cell interference.

In such scenario, improving the spatial FR by reducing the cell size may overcome capacity bottleneck and enable a uniform user experience. Furthermore, replanning the network sites deployment, by reducing the Inter-Site Distance (ISD), permits to keep low the number of additional BSs. However, this deployment process is complex and iterative. Moreover, site acquisition for M-BSs with towers becomes more difficult and expensive in dense urban areas.

Upgrading the radio access of the current BSs may greatly enhance network capacity by increasing the network SE and limiting the effect of co-channel interference. However, bandwidth is a scarce and expensive resource, and future wireless technologies could not rely on further increasing the spectrum availability. Moreover, cooperative communications and Multiple-Input Multiple-Output (MIMO) techniques are showing performance that are still far from the theoretical bounds, especially for UEs characterized by very low Signal to Interference and Noise Ratio

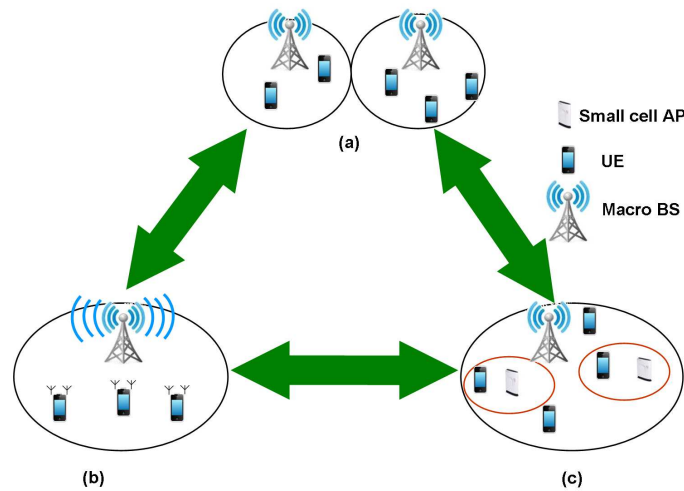


Figure 2.3: Solutions to achieve a uniform broadband wireless service [12]: a) Densifying the homogeneous cellular network by reducing the ISD; b) Upgrading the radio access by implementing ICIC, increasing the available bandwidth, signal processing capabilities, and number of antennas; c) Locally deploying low-cost nodes.

(SINR), such as indoor and cell-edge UEs. These users exhibit very poor performance due to notable propagation and penetration losses, which affect the link between terminals and APs. A different approach to improve the system SE is to integrate CR capabilities into cellular networks. In the last ten years, CR has emerged as a way to improve the overall spectrum usage by exploiting spectrum opportunities in both licensed and unlicensed bands [13]. CR has been mainly proposed as an enabling technique for ad-hoc wireless networks and the implementation of this paradigm in cellular network leads to new challenges in terms of complexity, overhead, and QoS constraints.

The third solution aims to provide a uniform broadband experience to users anywhere in the network through the local deployment of heterogeneous nodes. Such nodes can be either deployed in outdoor or in indoor environment. Moreover, they can act as network APs or relaying the message generated by the M-BS towards cell-edge users. Complementing the macro networks with low power nodes, such as micro and pico BSs, has been considered a way to increase capacity for nearly 3 decades [14, 15]. This approach offers very high capacity and data rates in areas covered by the low-power nodes. However, due to their reduced range a dense deployment of local APs may be required. Therefore, in such a novel heterogeneous network architecture, a high number of cells of different characteristics may share the same spectrum in a given geographical area, increasing the inter-cell interference. Moreover, due to the limited capacity of the backhaul, inter-cell coordination for interference mitigation purpose is a challenge.

The three approaches that have been briefly introduced in this section are summarized on Figure 2.3. Note that, it is not possible to identify a unique methodology to meet future capacity demand. On the contrary, it is probable that operators will use all three strategies to improve system performance. How these solutions are combined depends on the network characteristics and targeted capacity, as well as the technical and economical feasibility of each approach.

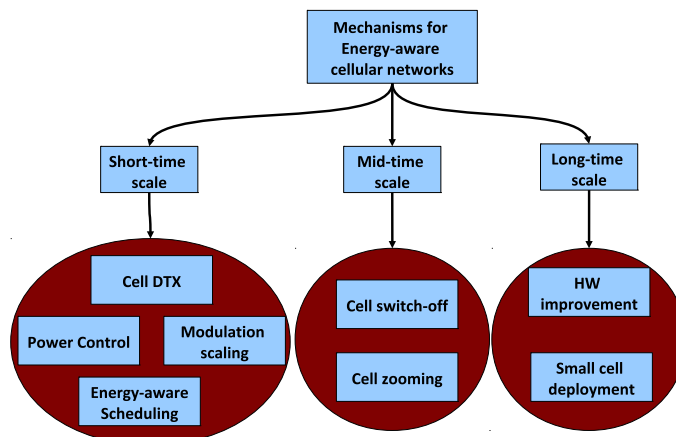


Figure 2.4: Time-scale classification of energy-aware mechanisms for broadband heterogeneous cellular networks.

2.1.3 Fundamental Approaches for Sustainable Cellular Networks

State-of-the-art mobile networks have a strong potential for energy savings. The design of mobile networks has until now focused on reducing the energy consumption of terminals, whose battery power imposes stringent requirements on energy consumption. However, according to a recent survey, nearly the 80% of the energy consumption of a typical cellular network comes from the BS side [16]. Furthermore, the 70% of this consumption is due to Power Amplifier (PA) and air conditioning, which are used to keep the BS active even though there is no traffic in the cell (i.e., to guarantee coverage). Consequently, the optimization of the radio access and in particular of BSs should have a large impact on the overall cellular network EE.

A general classification of network level and RRM approaches, which aim to design an agile and sustainable broadband mobile cellular network, can be realized according to the temporal scale in which they operate (see Figure 2.4).

Short-term mechanisms allow the system to self-adapt to fast changes in the network, such as load, interference, and mobility. Such a capability permits to avoid resource wastage and increase the system efficiency; however, the amount of energy saving may be limited for two basic reasons. First, due to the integration of PAs whose power consumption does not vary with the irradiated power, the energy consumption of small cell slightly depends on the cell load [17]. Second, as already mentioned, most of the network power consumption is used to maintain the BSs activated and it is not related to transmissions.

On the contrary, mid-term and long-term solutions exploit statistical characterizations of the network traffic to predict the average amount of resources necessary in a given region during a period of time (i.e., hours, days, and weeks). These approaches may lead to much higher gain with respect to the short-term solutions, however, estimation errors can result in poor performance due to coverage holes and traffic bottleneck. Finally, it is important to note that, amongst the long-term solutions, hardware improvements and the usage of alternative energy sources have an important role to improve the cellular network sustainability. To achieve important energy saving by exploiting adaptive mechanisms, such as cell DTX [2], hardware should allow fast BSs activation/deactivation according to the cell load. Moreover, extending wireless networks

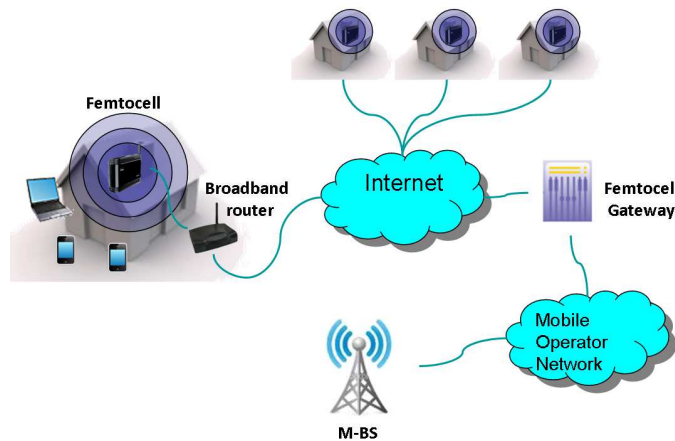


Figure 2.5: A generic femtocell architecture.

beyond electricity grids and diesel generators with alternative energy solutions, such as wind and solar, at industrial scale can greatly limit the overall carbon footprint. Due to the high power consumption of M-BSs, today the number of sites powered by alternate energy is quite small; however, improving the cellular network EE may enable the proliferation of BSs with low CO_2 emissions. The interest on this eco-friendly technology is increasing, and Alcatel-Lucent envisions a global market potential of more than one hundred thousand solar powered sites in 2012 [18].

2.2 Femtocell Networks: an Overview

2.2.1 Notions, Concepts, and Definitions

As underlined in the previous section, the local deployment of additional low-power nodes, may enable future cellular networks to ubiquitous offer broadband wireless services in sustainable way.

Amongst the different technical solutions available at mobile operators, such as relays, picocells, radio remote header, and distributed antenna systems, femtocells have recently captured the attention of both industrial and the academic communities. Market investigations on mobile networks claim that more than 60% of traffic is generated indoors [19]; FAPs can enable cellular networks to take advantage of this evolution of usage. These APs offer radio coverage through a given wireless technology while a broadband wired link connects them to the backhaul network of a cellular operator (see Figure 2.5).

Such a technical solution presents several benefits both to operators and end consumers. The latter may obtain a larger coverage, a better support for high data rate services, and a prolonged battery life of their devices. The advantages mainly come from the reduced distance between an end-user terminal and the AP, the mitigation of interference due to propagation and penetration losses, and the limited number of users served by a FAP.

Originally envisioned as a means to provide better voice coverage in the home, FAPs are now primarily viewed as a cost-effective way to offload data traffic from the macrocell network.

In a cellular network, traffic is carried from an end-user device to the cell site and then to the core network using the backhaul of the mobile operator. With network offload, cellular traffic from the UE is directed to a local AP; then, it is carried over a fixed broadband connection, either to the

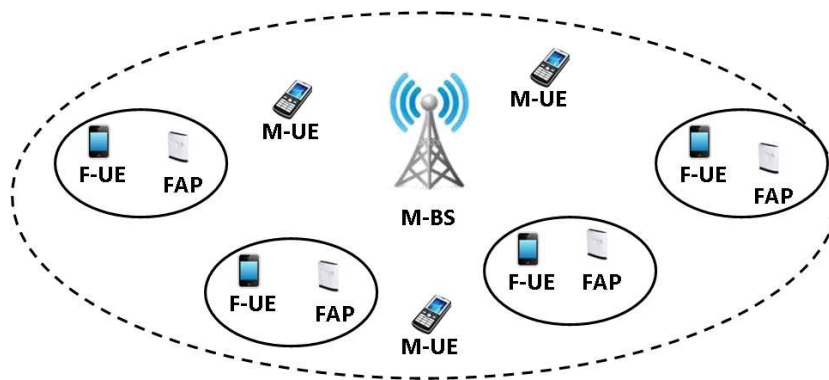


Figure 2.6: A two-tier cellular network.

mobile operator's core network or to another Internet destination. This reduces the traffic carried over the operator's radio and backhaul networks, thereby increasing available capacity.

The success of this novel technology is confirmed by market forecast: 2.3 million femtocells have already been deployed globally in 2011, and they are expected to be nearly 50 million by 2014 [20]. Moreover, Juniper Research forecasts that by 2015, 63% of mobile data traffic will be offloaded to fixed networks through femtocells and WiFi APs [21].

In this novel network architecture, macrocells and femtocells may share the same spectrum in a given geographical area as a *two-tier network* (see Figure 2.6). Thus, *cross-tier interference* may drastically corrupt the reliability of communications. As shown, in Figure 2.7, cross-tier interference affects macro users (M-UEs) as well as femto users (F-UEs) creating dead zones around the interfered receiver. Similarly, neighbour FAPs belonging to same operators may also interfere with each other thus generating *co-tier interference* (see Figure 2.8).

ICIC schemes are classically used to mitigate inter-cell interference in cellular networks; however, femtocell is different from the traditional cells in its need to be more autonomous and self-adaptive. Additionally, the backhaul interface back to the cellular network is IP-based and likely supports a lower rate and higher latency than the standard X2 interface connecting macro and picocells [22]. Some RRM algorithms propose to use full time/frequency orthogonalization of concurrent transmissions in the macro and femto layers to avoid cross-tier interference (see for instance [23]). However, these approaches are far from the FR targets of mobile operators and they does not reduce interference amongst neighbour femtocells, which can strongly reduces users performance, especially in dense femtocell deployment scenarios.

The impact of interference is highly related to femtocell access control mechanism. Standard Development Organizations (SDOs) are currently investigating three different access control approaches: *closed access*, *open access*, and *hybrid access* [24]. Closed access scheme allows only a restricted set of users, which is named as Closed Subscriber Group (CSG), to connect to each femtocell; open access FAPs, referred to as Open Subscriber Group (OSG) FAPs, always permit a subscriber to access the mobile network; in the hybrid Access approach, FAPs allow the access to all users but a certain group of subscribers maintain higher access priority. In the CSG femtocells scenario, the issue of interference can become an important bottleneck with respect to QoS and performance of communications. On the contrary, OSG FAPs limit the interference problem although security issues and high signalling due to handover procedures can reduce the overall performance. Furthermore, due to resource sharing, open access limits benefits for the femtocell owner. Henceforth, according to a recent market research [25], the closed access scheme is the

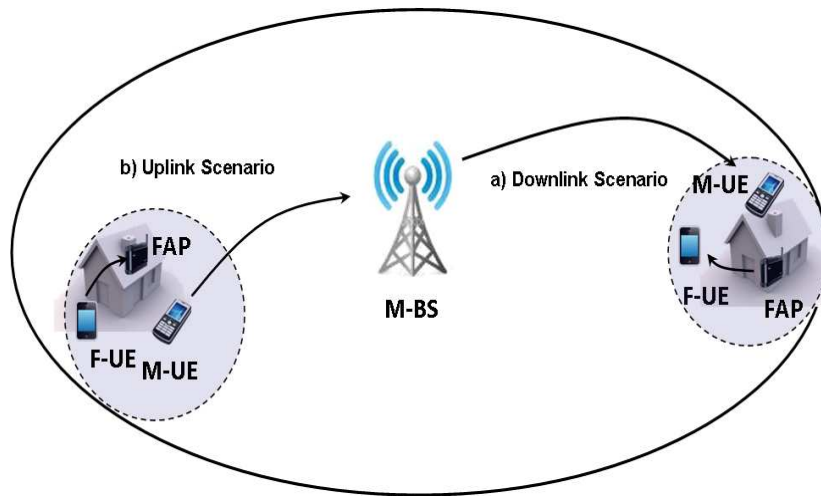


Figure 2.7: Near-far scenarios in two-tier cellular networks: (a) Downlink Scenario: FAP transmits to its F-UE and creates a dead zone for the cell-edge M-UE. (b) Uplink Scenario: cell-edge M-UE transmits with high power to its serving M-BS and creates a dead zone for the nearby FAP.

favourite access method of potential customers.

The following of this chapter focuses on main solutions proposed in the literature to enable the cost-effective and reliable deployment of femtocells. First, Section 2.2.2 presents recent advances in the femtocell network standardization and relevant studies realized in the framework of European projects. Subsequently, Section 2.3 presents CR concept and discusses its main functionalities. Section 2.4 overviews some important contributions, which deal with interference management and *green communications* in two-tier cellular networks, Eventually, Section 2.5 underlines open issues in the field.

2.2.2 Femtocell Reference Models and Scenarios

To successfully introduce femtocell networks in the telecommunication market, both operators and manufacturers are cooperatively working for the development of reliable femtocell technologies. Moreover, SDOs, such as the Third Generation Partnership Program (3GPP), are contributing to the definition of common standardized architectures.

The 3GPP and 3GPP2 partnerships propose solutions for Wideband Code Division Multiple Access (WCDMA), and beyond, and CDMA2000, respectively. IEEE 802.16 and WiMAX forum jointly cooperate to realize femtocells based on Worldwide Interoperability for Microwave Access (WiMAX). Broadband forum investigates the interoperability between FAPs and network equipment from different vendors. Furthermore, other non-SDO partnerships such as the Femto Forum and the Next Generation Mobile Network (NGMN) organizations, actively contribute to the development and diffusion of femtocells worldwide.

In early 2009, 3GPP published the first femtocell standard as a part of the Release 8 specification [26]. This standard defines WCDMA femtocell and includes initial baseline for Long Term Evolution (LTE) femtocells. 3GPP has continued to develop femtocell architecture in Release 9, which has been finalized in March 2010. Seidel and Saad present an overview of major enhancements introduced in the 3GPP Release 9 [27]. Release 10 has been frozen during 2011 and

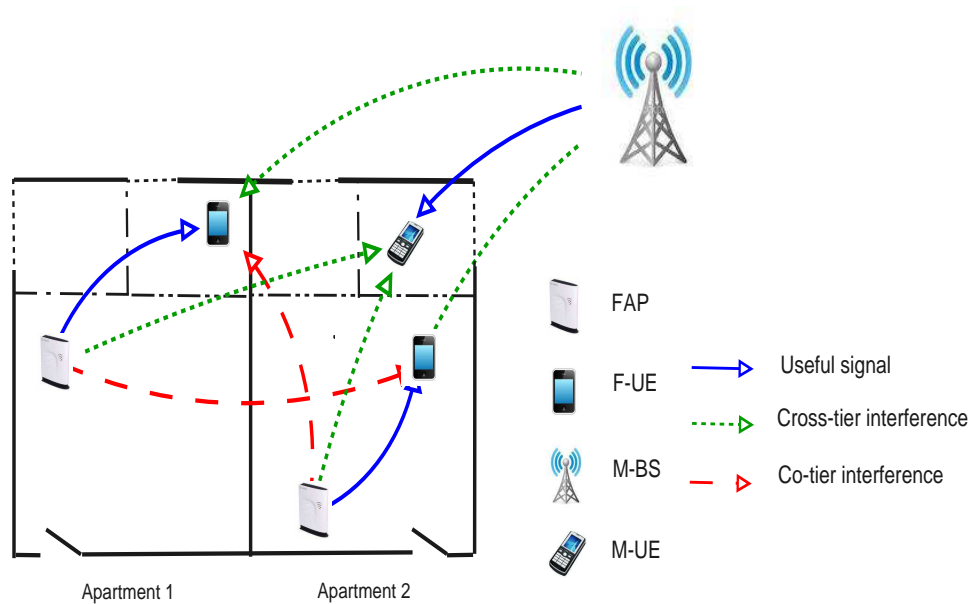


Figure 2.8: Downlink interference scenarios in two-tier cellular networks.

it introduces new functionalities such as support for mobility enhancements and Self Organizing Networks (SONs).

In April 2009, the Broadband forum announces the 'Femto Access Point Service Data Model' for 3G femtocells [28]. Further improvements, which integrate functionalities of both LTE and CDMA2000 femtocells, are expected to be announced in 2011. To prove the effectiveness of this standard, the Femto Forum and the European Telecommunications Standards Institute (ETSI) have recently organized the second femtocell plugfest event. During the plugfest event, interoperability tests were realized amongst FAPs, management systems, security gateways and femtocell network gateways. The plugfest also tested the IPsec/IKEv2 security protocols that permit femtocells to communicate over the public Internet to core networks.

In March 2010, 3GPP2 ended the first phase of standardization of CDMA2000 femtocells [29]. In June 2010 Femto Forum and WiMAX forum conjointly announced the publication of the first WiMAX femtocell standard. This standard allows manufacturers to produce femtocells and associated equipment based on the IEEE 802.16e physical layer characteristics. The specifications include a security framework, SON-like capabilities, and three different access modes [30].

Moreover, in the frameworks of standardization and European projects, industrial partners in conjunction with research centres have proposed use cases and models, which are the baseline of the research that aims to enable the successful deployment of femtocells networks. In particular, in the following we present three main contributions:

1. The femtocell deployment model for urban scenarios proposed by Alcatel-Lucent, picoChip Designs, and Vodafone in the 3GPP frameworks [31];
2. Some interesting femtocells usage cases [32] defined in the framework of BeFEMTO project, which are useful contexts for most of contribution in the literature;
3. The Energy Efficiency Evaluation Framework (E^3F) proposed in the EARTH project, which provides a reliable estimation of the BSs power consumption considering the different com-

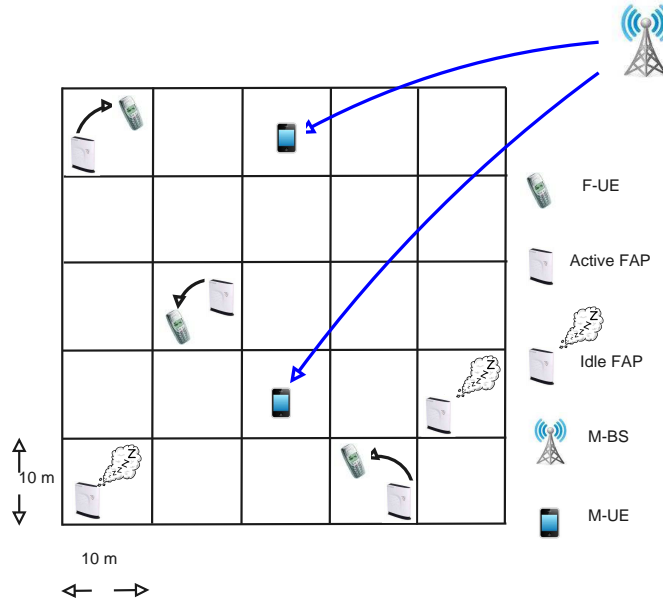


Figure 2.9: The femtocell grid urban deployment model.

ponents of the radio equipment [17];

2.2.2.1 Deployment of Femtocells and Path loss Models

The grid urban deployment model represents a single floor building with 10 m x 10 m apartments placed next to each other in a 5 x 5 grid (see Figure 2.9). To consider a realistic case in which some apartments do not have FAPs, a system parameter ρ_d called a *deployment ratio* indicates the percentage of apartments with a FAP. Furthermore, the 3GPP model includes ρ_a , another parameter called an *activation ratio* defined as the percentage of active FAPs. Whenever a FAP is active, it transmits with suitable power over the traffic channels; otherwise, it only transmits only on the control channel.

Two different models are used to capture the signal propagation effect:

1) *Transmissions from M-BSs to cellular users:*

$$PL(dB) = 15.3 + 37.6 \log_{10} d + L_{ow}, \quad (2.1)$$

where d is the distance between the transmitter and the receiver (in meters) and L_{ow} is the penetration losses of an outside wall equal to 20 dB.

2) *Transmissions from FAPs to cellular users:*

$$PL(dB) = 38.46 + 20 \log_{10} d + 0.7 d_{2D,indoor} + 18.3 n^{((n+2)/(n+1)-0.46)} + q \cdot L_{iw}, \quad (2.2)$$

where d is the distance between the transmitter and the receiver (in meters), $d_{2D,indoor}$ is the two dimensional separation between the transmitter and the receiver (in meters), n is the number of penetrated floors, q is the number of walls that separate the user apartment and the transmitting FAP apartment, L_{iw} is the penetration loss of walls within the grid of apartments equal to 5 dB. The third term in the above expression represents the penetration loss due to walls inside an apartment.

This attenuation is modelled as a log-linear value equal to 0.7 dB/m. The fourth term represents the penetration loss through different floors. In the considered single floor building scenario, $d = d_{2D,indoor}$ and $n = 0$.

2.2.2.2 Femtocell Use Cases

Here, we describe two femtocell deployment scenarios, which characterize a broad range of femtocell-based services, and we discuss their usage, architectural challenges, and main benefits. The proposals of this are developed within the context of the scenarios listed below:

1. Indoor stand-alone femtocells for residential deployment;
2. Large interconnected femtocell networks (i.e., enterprise femtocell networks).

Femtocells have been originally designed to offer high quality service to customers in residential environments. In such scenario, a FAP is installed in an ad-hoc manner without traditional RF planning, site selection, deployment and maintenance by the mobile operator. Moreover, customers will likely restrain the access to their femtocell to guarantee their performance and also to protect their privacy. As already mentioned, several contributions underline that CSG femtocells can generate coverage holes to neighbouring UEs, which are served by a farther BS [33]. Moreover, in the femtocell stand-alone deployment scenario, inter-cell coordination is not feasible; therefore, self-configuration and network adaptation capabilities are necessary to avoid harmful cross-tier and co-tier interference. In particular, autonomous interference coordination, through power adjustment and distributed spectrum access, it is a required feature in standalone femtocells. Due to these challenges, the deployment of residential femtocells is generally investigated in the framework of SONs [34] or modelled as CR networks [6].

On the contrary, networked femtocells are designed in particular for large offices, enterprises, and shopping mall. Such an architecture is characterized by a large number of users, a dense femtocell deployment, and therefore, a potential higher co-tier interference and handover frequency. Another characteristic that distinguishes networked femtocells from residential ones is the access control mechanism: in such scenario, open access and hybrid access modes will likely be preferred to the closed access, especially due to the interference issue [35]. Up to the current 3GPP release 10, the standard does not allow direct coordination amongst CSG FAPs or amongst FAPs and M-BSs [22]. Exchanging coordination message via the IP-based backhaul, which connects FAPs to the backhaul network of a cellular operator, can support only long-term coordination due to high latency that can be introduced by such a link [36]. However, in release 10, X2 interface has been introduced at OSG femtocells as a part of the mobility enhancement for F-UEs [22]. This interface may enable dynamic inter-cell coordination amongst neighbouring FAPs and alleviate co-tier interference.

Whenever the X2 interface is not available, the exchange of coordination messages could be realized Over-The-Air (OTA). Two approaches can be used to enable OTA-based cooperation: direct coordination can be implemented amongst neighbouring FAPs, however, to enable bidirectional communication FAPs are required to be equipped with both downlink reception and uplink transmission capabilities, which increase the cost of the AP; a different solution, which limits the hardware complexity, is to implement dynamic inter-cell coordination through UE's relaying [37]. Moreover, the cooperation process can be implemented in both a distributed or centralized fashions. Centralized approaches require a local node, which acts as FAPs coordinator, to be introduced into the femtocell network architecture. It is important to note that, although centralized schemes often permit higher performance and reduced overhead, distributed solutions do not rely on the central node and therefore are generally preferred.

2.2.2.3 EARTH Energy Efficiency Evaluation Framework

The EARTH E^3F maps the radiated RF power to the power supply of a BS site and underlines the relationship between the BS load and its power consumption. Furthermore, it investigates the impact of the different components of the BS transceivers on the aggregate power consumption. Such a study is based on the analysis of the power consumption of various LTE BS types as of 2010. The effect of the various components of the BS transceivers is considered: Antenna Interface, PA, the small-signal RF transceiver, baseband interface, a DC-DC power supply, cooling, and AC-DC supply. Therefore, the E^3F proposes a linear power consumption model that approximates the dependency of the BS power consumption to the cell load:

$$P^* = \begin{cases} P_0 + \Delta_p P^{RF}, & 0 < P^{RF} \leq P_{max}; \\ P_{sleep}, & P^{RF} = 0. \end{cases} \quad (2.3)$$

where P^* is the BS input power required to generate the irradiated P^{RF} power and Δ_p is the slope of the load-dependent power consumption. Moreover, P_{max} , P_0 , and P_{sleep} indicate the RF output power at maximum load, minimum load, and in sleep mode, respectively.

Table 2.1 shows the classical values of P_{max} , P_0 , and Δ_p for M-BSs and FAPs. Note that the value of P_{sleep} depends on the hardware components that are deactivated during sleep intervals. However, more deactivated hardware components result in a slower reactivation process.

BS type	P_{max} [W]	P_0 [W]	Δ_p
M-BS	40	712	14.5
FAP	0.01	10.1	15

Table 2.1: BS Power model parameters.

Figure 2.10 shows the operating power consumption of M-BSs (left) and FAPs (right) with respect to the traffic load according to the model in [17].

Such representations evidence that:

- M-BS power consumption is fairly related to the load, thus, macro offloading via femtocells deployment can greatly enhance the overall cellular network EE;
- FAP power consumption does not vary much with the load, thus, the EE of these cells is reduced in lightly load scenarios;
- Retransmissions have a higher impact on macrocell performance and slightly affect femto EE; therefore, retransmissions towards M-UEs should be performed by neighbouring small cells;
- Low cost PAs designed to scale their power consumption with the load could improve the energy performance of femtocell networks;
- Dynamic cell switch-off techniques can adapt femtocells activity to the load to operate only in high EE state.

It is important to note that femtocells normally work in low load scenarios. Due to the limited number of UEs that can be simultaneously served by a FAP and the short distance between the AP and the user terminal, spectrum/power resources are often underutilized at FAPs. Furthermore, the femtocells density in urban scenarios is expected to be very high. A high number of low energy efficient FAPs can have a detrimental effect on the aggregate cellular network performance.

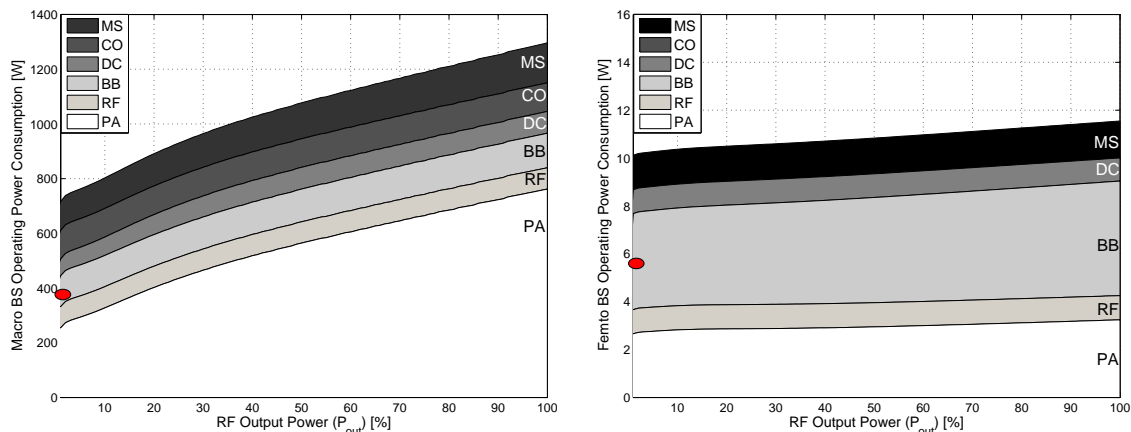


Figure 2.10: M-BS (left) and FAP (right) power consumption dependency on relative output power [17]. Legend: PA=Power Amplifier, RF=small signal RF transceiver, BB=Baseband processor, DC: DC-DC converters, CO: Cooling (only applicable to the M-BS), PS: AC/DC Power Supply, the ellipse indicates the BS power consumption in sleep mode.

2.3 Medium Access Control Strategies for Cognitive Radio Ad-Hoc Networks

In our vision the femtocell deployment requires adaptive mechanisms inspired by the CR paradigm to deal with its inherent issues. A CR network is capable to observe its environment (i.e., it is context-aware) and dynamically react to the acquired stimuli to improve its users' performance while limiting co-channel interference. Moreover, it learns from the past and ameliorates its strategies. The integration of such a paradigm in femtocell networks may allow to either solve or limit the impact due to, for instance, the co-channel interference and the limited backhaul capacity.

As already mentioned, CR has been mainly considered as enabling technology to enhance the SE in ad-hoc wireless networks. Therefore, in this section, we introduce the principles of CR and overview the main contribution in this field. On the contrary, next section discusses recent studies that propose adaptive mechanisms based on CR principles for improving performance in femtocell networks.

Spectral resource demand has greatly increased in the last two decades due to emerging wireless services and products. Although frequency allocation charts reveal that almost all frequency bands have already been assigned (see Fig. 2.11), traditional static spectrum allocation strategies cause temporal and geographical holes [13] of the spectrum usage in licensed bands. In addition, in recent years, Industrial, Scientific, and Medical (ISM) unlicensed bands have allowed the development of technologies such as WiFi, Bluetooth, and cordless phones. The great success of this band has given rise to the problem of coexistence of heterogeneous systems that might interfere each other.

CR emerges as a way to improve the overall spectrum usage by exploiting spectrum opportunities in both licensed and unlicensed bands. The cognitive cycle [38] begins with sensing the RF medium: radios are able to exploit information about the wireless environment to be aware of local and temporal spectrum usage. Opportunistic users may dynamically select best available channels,

problem [40]. A cognitive node may exploit, however, increased sophisticated sensing functionalities; it distinguishes between primary and secondary users, and provides protection to licensed transmissions. The number of channels available at each user is fixed in a multi-channel network, although it varies with time and space in a cognitive network. Furthermore, the time-scale in which a cognitive network operates is very different from that of a classic ad-hoc network: secondary users must exploit periodical sensing to be aware of the wireless environment evolution, and must rapidly adapt their behaviour to reach QoS and comply with interference constraints.

Industrial and research communities have been proposed a multitude of studies related to the CR MAC. A few surveys have already been out to review existing work, and to assess the fundamental goals of cognitive radio. Akyildiz *et al.* provided a general overview of critical issues in CR network spectrum management [41]. Another survey discussed main characteristics of some existing multi-channel MAC protocols underlining the additional functionalities that each multi-channel protocol should offer to operate in the opportunistic context [42]. Furthermore, CR MAC protocols are classified according to exploited mechanisms of channel negotiation/reservation. Wang *et al.* discuss the main differences between classical multi-channel protocols and CR MAC protocols [43, 42]. The former contribution presents, moreover, sensing policies and channel selection algorithms of some distinctive CR MAC protocols. Krishna and Das have analysed opportunistic networks according to the type of infrastructure [44]. Centralized networks are then classified depending on whether the controller takes part in data transmission among the secondary users. On the contrary, decentralized networks are classified according to how signalling and channel negotiation are managed into the network. Moreover, several CR MAC protocols are reviewed according to the proposed classification. Cormio and Chowdhury proposed to classify infrastructure-based and ad-hoc cognitive MAC protocols according to the exploited medium access scheme and the number of required radio transceivers [45]. Pawelczak *et al.* divided CR MAC protocols into four groups according to how control information is exchanged [46]. Moreover, to compare these groups from the throughput perspective, the authors exploited an extended version of the framework proposed by Mo *et al.* [47].

With respect to these previous surveys, the contribution of this section is, therefore, threefold. First, in an attempt to make order within different existing proposals, we present a global CR MAC protocols classification. Second, spectrum management issues and functionalities are discussed. Third, a comprehensive overview of classical and recent CR MAC protocols is presented. In particular, Section 2.3.1 introduces the proposed CR MAC protocol classification; Sections 2.3.2, 2.3.3, 2.3.4, and 2.3.5, discuss CR MAC main issues and present existing algorithms dealing with spectrum sensing, opportunistic channel allocation, dynamic spectrum sharing and spectrum mobility, respectively.

2.3.1 Classification of MAC Protocols for Cognitive Radio

A general presentation of cognitive MAC protocols can be obtained by following the approach proposed by Xiao and Hu [48], where protocols are classified according to the following features:

1. complexity;
2. protocol architecture;
3. level of cooperation within the network;
4. how signalling and data transfer are managed during communication.

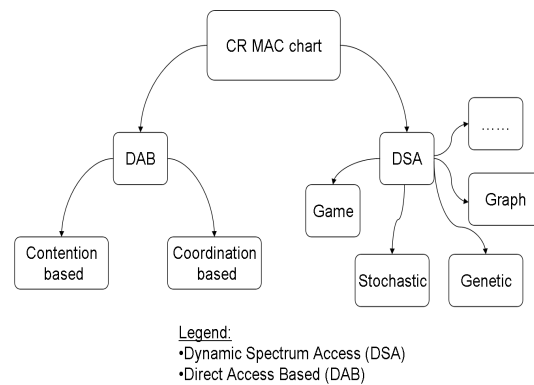


Figure 2.12: Cognitive radio MAC protocols chart.

Figure 2.12 shows that two main MAC protocols categories can be distinguished: Direct Access Based (DAB) and Dynamic Spectrum Allocation (DSA). DAB protocols do not allow any global network optimization since each sender-receiver pair tries to maximize its own optimization goal. Moreover, resource negotiation is classically addressed with a sender receiver handshake procedure [49, 50], and a simple protocol architecture limits computational cost and latency. DSA classification refers to protocols that exploit complex optimization algorithms to achieve a global purpose in an adaptive fashion. Both DAB and DSA protocols can be implemented in centralized or distributed architecture. As already mentioned, distributed protocols are more robust since they do not rely on reliability of the central node (also indicated as clusterhead or cluster leader), whereas in centralized protocols, a single node coordinates control information exchange and radio access. The latter architecture can potentially be more efficient in resource usage, by exploiting coordination and global information on network status. Moreover, the cluster leader often has access to complementary information on the wireless environment that permits to improve coexistence with primary users (e.g., the DIMSUMNet architecture [51] or the Cognitive Pilot Channel (CPC) scheme [52]).

Control information exchange in CR networks

The amount of signalling information exchanged in a CR network is substantially larger than in a classical wireless network. Thus, most of CR MAC protocols exploits an out-of-band control channel to perform resource negotiation and share results of spectrum sensing. This channel is physically separated from the in-band channel where data transmission occurs. A dedicated control channel, moreover, may allow network synchronization and broadcasting. Two strategies are suitable for the selection of the out-of-band control channel: it can be a dedicated licensed channel [50] or a shared channel [53, 54]. Although a licensed channel is often assumed to be interference free, in the latter solution heterogeneous networks may coexist on the same channel. Both solutions have drawbacks; in the first case, the common channel bandwidth should be adaptable to traffic load to limit resource wasting, or saturation, as the number of users increase. In the second case, the common channel should be continuously monitored because collisions of negotiation data could drastically affect system performance. When channel quality or its availability varies, it is necessary to vacate the selected channel and select a better one. Moreover, several protocols assume that a global control channel is available [49, 55], although the probability that an opportunistic channel is available for all nodes in a cognitive network might be dramatically small. A local common channel is proposed to overcome this drawback [56, 57], and two approaches are investigated in the literature to manage the out-of-band control channel: the Common Control

Channel scheme and the Split Phase scheme.

Common Control Channel: users share a dedicated channel to exchange signalling information, sensing outcome, and perform channel selection. This scheme does not require time synchronization, hence, to avoid that network nodes miss control messages, a dedicated transceiver should be tuned on the common channel ([55, 54]).

Split Phase: this approach permits to exploit only one transceiver, but with a cost in terms of synchronization overhead. Split Phase protocols divide time frames into two parts: a first part named control phase and a second part named data phase [53, 58]. During the control phase each terminal overhears control messages to be aware of the network status; then in the data phase, transmissions are performed. Hence, free data channels are wasted during the control phase, and system efficiency is reduced, although, the control channel can be used for data transmissions during the data phase.

To overcome the out-of-band control channel drawbacks, several solutions have been proposed to handle signalling exchange and data transmissions over the same channel (in-band signalling). In IEEE 802.22 [59] a logical in-band control channel is exploited and Chowdhury and Akyildiz have investigated a solution where sensing results are piggybacked over data transmissions [60]. On the contrary, in Frequency Hopping Sequence, cognitive users share a hopping list and keep moving from one channel to the other, until they are involved in a communication [61, 62]. In this approach, transmissions are more reliable because resource negotiation accuracy does not depend on the status of a single common channel. Frequency hopping requires, however, a tight synchronization among network nodes. Furthermore, to be suitable to a licensed scenario, it is necessary that the hopping sequence list may dynamically adapt to channel availability. This adaptation relies on spectrum usage prediction and its reliability influences system performance. Additionally, sensing output time-space dependence affects the possibility that different cognitive users may share a common hopping sequence and communicate.

Figure 2.13 highlights the main differences between the Common Control Channel, the Split Phase, and the Frequency Hopping Sequence approaches.

As already underlined, the Common Control Channel scheme requires two radios to efficiently manage signalling and data transmissions; the use of only one radio decreases device costs and energy consumption but imposes to interrupt data transmissions to perform sensing and signalling exchange. Moreover, a MAC protocol with a single transceiver has to address the multiple channel hidden terminal problem that may cause collisions between packets transmitted by different users. A user equipped with a single transceiver can in fact only transmit or listen over one channel at a time. Thus, when a node is listening at a particular channel, it cannot hear communication taking place on a different channel. Consider for instance, the scenario of Fig. 2.14: node *A* wants to send a packet to node *B* and starts the Request To Send/Clear To Send (RTS/CTS) handshake on the control channel (channel 1). After negotiation, channel 2 is selected and node *A* starts communication. Node *C* does not hear, however, the RTS/CTS messages because it is listening to channel 3, and decides to initiate a transmission on channel 2, causing a collision.

Direct Access Based MAC protocols

In general, each DAB protocol belongs to one of the two following groups:

- **contention based protocols:** first, cognitive senders and receivers exchange their sensing outcome by means of a simple handshake. Then, the pair compares available resource and negotiates the channel where to communicate. The entire procedure is referred to as Channel Filtering Sender Receiver (CFSR) handshake.

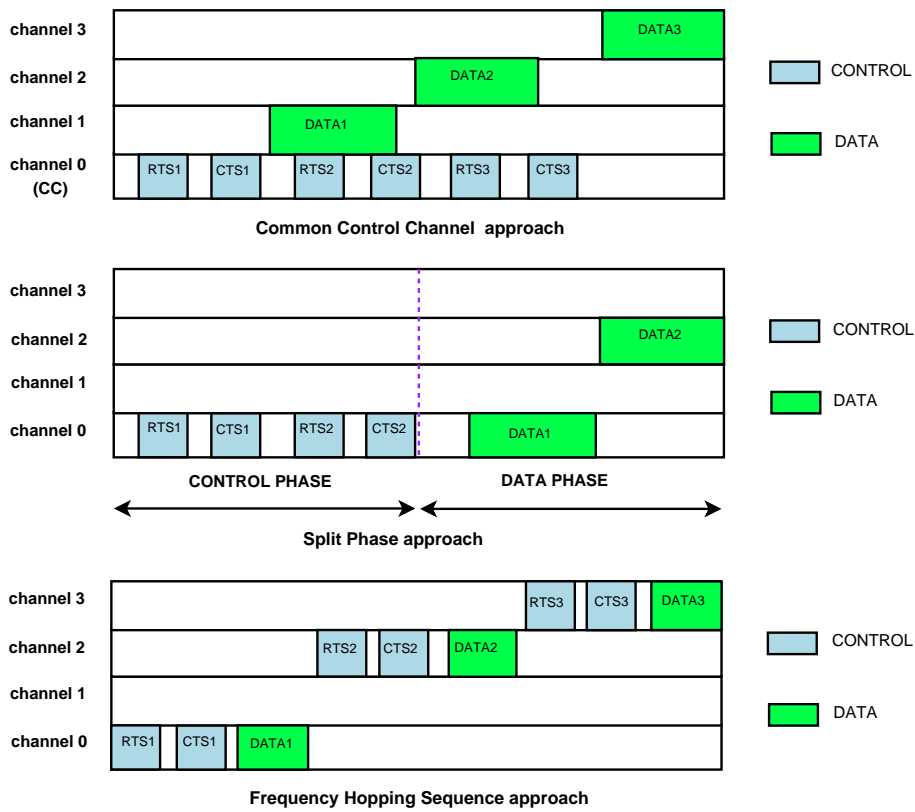


Figure 2.13: Dealing with signalling and data transmission in multichannel CR networks.

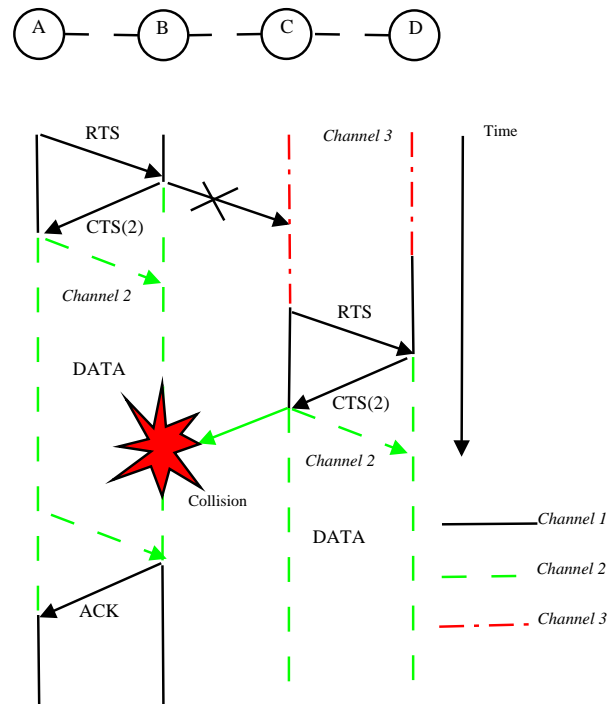


Figure 2.14: The multichannel hidden terminal problem.

- **coordination based protocols:** each node shares its channel usage information with its neighbours to increase sensing reliability, and improve overall system performance.

DAB protocols reviewed in this chapter are listed in Table 2.2, following the presented taxonomy.

Protocol	Cooperation	Signalling	Reference
HC-MAC	contention-based	out-of-band	[49]
IEEE 802.22	coordination-based	in-band	[59]
C-MAC	coordination-based	out-of-band	[53]
MMAC-CR	coordination-based	out-of-band	[58]
SU08	coordination-based	out-of-band	[50]
DOSS	contention-based	out-of-band	[55]
SYN-MAC	coordination-based	in-band	[62]
HD-MAC	coordination-based	out-of-band	[57]
CogMesh	coordination-based	out-of-band	[56]
COMAC	contention-based	out-of-band	[63]
OS-MAC	coordination-based	out-of-band	[64]
Ghaboosi08	not addressed	out-of-band	[54]

Table 2.2: DAB CR MAC protocols overview in this chapter.

Dynamic Spectrum Allocation MAC protocols

DSA-driven MAC protocols exploit advanced optimization algorithms to realize intelligent, fair and efficient allocation of the available spectrum. Each opportunistic user adapts its transmission parameters, such as modulation and coding, power transmission, and antenna configuration, to changes of the wireless environment, to efficiently exploit the available resource. Finding the system optimum that takes into account all the constraints of a cognitive system, requires, however, for practically relevant systems, prohibitively computational cost and a complete knowledge on the network status. Hence, although DSA algorithms promise global optimization and better performance than DAB strategies, they generally suffer from low scalability that affects negotiation delay and complexity. Therefore, to reduce complexity, decentralized approaches in which each node acts based on partial knowledge of network status (e.g., the localized variation of the island genetic algorithm [65]) have been proposed. Several approaches have been considered to model network interactions in DSA protocols, such as graph coloring theory [66, 67], game theory [68, 69], stochastic theory [70], genetic algorithms [71], and swarm intelligence algorithms [72].

Table 2.3 shows the list of DSA methods that will be examined in the following.

- **Graph theory algorithms:** a cognitive network can be modeled as a graph $G = (\mathcal{V}, \mathcal{E})$ where \mathcal{V} and \mathcal{E} indicate the vertex vs. the edge sets. Two kinds of representations are available: Node Contention Graph (NCG) and Link Contention Graph (LCG). In NCG, cognitive users are represented by nodes and edges indicate that two nodes are in the interfering range of each other. In LCG, the vertex set represents active flows, although edges represent a contention between different flows.
- **Stochastic algorithms:** the evolution of channel availability can be represented by a stochastic process. In particular, among the various proposed stochastic approaches, Markov chain

Name	Algorithm	Signalling	Reference
DH	Graph coloring	not addressed	[67]
Zheng05	Graph coloring	not addressed	[66]
G-MAC	Game theory	in-band	[68]
Zou08	Game-theory	out-of-band	[69]
DC-MAC	Stochastic model	in-band	[70]
BIOSS	Swarm intelligence	not addressed	[72]
Nainay08	Genetic algorithm	not addressed	[65]

Table 2.3: Presented DSA CR MAC protocols/algorithms.

formulation is the most applied. In these strategies, each node estimates channel usage based on the statistics of local spectrum sensing and its historical access experience. Hence, based on the observations, stochastic algorithm is expected to determine a strategy that maximizes the adopted utility function.

- **Game theoretic algorithms:** interactions within a cognitive network can be represented as a game. Game theory efficiently models the dynamics of a cognitive network: adaptation and recursive interactive decision process are naturally modeled by a repeated game. Moreover, with game theory each player may adopt a different utility function to pursue specific goals. Interactive behaviours among cognitive nodes is represented as a game $\Gamma = \langle \mathcal{N}, \{S_i\}, \{u_i\} \rangle$. \mathcal{N} is the set of game players, each sender-receiver pair is an element of this set; S_i represents the strategy space (such as MCSs, transmission power, antenna parameters) of player i ; u_i is the local utility function that models the scope of player i .
- **Genetic algorithms:** these are adaptive search algorithms based on the evolutionary ideas of natural selection. An iterative process starts with a randomly generated set of solutions called population. Best individuals are selected through the utility function (called here fitness function). Then, starting from this subset, a second population is produced through genetic operators: crossover and/or mutation. The new population shares many of the characteristics of its *parents*, and it hopefully represents a better solution. The algorithm typically terminates when it converges to the optimal solution or after a fixed number of iterations. Genetic algorithms are chosen to solve resource allocation problems due to their fast convergence and the possibility of obtaining multiple solutions.
- **Swarm intelligence algorithms:** Inspired by the collective behavior of social biological individuals, Swarm Intelligence algorithms model network users as a population of simple agents interacting with the surrounding environment. Each individual has relatively little intelligence, however, the collaborative behaviour of the population leads to a global intelligence, which permits to solve complex tasks. For instance, in social insect colonies, different activities are often performed by those individuals that are better equipped for the task. This phenomenon is called division of labour [72]. Swarm Intelligence algorithms are scalable, fault tolerant and moreover, they adapt to changes in real time.

2.3.2 Spectrum Sensing

Spectrum sensing is the functionality enabling cognitive nodes to be aware of spectrum usage and to detect spectrum opportunities. When two nodes want to communicate, source and destination

are responsible for performing sensing; they select a set of channels to sense, they estimate channel availability, then channel filtering is performed, and a communication link is set up. Both reactive (on-demand) and proactive sensing may be exploited in a cognitive network. During data transmission, periodic in-band sensing is performed to detect incumbent primary users and avoid harmful collisions, while the sensing process dealing with the search of new opportunistic resources is referred to as out-of-band sensing. Different techniques have been proposed in the literature to process observations and detect primary users (such as energy detection [73], matched filter [74], and feature detection [75]). MAC protocols are not necessarily aware of the adopted approach. The sensing outcome processing and available channel estimation can be realized in a distributed or centralized fashion. In the centralized approach, a leader fuses all sensing information according to a certain rule (for instance, AND, OR, or M-out-of-N rules [76]) and it evaluates spectrum opportunities. In the distributed solution, secondary nodes share observation data and independently take decisions regarding resource availability.

Sensing performance is limited by hardware and physical constraints. For instance, secondary nodes with a single transceiver cannot transmit and sense simultaneously. Moreover, users usually only observe a partial state of the network to limit sensing overhead. There is a fundamental trade-off between the undesired overhead and spectrum holes detection effectiveness: the more bands are sensed, the higher the number and quality of the available resource. This overhead is not only due to the sharing of the sensing outcome but also to the Quiet Period (QP) [59]. QP is the time during which a resource is not exploited for data communication to be sensed; transmission on the observed band is avoided during in-band sensing measurements to avoid intra-network interference. However, the overall system throughput is reduced when the network postpones scheduled transmissions to quiet the sensed channel.

Spectrum sensing in IEEE 802.22

The IEEE 802.22 [59] working group task is to develop CR based Wireless Regional Area Network (WRAN) Physical and MAC layers to exploit idle TV spectrum bands. The proposed MAC protocol is a contention based DAB protocol with a centralized architecture. Each WRAN cell consists of a BS and its associated secondary users. The BS and its users are responsible for performing both in-band and out-of-band sensing. BSs indicate to each of their serving nodes the channel to sense, the sensing period and false alarm/detection probability constraints. Measured values are transferred to the BS, which analyses them and takes appropriate action. IEEE 802.22 proposes a two sensing stages mechanism to realize in-band sensing, as represented in Figure 2.15. During fast sensing, rapid measurements (≤ 1 ms/channel) are performed by each network node, and processed at the BS. Depending on the fast sensing process outcome, a BS may require a more reliable sensing on a specific channel. Fine sensing requires longer sensing period than fast sensing (for instance, 25 ms/channel sensing is performed for primary users detection in the US digital television system), and exploits algorithms looking for particular signatures of licensed transmissions. Furthermore, to avoid intra-network interference during QPs, IEEE 802.22 exploits a synchronization algorithm permitting to BSs that operate in the same geographical region to perform reliable in-band sensing.

A Dynamic Frequency Hopping (DFH) strategy was proposed to increase IEEE 802.22 performance [61]. In the DFH mode, a WRAN cell, while communicating on channel i (the in-band channel), observes channel availability on the next working channel j (the out-of-band channel). Then, to avoid collision with licensed users, the cognitive cell hops on channel j to continue transmission and starts sensing channel i . Each user is equipped with two transceivers; hence, sensing and transmission can be performed in parallel. This operation is referred as Simultaneous Sensing and Data Transmissions, and represented in Figure 2.16. Guard bands separate in-band and out-of-

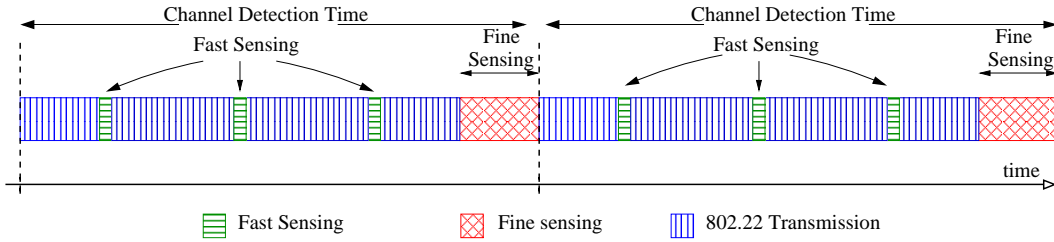


Figure 2.15: The IEEE 802.22 two stage sensing [59].

band channels to mitigate interference during simultaneous sensing and transmissions. Hence, the DFH strategy increases system throughput by avoiding transmission interruption. Moreover, coordination between neighbor WRANs is proposed to avoid mutual interference during the sensing phase. A DFH Community (DFHC) is a set of N coordinated WRANs: each DFHC is managed by a community leader and its members exchange information through a coexistence window located at the end of the MAC frame. The leader is responsible of periodically generating and broadcasting the channel hopping pattern. Coordination permits the DFHC members to operate by transmitting and sensing without interruption using $N+1$ vacant channels, as long as the length of a single transmission is larger than the product $N \cdot QT$ (QT is the length of the Quiet Period).

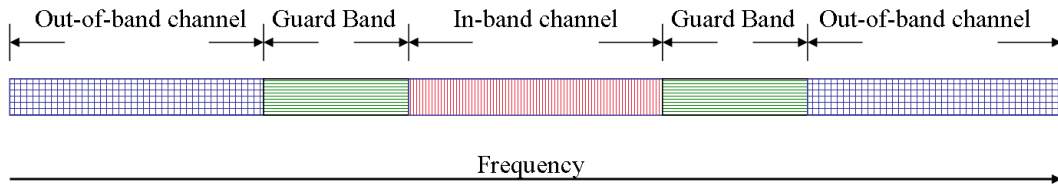


Figure 2.16: Simultaneous Sensing and Data Transmission in 802.22 DFH [61].

Double Hopping (DH) approach improves reliability of the DFH scheme [67]. Figure 2.17 shows the DH operating mode for three neighbour IEEE 802.22 cells. The time at which a cell is allowed to consecutively transmit is indicated as T_{data} . The minimum amount of time required to perform sensing is T_{sens} . To limit interference, transmissions are not allowed on sensing channels during the QP. T_{quiet} defines for how long a frequency cannot be used because of the sensing process. Hence, in the DH operating mode each cell exploits a dedicated working frequency and shares a sensing frequency with all the cells within its network. Transmission starts on the working frequency, then when T_{data} expires, a cell hops on the sensing frequency to continue its communication while performing periodic sensing on its working frequency. After T_{quiet} , it can hop back on its working frequency and let the sensing frequency free. In Figure 2.17, the sensing slots for the working frequencies and the sensing frequency are referred to as N_{wf} and N_{sf} , respectively. The maximum number of neighbour cells that can share a sensing frequency and be supported by the DH strategy is $N_q = T_{data}/T_{quiet}$.

The DH approach permits to reduce the number of frequency channels exploited by each WRAN cell. In the classic DFH scheme, each cell hops on $N+1$ channels (N is the number of cells in the network) according to the pattern generated by the cell leader. Oppositely, in the DH approach, a CR cell hops between two frequencies only. This approach has some advantages: first, when a primary user appears on a working frequency only the cell attached to that channel has to shift to another channel; second, managing network coordination is simpler because cells share only the sensing frequency.

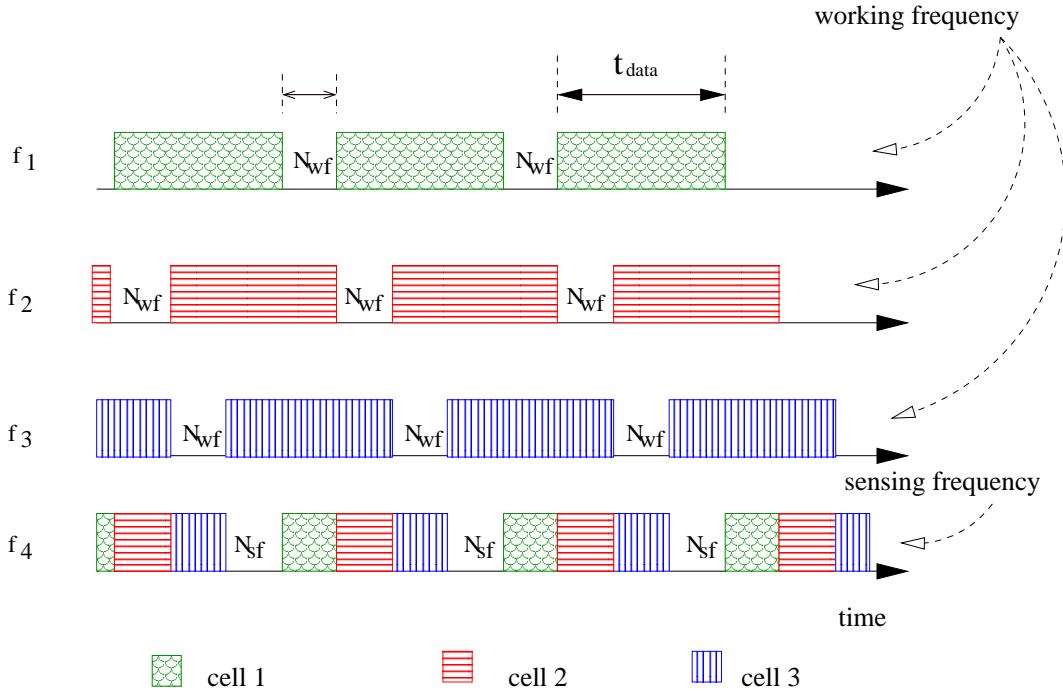


Figure 2.17: Double Hopping operating mode for three neighbouring cells [67].

Spectrum sensing optimization

To improve the spectrum sensing process, several CR MAC protocols have proposed different strategies to limit resource waste. A first approach is presented in the Hardware-Constrained Cognitive MAC (HC-MAC) [49]. HC-MAC is a contention based DAB protocol that represents the sensing process as an optimal stopping problem to determine how long a cognitive radio should observe the wireless bands to optimize its expected throughput. The stopping rule is defined by two objects:

- the observation sequence, modelled as random variable, X_1, X_2, \dots ,
- a reward sequence, which is a function of the observation, $y_0, y_1(x_1), y_2(x_1, x_2), \dots$.

After n observations, a cognitive node can choose to stop sensing to collect corresponding rewards, or continue probing until it reaches its goal. The goal is to choose a time for stopping such that the reward is maximized. In OFDM radios, this decision is constrained by the maximum fragments number (the spectrum holes) that can be merged, and also by the limited width of the aggregated band. If there is a maximum number of channels that a radio can sense before taking the stopping decision, the stopping problem has a finite horizon. The finite horizon stopping problem can be optimally solved by the method of backward induction [77]. This solution has, however, an exponential complexity and it is thus necessary to reduce computational cost to a reasonable level, especially for large numbers of fragments. HC-MAC authors propose a truncated version of the optimal rule named $k - stage\ look - ahead$. This suboptimal algorithm computes, at stage n , the expected reward for sensing during $n + k$ stages. Hence, it decides whether to stop or to continue probing, comparing the reward function value with throughput constraints.

Kim and Shin investigated the optimization of the sensing period to maximize the discovery of spectral opportunities while minimizing sensing overhead [78]. The authors have considered a single hop cognitive wireless network coexisting with a primary network. Each opportunistic user

is assumed to be equipped with a single antenna, which can be tuned to any combination of N consecutive licensed channels. Hence, transmission and sensing cannot be performed at the same time, and communications have to be periodically interrupted. Channel sensing is performed during QPs in which nodes cooperatively participate in sensing to enhance primary users detection. Channel usage is modeled as an ON-OFF source; when a cognitive node discovers an OFF period the available channel is merged into a set with capacity equal to the sum of all available found channels. Then, nodes within the opportunistic network contend the exclusive access to the logic channel. Hence, the problem of finding the optimal sensing period for the N channels that minimize the Unexplored OPPortunities (UOPP) and the SenSing OverHead (SSOH) can be expressed as

$$\underline{Tp}^* = \arg \min_{Tp} \left[\sum_{c=1}^N (SSOH^c(Tp^c) + UOPP^c(Tp^c)) \right] \quad (2.4)$$

where \underline{Tp}^* is the vector of optimal sensing periods. $UOPP^c(Tp^c)$ is defined as the average fraction of time during which channel c 's opportunities are not discovered because c is sensed with a sensing period Tp^c . Moreover, $SSOH^c(Tp^c)$ is defined as the average fraction of time in which channel c 's discovered opportunities are not exploited due to the QP.

In the Decentralized Cognitive MAC (DC-MAC) [70, 79], authors propose a channel sensing/access policy which considers the partial knowledge of licensed channels state at secondary users. Furthermore, this strategy handles spectrum sensing errors limiting interference to primary network. The proposed DC-MAC exploits the theory of *partially observable Markov decision process* where traffic characteristics of the primary users is represented as a Markov chain. Considering a band composed by N channels, the network can assume one of $M = 2^N$ state (Figure 2.18 shows a network state diagram for $N=2$). At the beginning of each slot, cognitive users, exploiting

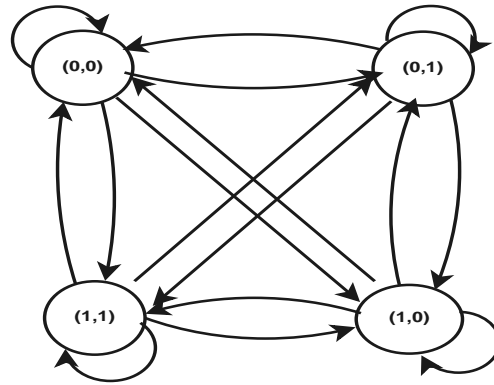


Figure 2.18: The Markov model representing a network state transition $\{0$ (idle), 1 (occupied) $\}$.

their knowledge of the network state, select the set of channels to sense to maximize the global reward collected in T slots, while limiting the primary user miss-detection probability. The optimal strategy represents past decisions and observations with the *belief* vector $\mathbf{\Lambda}(t) = [\lambda_1(t), \dots, \lambda_M(t)]$. $\lambda_j(t)$ is the conditional probability that the network state is j at the beginning of slot t , prior to the state transition. Action chosen at each slot affects the reward function in two ways: it gives an immediate reward (the access to selected channels), furthermore, it permits to update the belief vector according the observed state of the network. The optimal strategy defines a balance between gaining immediate rewards and achieve information to improve future behaviour. This strategy may, however, hardly be implemented because the dimension of the statistic $\mathbf{\Lambda}(t)$ grows exponentially. Hence, the authors propose a sufficient statistic $\mathbf{\Omega} = [\omega_1, \dots, \omega_N]$ whose dimension

grows linearly with N . This statistic can be exploited only when the N channels evolve independently. The element $\omega_c \in \Omega$ is the probability (conditioned to the sensing and access history) that channel c is idle at the beginning of a slot. Moreover, a suboptimal greedy approach that maximizes the expected reward per slot is presented.

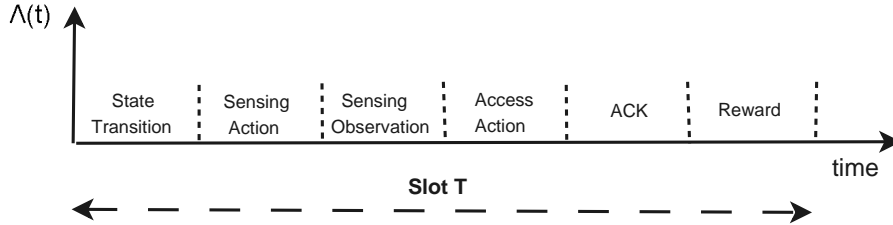


Figure 2.19: The DC-MAC sequence of operations [70, 79].

Hence, the proposed DC-MAC operations are represented in Figure 2.19 and can be resumed as follows:

- At the beginning of each slot, transmitter and receiver select the channel a to sense according to the belief vector Ω . The two users exploit the same belief vector, this ensures that they tune to the same channel.
- If the sensed channel is available, the transmitter generated a random back-off time. To limit collisions with incumbent primary/secondary users, the sender continues to monitor the channel c during this period. If c remains idle, the transmitter starts a RTS/CTS handshake to verify if the sensed channel c is also available at the receiver side.
- The transmitter sends data over channel c . If the data are successfully received the receiver transmits an acknowledgement message. Finally, both the sender and the receiver update their belief vector.

DC-MAC is one of the few opportunistic MAC protocols that include sensing errors in its design, however, its implementation is limited by the assumption that the transition probability in the Markov channel model are known. In practice, this may not be available.

Cooperative detection

Licensed users detection effectiveness is compromised by noise uncertainty, lack of information about the primary receiver location, fading, and shadowing effects. The MAC layer optimizes the sensing strategy by dealing with these limitations and by taking into account possible sensing errors. Collaborative sensing allows different secondary users to share their sensing outcome. This strategy exploits inherent multiuser spatial diversity to improve detection, and decrease missing and false alarm probabilities [80]. Increased performance comes at the expense of increased latency and communication overhead. Cooperation can also solve the hidden terminal problem as well as reduce sensing observation time and bandwidth [81]. Furthermore, it also permits to decrease the effects of malicious sensing nodes [82].

In C-MAC [53] collaborative detection is implemented through beacons transmitted among network channels. C-MAC is a Split Phase distributed DAB protocol. It assumes that each cognitive user is equipped with a half duplex radio and that each channel is organized in superframe. The superframe is composed of two consecutive parts: Beacon Period (BP) and Data Transfer Period (DTP). In-band and out-of band sensing are performed during the QP of the corresponding

channel. Primary users detection is notified through the beacon frame transmitted in each superframe. To allow cognitive users to decode the sensing output message even in presence of the primary user interference, the beacon frame is transmitted using the most robust Modulation and Coding Scheme (MCS). Synchronization within the cognitive network allows different users to broadcast beacons without overlapping across all the available channels. During BPs secondary users switch among the network channels by listening beacon frames and acquiring information about channels state. Moreover, cognitive nodes periodically visit a common channel, named Rendezvous Channel (RC), to gather information about primary and secondary users discovery and get resynchronized. Collected data are processed to realize a more reliable picture of spectrum usage.

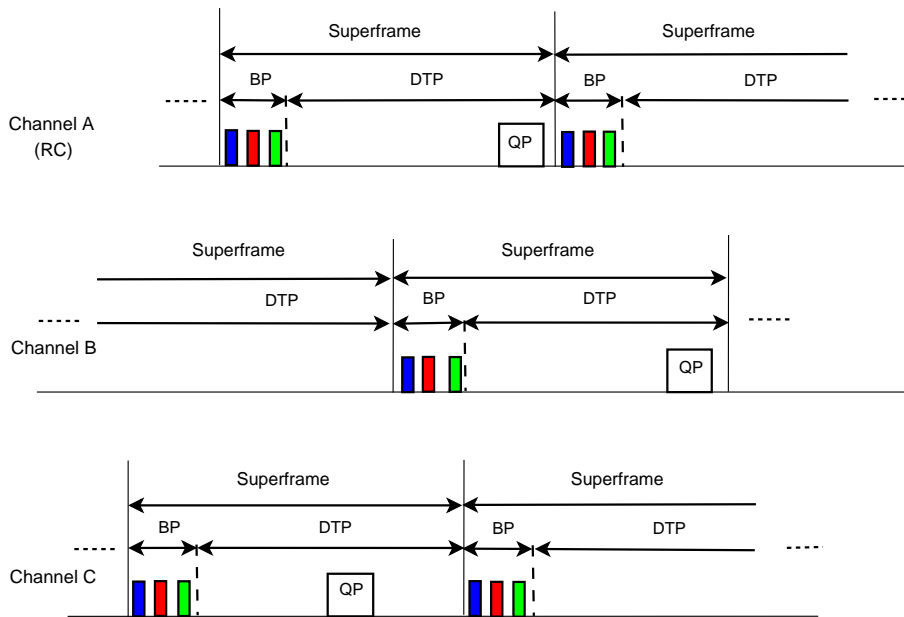


Figure 2.20: Channel superframe structure in C-MAC [53].

Timmers *et al.* have proposed a MAC protocol for CR ad-hoc networks [58]. The Multichannel MAC protocol (MMAC-CR) is a Split Phase protocol which takes advantages of a two stage sensing (fast/fine sensing) mechanism and a cooperative detection scheme. A dedicated control channel is used to perform network synchronization and common information exchange. In this protocol, time is divided into two phase: the Ad-hoc Traffic Indication Message (ATIM) window and the DATA window. During the first phase the following operations are performed:

- IEEE 802.11 timer synchronization function [83] is run to permit tight synchronization within the network;
- CRs perform fast sensing;
- neighbour users share sensing outputs and update their local view of spectrum opportunities;
- medium access coordination is performed via a two way handshake.

During the second phase CRs

- exchange their data;

- perform fine sensing;
- enter in a doze state if they have not to data to exchange or channels to sense.

Communicating and sensing on different channels can be performed in parallel (i.e., one radio is dedicated to sense the spectrum medium), which significantly reduces the impact of sensing. When a user joins the network, it performs a fast scan on each channel and constructs the Spectral Image of Primary users (SIP) vector. $SIP[c]$ represents the spectrum usage estimation of the channel c :

- When no primary users are active on channel c , $SIP[c]$ is set to 0;
- When a primary user is active on channel c , $SIP[c]$ is set to 1;
- When the presence of primary users is uncertain $SIP[c]$ is set to 2;

When the SIP of a channel is not 0, it will be excluded from the list of channels available for data transmission. Moreover, if the presence of PU on the channel is uncertain, a fine sensing will be performed on that channel during the DATA window. SIP values are periodically updated during the ATIM window through fast sensing. Primary user presence is estimated by implementing the OR fusion rule. Cooperative detection is performed during a mini-frame in the ATIM window. This frame is divided into C slots, one for each licensed channel. Cooperating nodes transmit a busy tone in the corresponding slot for every channel their SIP is not 0. If a slot is sensed as busy, then the corresponding channel is excluded for CR communication.

Synchronization within cooperating users is achieved through the *scan result packet*, which indicates the beginning of the mini-frame. During the ATIM window, after the sensing process, each node tries to send an scan result packet frame to initiate cooperative detection. The access on the common control channel to transmit scan result packet packets is managed with the IEEE 802.11 Distributed Coordination Function (DCF) [84]. Although MMAC-CR has the advantage to be energy efficient, it requires tight synchronism within the CR network. Moreover, MMAC-CR reliability strongly depends on the control channel quality.

Su and Zhang have proposed two novel sensing policies to improve the cognitive network awareness of the spectrum usage [50]. In the investigated coordination-based cognitive DAB protocol each secondary user is equipped with two transceivers. The control transceiver, is used to exchange sensing information and contend the available channel on the dedicated control channel. The software-defined radio transceiver is exploited to sense and transmit/receive data on the licensed channels. The control channel and licensed channels are time-slotted and synchronized. Furthermore, each licensed channel is modelled as an ON-OFF source and its state is characterized by a two state Markov-chain.

Time slots in the control channel are divided into two phases: a *reporting phase* and a *negotiating phase*. Reporting phase is still divided into n mini-slot, each one corresponding to one of the licensed channels. This phase permits secondary users to share their sensing outputs. Negotiating phase permits cognitive users to contend the access to the overall set of available channels in the next time slot. The proposed scheme is illustrated in Figure 2.21. According to the *random sensing policy*, at the beginning of each time slot, secondary users randomly sense one of the licensed channel. If the sensed channel is idle, the cognitive user transmits a beacon in the corresponding mini-slot within the reporting phase. Basically, the reporting phase, is a physical implementation of the AND rule. Clearly, the higher the secondary users number, the higher the number of the sensed channels. The basic idea of the *negotiating sensing policy* is to let secondary users know which channel have been sensed by their neighbors, and then select different channels to sense in the next slot. During the negotiating phase, cognitive users include the information about the

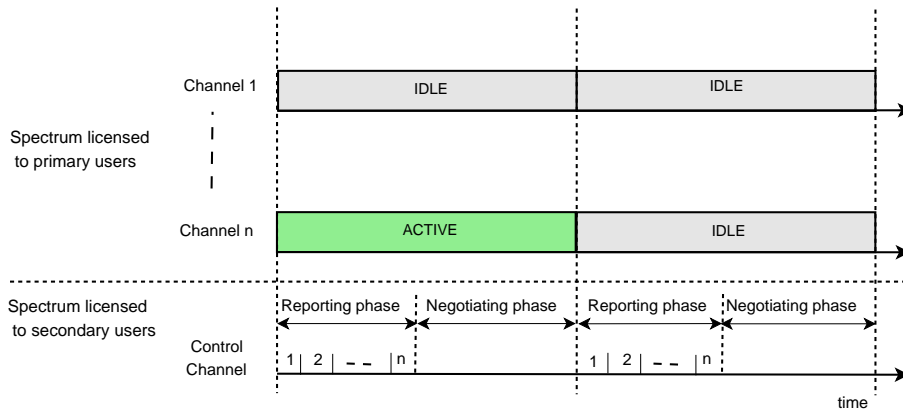


Figure 2.21: Reporting and negotiation phases in the work proposed by Su and Zhang [50].

channels they sensed in the negotiating (RTS/CTS) messages. When a cognitive user discovers that it sensed the same channel of one of its neighbors, it selects a different channel to sense for the next time slot. The new channel is randomly picked from the set of channels for which the user has not received any beacon during the reporting phase. This set is made up by the channels that have been sensed busy and the channels that have not been sensed. Eventually, using the proposed negotiating sensing policy the number of sensed channels monotonically increases with time. It should be noted, however, that the implemented AND rule could be too aggressive with respect to the primary user. For instance, a more conservative approach has been proposed by Timmers *et al.* [58].

Exploiting location awareness to improve spectrum sensing

Chowdhury and Akyildiz have proposed a novel approach to perform spectrum sensing in a cluster-based mesh architecture [60]. The proposed scheme permits to identify primary users' frequencies without any change to the IEEE 802.11 standard for Wireless Mesh Networks. In the investigated architecture, a number of Mesh Routers (MRs) serve as APs for a community of Mesh Clients (MCs), which exchange data over the Internet. The APs form the backbone of the network and they forward traffic over the backbone, in a multi-hop manner, towards an Internet gateway. Both MRs and MCs are equipped with a single IEEE 802.11b transceiver, which can be tuned on both the ISM and licensed TV bands. In each cluster, MCs periodically piggyback sensing results over the data transmission to the cluster AP. The MR combines received information, and forwards it to the internet gateway where it is stored in a centralized database. Then, this data is regularly included by the gateway in the downlink stream and exploited at each cluster to optimize the MAC layer. Authors propose a sensing scheme that enables MCs to monitor licensed channels while avoiding MCs miss data packets transmitted on the ISM band. The proposed algorithm requires MCs to estimate their distance from primary BS, when necessary. A cognitive node is allowed to perform spectrum sensing only when its operating channel is busy but the node is not the intended receiver. Whenever a MC hears a message over the cluster channel, it decodes the MAC layer header in the received message; if the node is not the packet intended receiver, it can hop to a licensed channel and perform spectrum sensing. All the *free* MCs within a cluster tune to the same licensed channel and evaluate the received energy. This energy is due to the superposition of signals emitted by different TV transmitters. These transmissions may lay on different carriers, and only a part of their power overlaps on the channel in which sensing is performed. Hence, MCs forward energy measurements and the estimated distances between each MC and primary receivers to the MR.

Then, the MR estimates the carriers in which there are active transmissions exploiting the received information, the knowledge of the entire set of carriers available to the primary users, and the spectral overlap factor between licensed channels. Furthermore, authors propose a decentralized version of the proposed sensing scheme to equally share the computational cost among nodes within a cluster.

Wang and Chen have proposed a novel approach to improve coexistence between an infrastructure-based primary network and a cognitive ad-hoc network [85]. The presented scheme can drastically reduce the need to perform spectrum sensing. Authors consider a scenario in which both primary and secondary users stay fixed or hardly move. Therefore, an opportunistic node that has location information about neighbour primary and secondary users can identify the coexistence region (R_{CT}) in which primary and secondary nodes can perform concurrent data exchange on the same frequency channels. R_{CT} can be computed as the area in which contemporary primary and secondary users transmissions are not in outage. To estimate this region, when a new node joins the ad-hoc network it should perform positioning and geographical routing to acquire its position and learn the position of its neighbours.

Therefore, authors believe that additional energy consumption and memory space due to the position and location update could be relatively small. However they have not provided comparison between the proposal and the classical sensing techniques neither in terms of energy consumption nor in terms of computationally costs. Nevertheless, classic spectrum sensing is still necessary when a secondary sender receiver pair is outside the concurrent transmission region R_{CT} .

2.3.3 Dynamic Spectrum Allocation

In traditional static spectrum assignment policies, the radio spectrum is divided into separate bands of fixed width, identified by their range of frequencies. A band is allocated to a licensee having the exclusiveness of using this resource. Quality constraints can be guaranteed because interference between heterogeneous systems is avoided. In a cognitive network, based on the sensing outcome, a resource allocation function assigns available channels to the contending users by attempting to maximize a utility function. Bandwidth and channel availability time-space dependency introduces, thus, new challenges with respect to classic wireless technologies.

Spectrum allocation in DAB algorithms

In DAB protocols, each sender-receiver pair selects channels to access according to personal constraints without considering network optimization.

COMAC [63] is a contention based protocol that tries to satisfy QoS constraints by limiting the number of used channels per user. Authors have considered a scenario in which an ad-hoc cognitive network coexists with M primary networks. Each opportunistic user A maintains a list of its locally available channels \mathcal{L}_A , which is the set of channels that are not currently used by any of A 's CR neighbours. \mathcal{L} is continuously updated through the overheard of control packets. When an opportunistic pair wants to initiate a communication, the sender and the receiver exchange their \mathcal{L} s over the network control channel, and then the receiver selects channels where to communicate. Three parameters impact channel selection:

1. Spectrum state information;
2. Maximum allowable transmission power for channel;
3. Requested data rate.

According to these parameters, when the receiver B receives the sender A 's RTS packet:

- It compares the set of its available channel \mathcal{L}_B with the sender's list \mathcal{L}_A . Then it computes $\hat{\mathcal{L}} \doteq \mathcal{L}_A \cap \mathcal{L}_B$;
- The channels within $\hat{\mathcal{L}}$ whose received SINR is below a fixed threshold are removed from the list;
- Then the receiver sort the rest of available channels in descending order of their data rate;
- Selected channels are chosen from the sorted list until the the requested data rate is satisfied or the list is exhausted;
- If the data rate condition is satisfied the receiver transmits to the sender a CTS message including the list of the selected channels. Otherwise, B will not respond to A 's RTS and the sender will reschedule its transmission.

The Heterogeneous Distributed MAC (HD-MAC) proposes a channel selection metric that jointly considers traffic load, connectivity, and interference [57]. HD-MAC is a modified version of the IEEE 802.11 MAC protocol proposed by So and Vaidya [40] that enables distributed coordination of local clusters in a multi-hop CR network. In HD-MAC neighbouring secondary users self organize in local group where coordination is handled through a local common channel. The MAC structure is organized in super-frames consisting in a BP, a coordination window (CHWIN), and DATA period . During the CHWIN period users hop to the coordination channel to manage channels contention. Access during the CHWIN is realized according to the carrier sense multiple access with collision avoidance protocol. A general node i , maintains a score $u_i(c)$ for each channel c , defined as follows:

$$u_i(c) = \lambda_{in}Q_{in}(c) + \lambda_{out}Q_{out}(c) - \lambda_fQ_f(c) \quad (2.5)$$

where,

- Q_{in} represents the estimation of incoming traffic load on channel c ,
- Q_{out} represents the estimation of outgoing traffic load on channel c ,
- Q_f represents the estimation of traffic load that may interfere with neighbour's transmissions using channel c ,
- λ_{in} , λ_{out} and λ_f represent the weight of each traffic type.

Q_{out} is updated at the beginning of CHWIN period based on the currently outgoing queue of node i , on the contrary, Q_{in} and Q_f are estimated based on neighbour queues. In HD-MAC, each node includes its queue status in coordination messages. Channel negotiation is realized through CFSR handshake. When sender i transmits a channel request to receiver j , it includes its queue size related to j and a channel information message $\theta_i = \{c, u_i(c)\}_{c \in \mathcal{L}_i}$ related to its available channel list \mathcal{L}_i . The receiver chooses the common channel that maximizes $\min\{u_i(c), u_j(c)\}$, and transmits to the sender a channel respond message that includes its selection and the volume of pending packets. If there is no feasible channel, the receiver sends a message of transmission failure. Upon receiving the channel respond message, i sends a channel confirmation message to j . This message confirms the selected data channel and includes the length of the pending packets. Neighbour nodes that overhear the channel confirmation and channel respond messages obtain traffic information and update the channel score accordingly. Eventually, sender and receiver mark the selected channel as "outstanding". They will tune on this channel for all the DATA period,

hence, their subsequent negotiations during the current CHWIN are based on the outstanding channel only.

In the MMAC-CR [58], channel selection is performed to minimize the expected interference. As explained in Section 2.3.2, after the transmission of the scan result packet over the control channel, secondary users are aware of primary users activity on the observed band. The MAC frame is divided into two period: the ATIM window and the DATA window. During the ATIM window cognitive users that have buffered data perform a three-way handshake to realize data channel selection and inform neighbours about their traffic load. This handshake starts when the transmitter sends an ATIM packet on the control channel. Such a packet contains the selected channel and queue status of the transmitter. If the receiver agrees on the selected channel, it responds with a ATIM-ACK and then it waits for the beginning of the DATA window. Finally, the sender confirms the channel selection broadcasting an ATIM-RES frame on the control channel. Hence, cognitive users that overhear ATIM packets estimate the opportunistic traffic load on each channel and stocks this value in the secondary users channel load vector. When a user wants to start a communication, it selects the channel with the lowest secondary users channel load value.

Spectrum allocation in DSA algorithms

In DSA protocols, the utility function is often made up of two components: a reward and a price. The reward describes the gain achieved by a certain node when choosing a particular channel, the price represents the cost that this choice implies for the overall network.

For instance, GMAC [68] is a game theoretic DSA protocol that exploits a function to maximize overall network throughput by limiting transmission power. Nash Equilibrium (NE) is achieved through a distributed recursive game.

Zheng and Peng have proposed different centralized and distributed strategies that optimize system throughput and fairness while minimizing interference [66]. Frequency assignment is based on a graph coloring algorithm and the cognitive network is represented as a NCG (see section 2.3.1). Authors have considered a graph $G = (\mathcal{V}, \mathcal{E}, \mathcal{L})$ where \mathcal{V} is the set of users sharing the spectrum, \mathcal{L} represents the channel availability list at each vertex, and \mathcal{E} the edges set modelling the interference constraints. For instance, given $i, j \in \mathcal{V}$, if i, j interfere when using simultaneously a channel c , c is an element of \mathcal{E} , and an edge labelled c is present between i, j . Figure 2.22 illustrates an example of a graph obtained according to this representation. In the proposed schemes channels assignment follows the order of the nodes that mostly contribute to maximize system utility.

DH [67] is a DFH scheme that proposes a distributed algorithm to generate a hopping pattern that minimizes the number of used frequencies. Maximizing the number of used channels for a transmission would reduce the interference to primary users. However, this may lead to channel overassignment and the system would not be able to guarantee QoS to secondary users. In DH, frequency assignment is again based on a graph coloring algorithm. Authors have investigated a scenario in which several CR cells contend the access to spectrum medium. Each cell consist of a BS and a number of associated terminals. The network is represented by an interference topology graph $G = (\mathcal{V}, \mathcal{E})$. The elements of the set $\mathcal{V} = \{v_1, \dots, v_n\}$ are the cognitive cells and \mathcal{E} is the set of interference relationships between network cells. Additionally, the set of the neighbouring cells \mathcal{V}_i^* is defined for each cognitive node i .

To generate hopping patterns, authors have modelled the problem as an *integer linear program* and they have presented a centralized optimal frequency assignment algorithm that minimizes the number of used channels. Furthermore, they have proposed a distributed sub-optimal approach named as *distributed frequency assignment*, which is based on the *distributed largest first* [86] strategy. Accordingly, the order in which nodes choose channels depends on their interfering

degree: a cognitive user does not choose its channel until it receives the decision of its neighbours with higher degree. Although the optimal scheme slightly outperforms the sub-optimal approach in terms of used channels, the computational complexity of the distributed scheme is lower and it also requires a constant signalling overhead, which results in a better scalability.

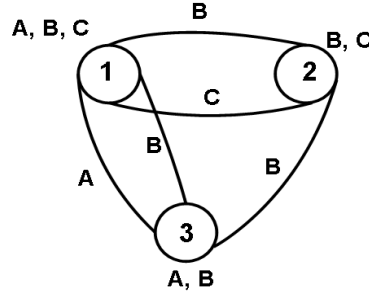


Figure 2.22: A NCG representation of channel availability and interference constraints [66].

Atakan and Akan have proposed a distributed approach to manage channel allocation in cognitive radio network [72]. The BIOlogically-inspired Spectrum Sharing (BIOSS) algorithm is based on the adaptive task allocation model of an insect colony. In this model, each element performs its task when the associated stimuli exceeds a fixed threshold. In the proposed algorithm, the stimuli associated to each channel is the maximum allowable transmission power. Instead, the response threshold is the required transmission power to achieve QoS constraints. Hence, the probability $P_r(i, c)$ that a cognitive user i access to the channel c is:

$$P_r(i, c) = \frac{P_{max,c}^n}{P_{max,c}^n + \alpha P_{i,c}^n + \beta L_{i,c}^n} \quad (2.6)$$

where

- $P_{max,c}$ is the maximum permissible power on channel c ;
- $P_{i,c}$ is the power that meets users requirements;
- $n \geq 1$ represents the steepness of the channel selection probability;
- $L_{i,c}$ is a learning factor which influences the access probabilities according to the perceived performance history;
- α and β are positive constants;

The learning factor is updated according to the performance experienced by cognitive users:

$$L_{i,c} = \begin{cases} L_{i,c} - \xi_0 & c \text{ does not satisfy QoS constraints} \\ L_{i,c} + \xi_1 & \text{elsewhere} \end{cases} \quad (2.7)$$

where ξ_1 and ξ_0 are the forgetting and the learning coefficients, respectively. Hence, the BIOSS algorithm works as follow:

1. each unlicensed user detects the set of available channels;
2. it estimates the maximum allowable power in each channel;

3. it initializes the learning factor, the forgetting and learning coefficients;
4. cognitive user computes the access probability for each available channels;
5. according to its QoS constraints the secondary user selects the set of channels with the highest channel selection probability;
6. finally, the learning factor is updated according to (2.7).

The access probability increases with the positive difference between the maximum estimated allowable power $P_{max,c}$ and the minimum required power $P_{i,c}$. The major drawback of the proposed scheme is that users with either tight or weak transmission constraints ($P_{i,c}$) both prefer channels with larger permissible power. On the contrary, the overall spectrum efficiency could be increased if users with weaker power constraints would select available channels with smaller permissible power.

Nainay *et al.* have proposed a genetic algorithm to solve a distributed channel allocation/power control problem for an ad-hoc CR network [65]. This study extends a previous work where an island genetic algorithm is used to deal with the channel allocation problem [87]. Moreover, although the latter algorithm exploits a global knowledge about the network state, the former presents a localized version of this algorithm, which reduces the signalization overhead.

The proposed CR network model consists of a set of nodes \mathcal{N} , and each node $i \in \mathcal{N}$ is able to simultaneously transmit and receive on different channels. Authors define \mathcal{E}_i^C as the set of outgoing communication links originating from i and any node within its range of interference. Then, given a link $e_{j,k} \in \mathcal{E}_i^C$, $\mathcal{H}_{j,k}^i$ and $Q_{j,k}^i$ are the set of the available channels and the set of the available power levels for the link $e_{j,k}$, respectively. Finally, $\mathbf{h}\mathbf{q}_i$ is the channel-power level assignment vector, where $\mathbf{h}\mathbf{q}_i \in (\mathcal{H}_{j,k}^i \times Q_{j,k}^i)$. Hence, each user i try to optimize the fitness function

$$\max_{\mathbf{h}\mathbf{q}_i \in (\mathcal{H}_{j,k}^i \times Q_{j,k}^i)} \left[f(\mathbf{h}\mathbf{q}_i) = \sum_{e_{j,k} \in \mathcal{E}_i^C} \left(\frac{W_{j,k} \cdot P_{j,k}}{1 + |\mathcal{E}_{j,k}^{\mathbf{h}\mathbf{q}_i}|} \right) \right], \quad (2.8)$$

where $W_{j,k}$ and $P_{j,k}$ are the bandwidth and the power assigned to the link $e_{j,k}$, respectively. $|\mathcal{E}_{j,k}^{\mathbf{h}\mathbf{q}_i}|$ is the cardinality of the set of links that belong to \mathcal{E}_i^C and can not be active at the same time as link $\mathcal{E}_{j,k}$ under the assignment $\mathbf{h}\mathbf{q}_i$. To find the solution of Eq. (2.8) a genetic algorithm is implemented. Each node generates its initial population, consisting of M individuals. Each element of the population randomly allocates a channel-power level $\mathbf{h}\mathbf{q}_i$ to each link $e_{j,k} \in \mathcal{E}_i^C$. Hence, Eq. (2.8) is computed for each individual then, based on a parameters called as *keep rate*, the worst $[(1-\text{keep rate}) \cdot M]$ elements are eliminated and the remaining $(\text{keep rate} \cdot M)$ elements are selected to perform crossover and to generate new individuals. To perform crossover, first a triplet of parents is randomly selected, then the couple of parents with higher values exchanges part of their set $\mathbf{h}\mathbf{q}_i$. The crossover process is illustrated in Figure 2.23. Hence mutation is performed: according to the *mutation rate*, each element of the population, excluding the one with the best fitness, replaces part of values in $\mathbf{h}\mathbf{q}_i$ with randomly selected couple of channel-power levels. Furthermore, after a fixed number of iterations (*the migration interval*) each node share $\mathbf{h}\mathbf{q}_i$ values of its best individual with all the nodes within its interfering range. If the received information gives better fitness, it is included in all individuals of the node, otherwise the node merges the received data with only a part of its population. Finally, the implementation of the algorithm stops after a fixed number of iterations. The proposed localized island genetic algorithm reduces the signalling overhead and computation cost in each node, hence it is more scalable; it needs, however, a larger number of iterations to converge.

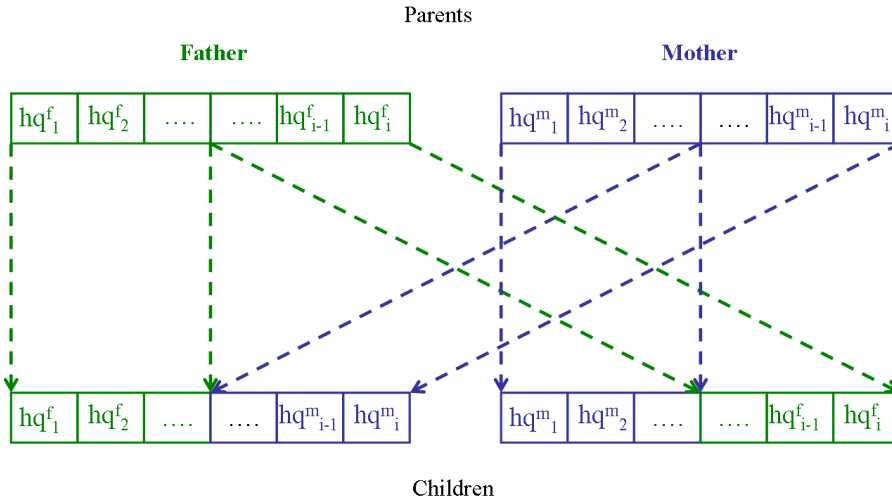


Figure 2.23: One point crossover operation in [65].

Chowdhury and Akyildiz have investigated opportunistic spectrum access in a cluster-based mesh architecture [60]. The proposed COgnitive Mesh NETwork (COMNET) framework allows nodes within a cluster to shift working into the licensed TV bands. The goal is to equally distribute the cognitive network load between licensed and the unlicensed bands while limiting the generated interference. Each cluster is managed by a MR, which acts as an AP for MCs of its cluster. The region in which the mesh network operates is represented as a grid. MRs share information about the mesh network state (number of clients and positions of their APs) and the output of sensing stage (occupied licensed channels) to estimate the interference generated by the mesh network at the center of the grid blocks. Hence, each MR autonomously selects the set of clusters that are allowed to shift into the free part of the licensed band and finds operating frequencies. All MRs have the same constraints and inputs, hence, they independently arrive at the same solution. This optimization problem is modelled as an integer linear program where selection is made in such a way as the total interferences in the licensed band is limited. Furthermore, the mesh load is equally divided into the ISM and the licensed bands.

2.3.4 Dynamic Spectrum Sharing

The MAC spectrum sharing functionalities face the problem of coexistence between heterogeneous users accessing the radio resource. Typically, primary users are licensee owners of the spectrum resource and opportunistic users should not interfere with their transmissions. Goldsmith *et al.* have investigated three different cognitive transmission access paradigms: underlay, overlay and interweave [88]. In underlay transmissions, secondary users are allowed to operate while generated interference stays below a given threshold. Due to the associated interference constraints, the underlay technique is mainly useful in short range communications [89]. In 2003 the federal communications commission defined the *interference temperature* [90] as a way to measure and limit the interference perceived at primary users. However, implementation of this model results in poor performance compared to the amount of generated interference it can cause to primary users. Hence, this model has been abandoned by the federal communications commission in 2007 [91]. In overlay transmissions, cognitive users exploit the knowledge of non cognitive user messages to either cancel or mitigate interference at both primary and secondary users side. In interweave

transmissions, opportunistic radios transmit only in spectrum holes; if during in-band sensing a secondary user detects a licensed one, it vacates its channel to avoid harmful interference.

Contentions between secondary nodes can be avoided through coordinated access both in centralized (see, for instance IEEE 802.22 [92, 61]) and distributed architectures [53]. When coordination is absent, a random approach could be exploited to contend for access to available channels [55, 79]. Otherwise, opportunistic users may exchange signalling messages to reserve the access to a data channel [50, 63]. The control handshaking mechanism, however, does not completely solve the hidden terminal problem, hence the busy tone scheme is often exploited to prevent hidden nodes [55, 69].

Interweave Spectrum Access

Due to the lack of information on primary receivers, nowadays most of CR protocols are developed according to the interweave transmission paradigm. Secondary users avoid contention with incumbent primary nodes by performing periodically sensing on the occupied channels. If an incumbent is detected, the channel is vacated, transmission is interrupted, and a communication link is set up on a different channel.

In IEEE 802.22 [92] self coexistence of neighbour WRAN cells is realized with the *coexistence beacon protocol*: at the end of each MAC frame, during a self-coexistence window, BSs transmit a beacon that permits communication and synchronization within a community of cells. The BSs receiving this beacon can schedule their transmissions in non-overlapping slots and avoid interference.

In the DFH proposition for IEEE 802.22 [61] the coordination of a DFH Community is realized by transmitting a broadcast announcement message on a communication management channel. This message contains information about the state of the BSs, a list of neighbours, hopping channel list, and priorities. Each community leader periodically exploits the received information to update the community channel hopping pattern. Then, the leader broadcasts the new pattern to its community members. A DFH community can be rearranged by a leader to:

- reduce the number of used channels,
- reduce interference between neighbour communities,
- reduce communication overhead within a community.

In particular, a leader can:

1. permit to a community member to shift from one community to the others;
2. split its community and select two new leaders;
3. merge two communities in a new one.

Coexistence between neighbour communities is dealt through the broadcast announcement messages that are exploited to mark used channels as occupied and avoid contentions.

In C-MAC [53], each terminal is requested to periodically broadcast a beacon during its BP. Each node receiving this beacon retransmits the embedded data by adding its own information about channel occupancy and the state of the network. In such a way, users can coordinate the access and exploit information about the neighbours of their neighbours. This strategy overcomes the multiple channel hidden terminal problem, however, it increases network overhead, which affects C-MAC scalability.

Another approach is proposed in the Dynamic Open Spectrum Sharing (DOSS) [55], which is a direct contention based DAB protocol. A data band, a control channel, and a busy tone band are exploited to manage communication, signalling, and contention, respectively. Spectrum negotiation is managed with a RTS/CTS handshake. A mapping rule is proposed to match the narrow band busy tones and the wide band data channels. Overhearing the busy tones, each node is aware of its neighbours communications and hidden/exposed terminal problems are avoided. DOSS effectiveness is impaired by the need for multiple transceivers and two separate bands to manage busy tones and common information exchange. Moreover, by increasing the allocated bandwidth, the probability that a primary user may be interfered increases: for instance, a data channel could be idle while its corresponding busy tone channel is unavailable.

Most DSA MAC protocols suffer from scalability issues. In large CR networks, it is necessary to limit the number of cooperating users to minimize overhead and delay of the optimization process. In the game theoretic DSA-driven framework [69], the authors have proposed a clustering algorithm to overcome these issues and to achieve coordination among the game players. Moreover, they have introduced a collision avoidance mechanism to protect the negotiation reliability from inter-cluster interference. Hence, four are the main components in this protocol:

1. the game;
2. the clustering algorithm;
3. the collision avoidance algorithm;
4. the negotiation mechanism.

Interactions among cognitive nodes are modelled as a repeated game $\Gamma = \langle \mathcal{N}, \{S_i\}, \{u_i\}, T_d \rangle$. \mathcal{N} is the set of game players, where a game player represents the sender-receiver pair; S_i represents the strategy space (transmission parameters) of player i ; u_i is the local utility function that player i wants to maximize; T_d is the players decision time indicating the time at which each radio can update its strategy. This clustering algorithm is geographical-position based. Each cluster is represented by a hexagon and identified by a cluster ID that depends upon the hexagon center coordinates. Arrivals and departures are handled with a *virtual header* mechanism. In this approach, the header of a cluster is not a node but a cluster-unique packet, which is named virtual header. After a CR node chooses its cluster, it broadcasts its cluster ID and coordinates. Hence, each node obtains all the information about its neighbours. The proposed clustering algorithm is scalable, distributed, and independent of the used DSA strategy. Collision avoidance mechanism is cluster-based and it exploits two busy tones to avoid interference and overcome exposed and hidden terminal problems:

1. *inside-cluster busy tone* (BT_i) is transmitted by the node that receives a message to prevent nodes outside its cluster to interfere.
2. *outside-cluster busy tone* (BT_o) is forwarded by the node that overhears the inside cluster busy tone to indicate that it is interfered by nodes belonging to a neighbour cluster. In such a way, the overhearing node prevents nodes within its cluster to communicate with it.

Figure 2.24 and 2.25 represent the BT_i/BT_o collision avoidance mechanism.

Negotiation mechanism manages the control messages exchange and permit node synchronization during the game. This process is divided into two successive stages: the inquiry stage and the formal negotiation stage. In the first stage, each node within a cluster is queried of its intention to communicate by a token packet generated by the virtual header. At the end of the inquiry stage,

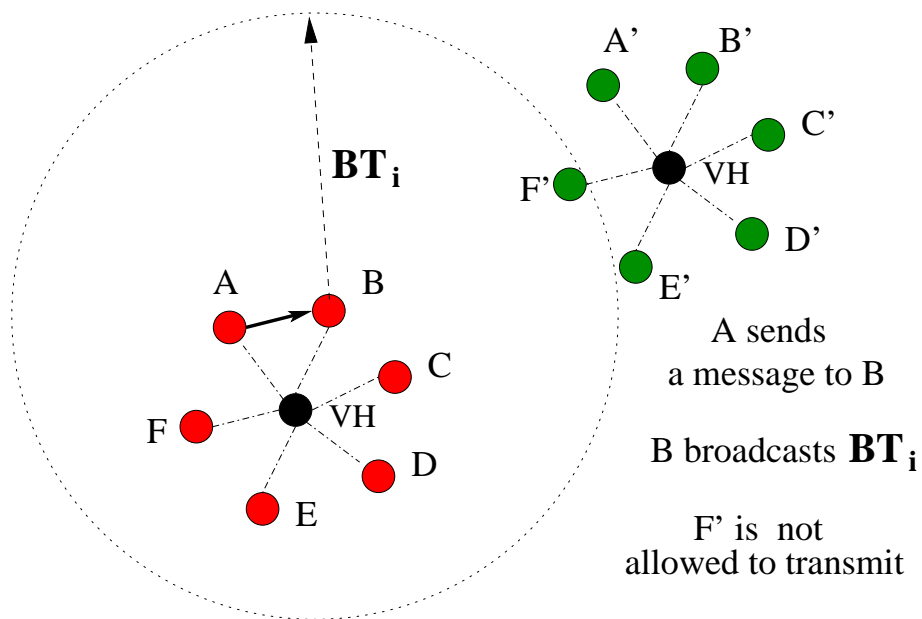


Figure 2.24: The BT_i collision avoidance mechanism according to the game theoretic DSA-driven protocol [69].

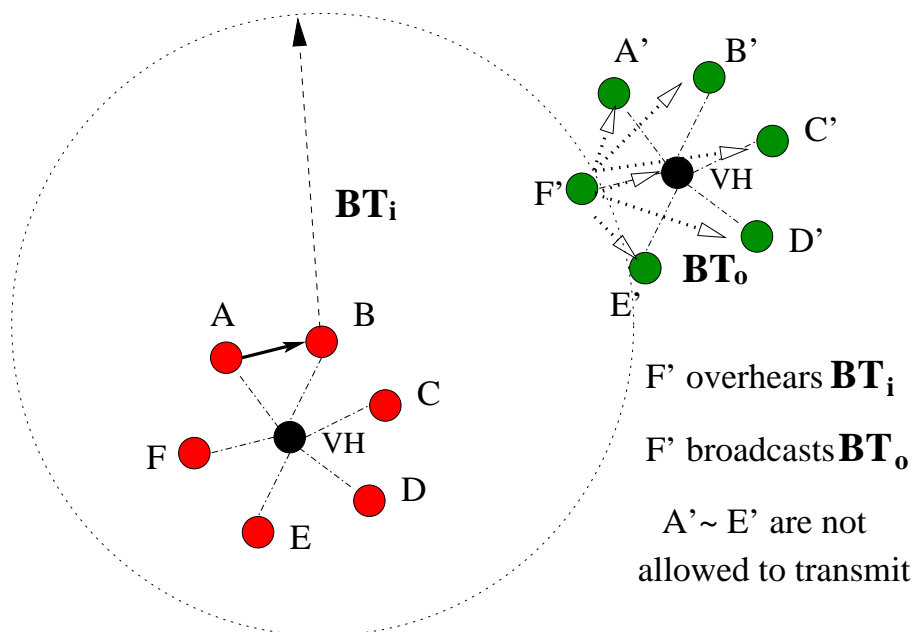


Figure 2.25: The BT_0 collision avoidance mechanism according to the game theoretic DSA-driven protocol [69].

the information collected by the token is exploited by game players to construct the game set and the strategy space. The advantages of a token based strategy is that it minimizes inter-cluster interference, and avoids intra-cluster interference during the negotiation process. Hence, during the formal negotiation stage, a negotiation token, which carries the dynamic game information is passed around the game players to update their local strategy. The process continues until the game converges to a NE.

Su and Zhang have proposed a MAC protocol that aim to improve coexistence between a secondary ad-hoc network and a primary network [50]. Two sensing policies are exploited to enhance spectrum opportunities detection (see Section 2.3.2). Moreover, the *p-persistent* carrier sense multiple access [93] protocol is used to manage reservation within secondary users. Negotiation is realized on the dedicated control channel which is licensed to the cognitive network. Each licensed channel is time-slotted and primary and secondary networks are synchronized. In the control channel, the slot is divided into two phases: the reporting and the negotiating phases. After the reporting phase each cognitive users is aware of the licensed channels that have been sensed idle by the nodes within its network. Then, secondary users with a non-empty queue negotiate the access to the overall set of available channels. Contention is managed during the control channel negotiating phase. In particular a sender listens to the control channel until it becomes idle. Then, it transmits a RTS packet with probability p . When the cognitive user successfully receives a CTS packet, it gets the reservation of all the available channels to transmit data in the next time slot. Although the medium access scheme proposed by Su and Zhang is a simple procedure, which profits from the cooperative detection benefits, it can not guarantee fairness to opportunistic users. Moreover, the scheme that would permit synchronization between primary and opportunistic networks is not investigated.

Ghaboosi *et al.* have proposed a cognitive MAC protocol for 802.11s wireless mesh networks [54]. In this protocol, a mesh entity called as cognitive extended service set is defined. This entity can be either a Mesh Point (MP) or a Mesh Access Point (MAP). Moreover, Cognitive Mesh Point (CMP) and Cognitive MAP (CMAP) are defined as MP and MAP with opportunistic capabilities. Although MP and MAP are able to operate only on the ISM band, CMP and CMAP can exploit also the licensed band. The licensed band is used by cognitive nodes to exchange data, although control signalling and transmission with non-cognitive nodes are realized on the ISM band. In this contention based protocol, cognitive users exploit two transceivers, which are dedicated to the control channel (ISM transceiver) and to data transmissions (non-ISM transceiver), respectively. After the sensing process, each cognitive node select a Long-Term Residency Channel (LTRC) and it tunes its non-ISM transceiver on this channel. Then, to inform all its next-hop neighbors, it transmits a channel switching frame on the control channel. Hence, when a cognitive source entity wants to initiate a communication with one of its next-hop neighbours, due to the fact that it already knows the destination LTRC, the channel negotiation phase can be avoided. Therefore, the cognitive source entity transmits an *eRTX* on the control channel indicating the receiver identity and its LTRC. This message permits to reach two important goals: first, the sender asks the receiver to establish a link layer connection, then it informs its neighbors about the on-leave situation and the corresponding absence time duration. When the cognitive destination entity correctly receives the *eRTX* message, it responds by sending an *eCTX* on its LTRC. Otherwise, when the cognitive source entity has an incorrect a priori information about the cognitive destination entity's LTRC, the receiver transmits the *eCTX* on the control channel, hence the sender can adjust its information and re-transmit the *eRTX* to avoid the distribution inconsistent information within the network. Upon reception of *eRTX* all neighbors of the sender are informed about the time period during which the cognitive source entity will not be present on its LTRC. Hence, those nodes that have already initiated a backoff cycle to start data transmission to the switching entity suspend the

counting down until it will come back on its LTRC. The discussed algorithm limits the use of the control channel and allows reducing the possibility of saturation. Moreover, it is more robust than the classic 802.11s to the hidden terminal problem, and it also reduces the resource wastage.

Kondareddy and Agrawal have proposed a frequency hopping DAB protocol for a multi-hop cognitive radio network [62]. This protocol, named SYNchronized MAC (SYN-MAC) avoids the exploitation of a common control channel to overcome its inherent drawbacks (see Section 2.3.1). Each node is equipped with two radios: one dedicated to control signal exchange and the other to data transmission. Nodes divide each frame in N slots each one assigned to a different data channel. During the network initialization state, at the beginning of each time slot, nodes broadcast a beacon in all available channels to exchange information about channels set and to synchronize their radios. When this phase is completed, nodes that are not involved in transmissions, continuously listen their channel set to:

- detect primary users,
- receive signalling information,
- avoid the multi-channel hidden terminal problem.

When a node wants to transfer data, it first chooses one of the channels that it shares with the receiver. Then it waits for the time slot representing the selected channel, and starts a negotiation process similar to the IEEE 802.11 DCF [84].

Although the proposed strategy has the advantage of avoiding a common control channel and solving the hidden terminal problem, it does not offer fast protection of primary users since their detection is notified to neighbours only in specific slots. Moreover, available channels are not efficiently exploited since they can only be used in one slot per frame.

On the contrary, HC-MAC [49] deals with medium access without requiring global synchronization or coordination among secondary users. The whole time frame consists in three phases: contention phase, sensing phase, and transmission phase. Secondary users contend the access in both control and data channel. During a contention window three packets are sent on the common control channel ch_0 :

1. C-RTS/C-CTS are used to start the handshake of the sender-receiver pair and to inform neighbours that the common channel is busy,
2. S-RTS/S-CTS are used by sender and receiver to exchange the sensing process outcome,
3. T-RTS/T-CTS notify the end of the transmission process.

A node, wanting to transmit, waits a backoff period and then sends a C-RTS on ch_0 . The receiver replies with a C-CTS on the same channel. Neighbours that overhear this packet defer their transmissions and wait for the S-RTS/S-CTS messages. After the handshake, sender and receiver are synchronized and sense each channel for the same amount of time. CFSR handshake is performed with the S-RTS/S-CTS exchange and permits the cognitive pair to agree on channel availability and to select the band where to communicate. After finishing transmission, the sender broadcasts the T-RTS and the receiver replies with the T-CTS: this packet exchange starts the next round of contention.

To reduce hardware costs, HC-MAC users are equipped with a single radio. The half-duplex radio, and the absence of a global synchronization, drive, however, to the multiple channel hidden terminal problem, which can cause collision during the transmission phase. Furthermore, a cognitive user may probe a channel where a hidden cognitive terminal is transmitting resulting in a false alarm event: authors refer to this problem as the *sensing exposed terminal problem*.

In a distributed CR ad-hoc network, it is desirable that nodes share a reliable control channel to provide the exchange of signalling information and to permit resource negotiation. Channel availability depends, however, on location and momentary conditions, and often a global control channel does not exist in the network. HD-MAC [57] adopts a distributed coordination scheme in which nodes self organize into local groups. Members of each group form a multi-hop network where a local common channel is exploited to realize coordination and communication. After neighbour discovery, each device shares its channel availability list and a common channel is elected through a voting process as the coordination channel. Only nodes into the same group can directly communicate with each other. Inter-group connection is realized through nodes located at groups boundaries: these nodes subscribe different coordination channels and act as *bridges* (see Fig. 2.26).

Each user is equipped with a half duplex radio and time is organized in superframes. Each frame is composed by a BP, a CHWIN, and a DATA period. During the BP, two kinds of beacons are transmitted within the network: a global beacon and a group beacon. Each node broadcasts the global beacon over all its available channels to discover new users; on the contrary, the group beacon is transmitted within its group to permit coordination and exchange information about neighbour discovery. During CHWIN users negotiate access to data channels. Additionally, to easily implement connection among neighbouring groups, HD-MAC divides bridges CHWIN structure in several slots, one for each coordination channel.

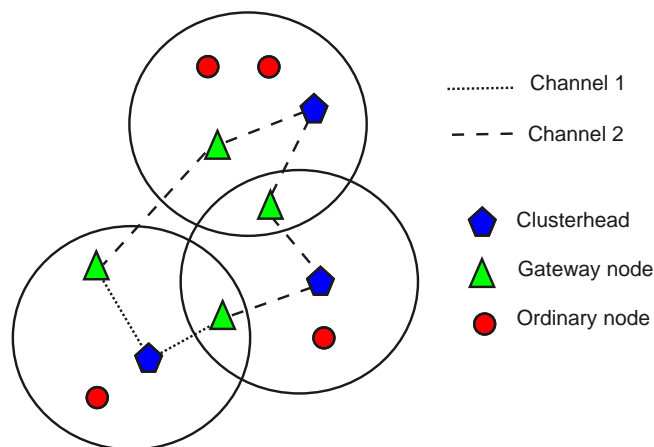


Figure 2.26: Multi-hop cognitive network clusters connected by gateway nodes [56].

Chen *et al.* have proposed a decentralized MAC protocol for a CR based mesh network (CogMesh) [56]. In CogMesh, a node forms a cluster on a particular channel and invites adjacent nodes sharing the same channel to join its cluster. The cluster leader and the common channel are named clusterhead and masterchannel, respectively. Clusterhead is responsible for intra-cluster channel access control and intra-cluster communication. Intra-cluster communication is realized through gateway nodes that act as bridges, as in HD-MAC [57]. The proposed MAC consists in a guaranteed access period to manage data transmission and a random access period to manage control message exchange. Channel access time is divided into super frames consisting of five periods (see Fig. 2.27). The BP is exploited by clusterheads to broadcast signalling information (such as resource allocation, synchronization, and control messages). The neighbor broadcast period is divided into mini slots in which each cluster node shares information about itself and its 1-hop neighbour list. During the data period, a TDMA approach is used to manage data communication. A quiet period is scheduled to quiet nodes within a cluster and realize spectrum sensing. The super

frame is ended with a private random access period and a public random access period that are used to manage intra-cluster and inter-cluster communications, respectively. Cluster formation, merging and termination processes are addressed in the proposed protocol. Eventually, a spread spectrum technique is proposed to realize the coexistence between different clusters and avoid the multichannel hidden terminal problem.

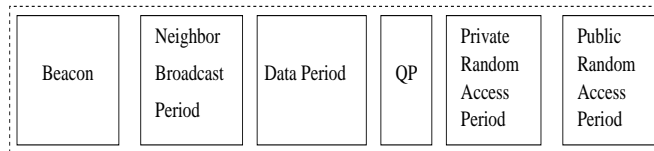


Figure 2.27: CogMesh MAC superframe [56].

Although both the strategies proposed in HD-MAC and CogMesh address the global control channel problem, several problems still remain. In particular, network topology is affected by the presence of primary users, and the overhead due to continuous cluster set up may be critical. Moreover, HD-MAC suffers from the multiple channel hidden terminal problem.

Chen *et al.* have introduced the concept of *cognitive cloud* to represent clusters dynamic size changes in a CogMesh network [94]. A cloud is a cluster that grows to cover as many secondary users as possible. Neighbouring nodes negotiate a common masterchannel to form fewer and larger clouds to simplify the exchange of signalling traffic through the network. A swarm intelligence approach is exploited to let nodes select as masterchannel a channel with sufficient quality, meanwhile being preferred by most neighbours. Although this approach decreases the overall system overhead, it may, however, impair the reliability of transmitted control data: for instance, this may be unacceptable in a cooperative sensing scenario.

The Opportunistic Spectrum MAC (OS-MAC) [64] is a coordination based DAB protocol for CR ad-hoc networks. As in CogMesh and HD-MAC, cognitive users self organize in clusters to manage the access in both licensed and unlicensed spectrum. Each Secondary Users Group (SUG) is formed by a set of users which want to communicate with each other. The group leader is indicated as Delegate Secondary User (DSU). DSUs acquire information about load in the data channel and share this information within their SUG. In the OS-MAC, the authors have supposed the existence of a global common control channel, which is used to perform clustering operation, and also to realize inter-cluster signalling exchange. Intra-cluster communication, on the contrary, is performed on the data channel selected by the cluster.

Secondary users are equipped with a single half-duplex transceiver; hence, they are not able to transmit and receive on different channels in parallel. At any time, in each SUG, only one node is allowed to broadcast data within its cluster. Nodes within a SUG that have buffered data contend the access to the data channel using the IEEE 802.11 DCF access mode [84]. Moreover, to limit the channel load, only one receiver will acknowledge the message reception.

The OS-MAC divides time into periods which are named as Opportunistic Spectrum Periods (OSPs). Each OSP is further split into three phases: the select phase, the delegate phase, and the update phase. At the beginning of the OSP, each DSU transmits load information acquired in the update phase of the previous period. Then, during the select phase, based on this traffic information, the SUG selects an available data channel. During the delegated phase, the first node that successfully delivers a message is elected as DSU. Finally, in the update phase, the DSU hops to the common control channel to inform other DSUs about the load in the current used data channel while nodes within its cluster continue to access to the data channel. To reduce inter-cluster interference, the OS-MAC implements a probabilistic channel selection mechanism which

reduces the probability that different SUGs choose the same data channel.

The main drawback in OS-MAC is that spectrum sensing and spectrum mobility functionalities are not addressed. Hence, a mechanism to protect licensed transmissions is not implemented. Furthermore, although the proposed inter-cluster information exchange scheme produces negligible overhead during the update phase, the common control channel may be mostly unused during the select and the delegate phases.

Underlay Spectrum Access

One of the few MAC protocols that exploit the underlay approach is COMAC [63]. COMAC permits cognitive users to exploit licensed band while limiting the generated interference. However, to exploit the available spectrum more efficiently, COMAC does not assume any predefined power mask. The proposed mechanism ensures that cognitive transmissions do not harm licensed users with probability $1-\beta$. More specifically, each secondary node determines the maximum transmission power over various channels such that primary receiver outage probability is guaranteed to be below a constant β . Authors consider a scenario in which M primary networks coexist within the same geographical space of a secondary network. A stochastic model is proposed for the aggregate interference within each primary network and for the primary to secondary interference. The proposed model assumes that:

1. Primary users are randomly located according a Poisson distribution;
2. The interference contribution to a generic opportunistic user is limited to all the active transmitters within a disk of radius r_c and centred at the cognitive receiver;
3. The M primary networks operate over M orthogonal bands;
4. There is a minimum distance between a primary receiver and the closest primary interferer within its network;
5. A channel occupied by a cognitive user cannot be simultaneously assigned to another secondary user in its vicinity. Hence, interference measured at a licensee user is mainly due at most one cognitive node.

Authors derive a close-form expression for the variance and the mean value of the two interferences. Furthermore they show through simulation that a lognormal function well approximates the distributions of these interferences. Hence, to guarantee primary users QoS, each cognitive user computes the upper bound on the transmission power that can be used on each licensed band. Each transmission power $P_{C,\beta}^{(i)}$ should satisfy the following condition:

$$P_{PR-PR,j}^{(i)} + g_{C,j}^{(i)} P_{C,\beta}^{(i)} \leq P_L^{(i)}, \quad (2.9)$$

where $P_{PR-PR,j}^{(i)}$ is the aggregated interference measured at the j th primary user generated by the transmitters within its network, $g_{C,j}^{(i)}$ is the gain between the cognitive user and the j th primary user and $P_L^{(i)}$ is the *interference power limit* of a user in the i th primary network. The $P_L^{(i)}$ value can be computed by the interference temperature limit which provides a metric for measuring the interference experienced by PR users. Following the methodology proposed by Clancy [95], the $g_{C,j}^{(i)}$ value is estimated based on the shortest distance between a primary receiver and cognitive transmitter. The proposed stochastic approach permits to mitigate interference perceived at primary users. However, contentions between secondary users are managed through a distributed carrier

sense multiple access with collision avoidance protocol. Signalling messages are transmitted over a specific control channel managed by a dedicated transceiver. In COMAC, each cognitive user A maintains a list \mathcal{L}_A , which consists of the data channels that are not currently used by A 's cognitive neighbours. A transmission region is associated with each channel within \mathcal{L}_A : this region is the area where transmissions sent over selected channel can be correctly decoded. The transmission range of channel j depends on its SINR and is defined by its radius a_j . To limit the hidden terminal problem, COMAC requires the following constraint on the transmission range (r_{ctr}) of the control channel region:

$$r_{ctr}(A) \geq 2 \max_{j \in \mathcal{L}_A} a_j. \quad (2.10)$$

This constraint reduces the probability that cognitive neighbours may transmit over the same channels.

Channels negotiation is managed with a sender-receiver handshake. Suppose that user A has data to transmit to user B at rate R_a . If A senses idle the control channel for a randomly selected back-off period it sends a RTS to user B . This packet contains \mathcal{L}_A , $r_{ctr}(A)$, $P_{C,\beta}^{(i)}(A)$ and the selected rate R_a . RTS refrains A neighbours to access on the control channel and permit to user B to check whether or not there exists a set of channel $\mathcal{L}^* \subseteq (\mathcal{L}_A \cap \mathcal{L}_B)$ that supported the request traffic constraint. If it exists, B sends a CTS packet which includes the \mathcal{L}^* set and the duration of the transmission T_{data} . CTS message refrains the receiver's neighbour to transmit to the channels within \mathcal{L}^* during data transmission. Finally A responds with a *Decided-Channel-To-Send* message, which informs its neighbours about \mathcal{L}^* and T_{data} , and then, it starts the transmission.

Although this scheme permits parallel transmissions to take place in the same vicinity, multi-channel hidden terminal is not completely solved due to possible collisions on the common control channel within neighbouring users transmissions. Furthermore, as previously underlined, interference temperature implementation typically results in poor performance, hence, investigation of new interference metrics should form object for future research.

Durantini *et al.* have proposed two *detect and avoid* algorithms that mitigate the interference generated by an Ultra-WideBand (UWB) network on Universal Mobile Telecommunications System (UMTS) and WiMAX systems [96]. In the detect and avoid approach, cognitive users implement the underlay paradigm through three operating modes: ranging, ordinary, and hold-off. During the ranging stage, UWB nodes perform all the signalling exchange, which is necessary to create a network. In the ordinary mode, users transmit data on a Time Division Duplex (TDD) basis. Secondary users can operate at a standard power P_{st} or at a limited power P_{red} . P_{red} is computed as the power that does not generate harmful interference to a primary user in the proximity of a secondary UWB terminal. Two time-out periods (T_{off} and T_{out}) are exploited to adapt power transmission to sensing results. During the hold-off stage cognitive nodes are idle to permit incumbent primary users to perform their first access to the primary network without being impaired by opportunistic users.

Coexistence with UMTS networks

UMTS networks operates in Frequency Division Duplex (FDD) mode. Hence, opportunistic UWB nodes periodically sense the uplink transmission to detect primary users presence and hence, they adapt their transmission power to mitigate interference generated toward the UMTS BS. When the power measured in the primary band (P_m) is greater than a certain threshold (P_{thr}), UWB users are constrained to limit their power to P_{red} . Otherwise, when opportunist nodes do not detect primary users for a time longer than T_{out} , the system supposes that there are not active UMTS terminals in the vicinity. Consequently UWB terminals are allowed to transmit with a power P_{st} .

Coexistence with WiMAX networks

Unlike UMTS, WiMAX terminals operate in TDD mode. Hence, subsequent frames are allotted

for uplink and downlink transmissions. Two time-out periods are defined to efficiently operate in this scenario, T_{out} and T_{off} . When $P_m \geq P_{thr}$ a WiMAX terminal is assumed to transmit in uplink, thus the opportunistic node can set its power to P_{st} and it accesses the sensed band. Otherwise, when opportunist nodes do not detect primary users for a time longer than T_{out} , the system supposes that a WiMAX downlink transmission is active. Consequently UWB terminals are obliged to limit their power to P_{red} . Furthermore, when primary transmissions are not detected for a time longer than T_{off} it is assumed that are not active primary users in the vicinity and, hence, transmissions are allowed at P_{st} .

Overlay Spectrum Access

Srinivasa and Jafar have investigated the overlay access paradigm comparing this approach with the classical interweave access [89]. The assumption of the overlay model is that the secondary transmitter has a-priori knowledge of the primary user's message. Furthermore, all channel gains are known to both transmitter and receiver. The overlay model is represented in Figure 2.28. Two

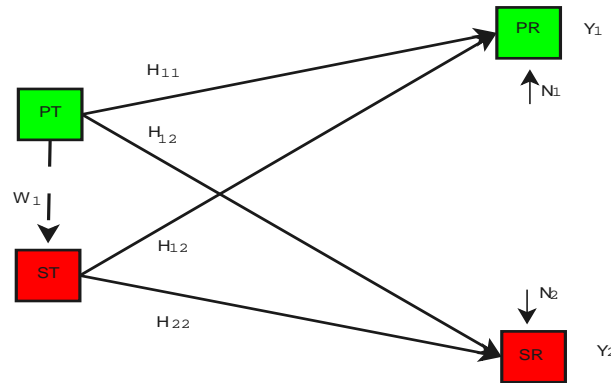


Figure 2.28: Overlay interference model [89]. PT, PR, ST, and SR represent the primary transmitter, the primary receiver, the secondary transmitter and the secondary receiver, respectively. Dashed curve represents the a-priori knowledge of primary message W_1 at the secondary transmitter.

underlay strategies are suitable at the cognitive transmitter accessing the licensed spectrum: The *selfish* approach and the *selfless* approach. In the former strategy, the secondary transmitter uses all its available power to transmit data to the secondary receiver. Furthermore, the transmitter exploits the knowledge of the primary transmitter's message to null the interference at the secondary receiver side (i.e., using the dirty paper coding strategy [97, 98]). In the selfless strategy the secondary transmitter uses part of its available power to relay the primary transmitter's message to the primary receiver. The remaining power is exploited to transmit data to the secondary receiver. The power distribution is calculated to guarantee SINR constraints at the primary receiver. Moreover, the cognitive transmitter precodes its data message to null interference at the cognitive receiver. The overlay technique has the further advantage to avoid primary hidden terminal interference because neighbouring primary transmitters are allotted on orthogonal frequency bands. Simulation results show how the underlay technique can potential outperform the achievable secondary network throughput with the interweave technique. However, as the knowledge of the licensed user message can be available at the cognitive side only if the two transmitters are located in close proximity, the overlay performance gain is strongly affected by this distance. Moreover, complicated precoding techniques must be available at the cognitive transmitter, and cooperation between

primary and secondary systems is necessary to estimate channel gains between transmitters and receivers.

2.3.5 Dynamic Spectrum Mobility

In wireless licensed scenarios, channel availability and quality change with space and time. Cognitive nodes coexist with primary users and interfering secondary users that dynamically access multiple channels. When a licensed user is detected, to realize seamless transmission, a cognitive node vacates its channel and reconstructs a transmission link on a different channel. The procedure that permits this transition from a channel to another with minimum performance degradation is called *handoff*.

MAC scope is to design spectrum mobility function such as it reduces delay and loss during spectrum handoff. The mobility management functionalities should be aware of the running applications and adapt to QoS constraints. For instance, File Transfer Protocol (FTP) traffic requires tight constraints on packet error rate: a retransmission protocol should be implemented to refrain from outage. Voice communication permits, however, a maximum delay for the channel handoff of 150 ms to avoid call interruption. In presence of collisions or sensing errors, the receiver should follow the transmitter in a new available channel: secondary pair tight time and frequency synchronization is required for successful communication in a CR network.

IEEE 802.22 [92] and C-MAC [53] deals with the spectrum handoff with the incumbent detection recovery protocol. This protocol allows the network to restore its normal activity maintaining an acceptable level of QoS. This procedure exploits a backup channel list that permit to reconstruct the communication link. To limit signalling and delay, the sender-receiver pair knows in advance where to restore their services if an incumbent is detected. Backup channels are identified by means of out-of-band sensing. Available channels are kept in a priority list used by devices during the recovery procedure. Users transmitting on the same channel share the same priority list to minimize signalling and rapidly recover communications.

Akyildiz *et al.* have investigated spectrum mobility issues for a CR ad-hoc network [3]. Two different strategies are presented: proactive spectrum handoff and reactive spectrum handoff. In proactive strategies, users, while communicating, predict events such as mobility and channel quality degradation that could cause handoff. Meanwhile they search new spectrum bands where rapidly switching and minimizing performance losses and delay. Proactive sensing requires, however, complex algorithms to estimate network behaviour, and two radios to perform out-of-band sensing and transmission in parallel. Reactive strategies need rapid channel switching without any preparation and cause performance degradation due to high handoff delays. Reactive handoff is realized when unpredictable events, such as the primary user appearance, occur, or in those cases where devices can not afford proactive handoff due to energy or hardware constraints.

Giupponi and Pérez-Neira have proposed a fuzzy-based distributed strategy to limit the spectrum handoff event [99]. This algorithm is realized through two fuzzy logic controllers; the cognitive node is assumed to be able to evaluate, by means of spectral estimation techniques, the primary user bit rate and consequently its Signal to Noise Ratio (SNR_{PU}). The first controller takes as inputs SNR_{PU} and the signal strength from the primary user to the secondary one (SS_{PU}). Then, it estimates the distance between primary and secondary users, and selects the allowed power for the cognitive node. The second controller is in charge of taking decision about spectrum mobility. Spectrum handoff is initiated if the secondary user is in outage, or if its transmissions harmfully interfere with a primary user. To avoid spectrum mobility, cognitive nodes can adjust their power to reduce generated interference. Reducing transmission power drives, however, to decrease the secondary user transmission reliability, which drives cognitive user to still decide to perform hand-

off.

Kim and Shin have proposed a sensing-sequencing algorithm that minimizes the *channel-switching latency* [78]. This metric is defined as the delay due to discovering of the first opportunity since the cognitive user has to vacate its channel. Authors have proposed to model channels as ON-OFF alternating sources and accordingly, they have estimated the probability that a channel i would be idle (P_{idle}) at a certain time t based on its sensing history. Hence, the presented scheme computes P_{idle} for each licensed channel except the channel that has been vacated. Therefore, the optimal strategy is to sense channel according the descending order P_{idle} . Furthermore, when no channels have found to be idle authors have recommended to avoid an instantaneous reply of the searching algorithm. A more energy-efficient strategy should consider a time T_{retry} , after which searching again for an idle channel.

2.4 A Critical Overview on Agile Strategies for Two-Tier Cellular Networks

As already mentioned, exploiting cognitive principles in two-tier network design may enable to the cost-effective deployment of femtocell networks, where spectrum sensing, dynamic resource allocation, and spectrum sharing, may be strategic in addressing issues that derive from the ad-hoc nature of FAPs.

In Section 2.4.1 we present spectrum sensing techniques that permit FAPs to be aware of spectrum usage at neighbouring cells, and monitor time-varying resource availability. Section 2.4.2 analyses dynamic resource allocation schemes that favour the compliance with QoS constraints, while limiting the generated interference and power consumption. Section 2.4.3 introduces spectrum access strategies that mitigate contentions to avoid harmful interference. Finally, Section 2.4.4 discusses cognitive-based approaches that are used to limit energy wastage in cellular networks.

2.4.1 Spectrum Awareness and Victim Detection

In this section we overview CR-based functionalities that enable FAPs to be aware of spectrum usage at nearby (macro and femto) cells and detect the presence of UEs that are served by neighbouring APs. Accordingly, cognitive APs can dynamically select available channels and adapt transmission parameters to avoid harmful interference towards contending cells.

A major misconception in the CR literature is that detecting the signal of the legacy transmitter is equivalent to discover transmission opportunities [100]. On the contrary, even when such a signal can be perfectly detected, this discovery is affected by three main problems: the *hidden transmitter*, the *exposed transmitter*, and the *hidden receiver*. These are well-known issues and have been investigated in depth in the ad-hoc wireless network literature [101]. Nevertheless, although the former problems have been solved, the hidden receiver is still an open problem. Due to wall attenuation, the occurrence of these scenarios is even higher in femtocell deployment scenarios. Furthermore, it is expected that the M-BS likely allocates all frequency resources when there is a high number of end-users to serve. Hence, a sensing analysis based on the classic *energy detection* [73] may detect few spectrum opportunities. However, since many M-UEs can be located far away from the FAP, their channels can be effectively reused in the femtocell [102]. More sophisticated and effective detection schemes, based on the knowledge of legacy users' signal characteristics, have been presented in the CR literature (cf. [74, 75]). Furthermore, infrastructure-based solutions

such as the CPC [103] and Geo-location database [104] have been proposed to assist cognitive networks across different Radio Access Technologies (RATs) and available spectrum resources.

Spectrum Sensing and LTE user detection

Sensing performance is limited by hardware and physical constraints. For instance, only cognitive devices equipped with two transceivers can transmit and sense simultaneously (such as in [105]). Moreover, users usually only monitor a partial state of the network to limit sensing overhead. There is a fundamental trade-off between the undesired overhead and spectrum holes detection effectiveness: the more bands are sensed, the higher the number and quality of the available resource. To improve the sensing process reliability in two-tier deployment scenarios, several approaches have been investigated in the literature.

Lien *et al.* have proposed a mechanism that optimizes both sensing period and frequency resource allocation to statistically guarantee femtocell user QoS [106]. Barbarossa *et al.* have introduced a strategy that jointly optimizes the energy detection thresholds and the power allocation under a constraint on the maximum generated interference [107]. Sahin *et al.* have investigated an opportunistic strategy that jointly exploits spectrum sensing and scheduling information obtained by the M-BS [102]. In this work, uplink sensing is used to individuate frequency resources that have been allocated to nearby M-UEs. Then uplink/downlink scheduling information is exploited to identify these M-UEs and their downlink frequency resources, respectively. Hence, this algorithm permits a reliable detection of the available spectrum opportunities at FAPs. However, it presents some drawbacks: first, the proposed coordination between M-BS and FAPs and limited availability of backhaul bandwidth result in scalability and security issues; second, the technique presented above may be ineffective in practice. This is due to dense femtocells deployment with consequent large population of interferers expected to be coordinated by the cellular operator. Due to such unsolved problems, direct coordination amongst femto and macro cells is not implemented in 3GPP Release 10 [108].

Lotze *et al.* have considered a scenario in which LTE-like femtocells are deployed in the GSM spectrum to avoid *cross-tier interference* [109]. In this scenario, neighbouring femtocells have to dynamically adapt their spectrum usage to prevent harmful *co-tier interference*. The authors have proposed a spectrum sensing technique that enable a FAP to detect the presence of neighbouring interferers without decoding their signals. The proposed approach combines the classic energy detection operations with a feature detection scheme that permits to discriminate between LTE transmissions (that have to be avoided) and other signals (that have no priorities). This technique allows the detection of weak signals at a complexity cost slightly higher than the classical energy detector. The proposed detection algorithm has been successfully implemented in the frame of the Iris platform [110].

Several studies related to *victim* aware interference management have been proposed in the 3GPP frame. DoCoMo have investigated a method for determining whether there are M-UEs in close proximity of a FAP [111, 112]. In this scheme M-UEs detect the cell IDentification (ID) of interferers, by listening to the Broadcast CHannel (BCH) of neighbouring FAPs. Then, based on the received Reference Signal Received Power (RSRP), each M-UE identifies most harmful FAPs and feedbacks this information to its serving M-BS. PicoChip and Kyocera have investigated a method where FAPs determine the presence of a M-UE by detecting its uplink reference signal [113]. A victim M-UE is often easy to detect because it likely transmits with relatively high power due to the experienced attenuation (composed mainly by path loss and wall losses). Furthermore, the authors have proposed to exploit the properties of the uplink reference signal, to discriminate between a single dominant transmission of a nearby victim and the aggregated power due to further away users. However, the above solutions are ineffective in the presence of an idle mode M-

UE. An idle M-UE neither transmits nor is able to report the presence of neighboring femtocells, thus, protecting M-BS downlink control channels is necessary. For instance, Qualcomm have recommended to introduce orthogonality between FAPs and M-BS control channels [114]. Further potential solutions are presented in [115].

Dedicated Architectures towards Geographical-based Interference Mapping

The SpectrumHarvest is an architecture that manages spectrum access in cognitive femtocell networks [116]. This architecture is composed of four components: a Multi-Operator Spectrum Server (MOSS), a Femto Coordination/controller Server (FCS), a cognitive FAP, and associated end-user terminals. The MOSS combines information on spectrum availability at different cellular operators with local measurements performed by different femtocells. After processing these inputs, the MOSS indicates to each FCS local available resources. The FCS has the role to provide the spectrum usage information to each of its served FAPs, joint with additional information such as power level of neighbouring femtocells and location of M-BSs/M-UEs. Each FAP is characterized by a Spectrum Usage Decision Unit (SUDU) that exploits information received by both the FCS and MOSS to allocate the required spectrum for each transmission. Furthermore, the SUDU performs local spectrum measurements to detect the presence/absence of neighbouring mobile terminals. Finally, end-user terminals support a new air interface operating in non-continuous channels across a multi-operator and multi-services ultra broadband.

Kawade and Nekovee have proposed to use TV White Spaces (TVWS) to support home networking services [117]. The TVWS spectrum comprises large portions of the UHF/VHF spectrum that became available on a geographical basis for opportunistic access as a result of the switch-over from analogue to digital TV.

Such an investigation is carried out using the database approach: a centrally managed database containing the information of free TV channels is made available to femtocells. Based on the Geo-location data and QoS requirements, FAPs query the central database for channel occupancy through the fixed-line connection. The database returns information about various operating parameters such as number of channels, centre frequencies and associated power levels for use in specific location. Simulation results show how TVWS can be an effective solution for low/medium rate services, although it should be used as a complementary interface for highly loaded traffic scenarios. Furthermore, the study underlines that, due to the lower propagation losses, operating in TVWS bands may result in a significant energy saving.

Haines, on the contrary, have investigated advantages and drawbacks of implementing the CPC in the femtocell deployment scenarios [118]. The CPC is a dedicated logic channel, and is used to disseminate radio context information permitting terminals configuration and interference mitigation. Moreover, the distributed deployment of the CPC (DCPC) is under investigation [119] to improve the coexistence of heterogeneous systems in a shared band. In the investigated scenario, several networks (such as WiFi and bluetooth), which exploit different technologies and bands, may coexist in the femtocell coverage area. In each household a Smart Femto Cell Controller (SFC-C) is proposed as interface with a centralized database managed by the cellular operator. The SFC-C is also able to collect and process the sensing outputs of different cognitive devices deployed in the area. Then, it sends interference information to neighbouring terminals to coordinate the access to common spectral resources and avoid mutual interference. Furthermore, a peer to peer link is established to permit neighbouring SFC-Cs, which coordinate different heterogeneous networks, to exchange local spectrum measurement and interference policies.

2.4.2 Dynamic Radio Resource Management

Classic RRM algorithms allocate different parts of the available spectral resource between macrocell and femtocell tiers [23]. The goal of these techniques is to avoid in-band concurrent transmissions using full time/frequency orthogonalization of transmissions. However, as already mentioned, these approaches are far from the FR targets of operators. The system SE can be enhanced by exploiting more flexible approaches.

FR schemes have been proposed to geographically reallocate to femtocells part of spectral resources used by the macrocell [120]. However, due to the high number of expected interferers in dense femtocell deployments, FR schemes can be ineffective. CR terminals can exploit awareness on the spectrum usage and dynamic RRM algorithms to break the capacity limit of classic macrocell networks.

Li *et al.* have proposed an opportunistic channel reuse scheduler that limits both *macro-to-femto interference* and *femto-to-femto interference* in downlink scenario [121]. In this scheme, each femtocell exploits sensing outputs to construct a two dimensional interference signature matrix. This model describes the local network environment in the time/frequency domains and permits to avoid high peaks of interference. When there is a user to serve, the scheduler assigns channel and power according to QoS and power constraints. First, it picks up the best available channel according to the user interference perception; then, the optimal transmission power is allocated to limit the femtocell power consumption. The authors investigate also to the uplink scenario [122], where the presence of M-UEs in the household of the femtocell may cause high level of macro-to-femto interference. This is a well-known issue, and it has been referred as the Kitchen Table problem [123]. In the above discussed cognitive scheme, the absence of coordination between neighbouring femtocells results in high scalability and low complexity. However, nearby cognitive FAPs, which experience similar level of interference, may simultaneously access same channels, thus interfering with each other. Furthermore, FAPs located at the macrocell edge may not be able to detect M-BS transmissions and subsequently cause strong cross-tier interference towards nearby M-UEs.

Xiang *et al.* have investigated the scenario in which cognitive femtocells access spectrum bands that are licensee to different legacy systems (such as macrocell and TVWS) to increase the aggregate network capacity [105]. Authors have proposed a joint channel allocation and power control scheme that aims to maximize the downlink femtocells capacity. The optimal allocation is found formulating a mixed integer non-linear problem, which is decomposed [124] and distributively solved at each femtocell. F-UEs are allowed to use only the channels that are temporally not used by the legacy system. Each FAP is equipped with two transceivers, one is dedicated to the data transmission and the other is used to continuously monitor the radio environment (i.e., sensing and transmission can be performed in parallel). Note that this approach improves the SE but it increases the cost of devices and also the system complexity. Whenever a FAP detects transmissions of the legacy system it stops its activity and updates channels assignment, accordingly. To increase spectral reuse and capacity, the proposed approach permits neighbouring femtocells to access the same channels as long as generated interference is not harmful. Furthermore, neighbouring FAPs share information about the presence of concurrent transmissions to cooperatively improve the primary UEs detection. However, this signalling exchange is realized on the cellular backhaul, thus the delay introduced by Internet limits the benefits of the cooperative detection. Eventually, on the opposite of the classic cellular technologies, each UEs can use only one channel, and the FAP is constrained to exploit a number of channels that is equal to the number of its served UEs.

As already mentioned, OSG femtocells may limit harmful interference in two-tier networks.

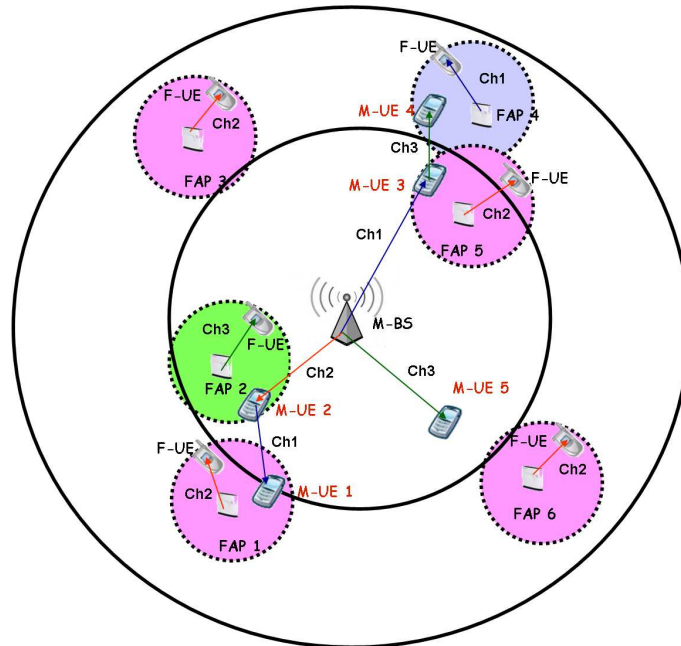


Figure 2.29: Two-hop cooperative transmission scheme for a two-tier cellular networks [127]: the M-BS is allowed to communicate with M-UE 1 and M-UE 4 through relays M-UE 2 and M-UE 3, respectively. Furthermore, due to the cooperative communication scheme, neighbouring FAPs are not interfered by macrocell transmissions .

In this scenario, FAPs do not restrict the access, and mobile users are allowed to connect to the closer femtocell in the vicinity. OSG femtocells deployment results in higher macrocell offload and enhanced network capacity [125]. As drawbacks, network signalling and frequency of handover increase. Furthermore, security issues emerge in this type of access. Torregoza *et al.* have considered a scenario in which both the M-BS and FAPs offer WiMAX services in their coverage areas [126]. Each femtocell has some private customers although public M-UEs to improve their performance, can access both the M-BS and neighbouring FAPs. In the presented model, a backhaul connection is introduced to permit communications between the M-BS and FAPs. A femtocell, which serves public M-UEs, receives a certain amount of the backhaul capacity as compensation for the poorer performance perceived by its private clients. Thus, a joint power control, BS assignment, and channel allocation scheme is proposed. This scheme improves the aggregate throughput while minimizing the need for femtocell compensation. To find the pareto optimal solution for both downlink and uplink scenarios, two multi-objective problems are formulated and solved through a sum weighted approach.

Jin and Li have analysed further potential benefits of applying CR techniques in WiMAX based two-tier networks [127]. In this scenario, F-UEs connected to WiMAX femtocells via a dedicated channel, experience guaranteed QoS. Oppositely, M-UEs are allowed to connect only to the central M-BS with best effort services. However, this deployment scenario permits a high number of spatial reuse opportunities. Femtocells are characterized by small coverage areas, few UEs per cell, and low transmission power; hence, outdoor M-UEs can opportunistically reuse channels utilized by far-away femtocells. Therefore, a two-hop cooperative transmission scheme is proposed to exploit the spatial diversity experienced by cognitive M-UEs (see Figure 2.29). In

classical CR networks, sender and receiver periodically exchange their sets of available channels; then, to find a common available resource where to communicate, a channel filtering procedure is realized [6]. Thus, when there are no common opportunities between the M-BS and a M-UE, the presence of a cognitive relay introduces further possibilities to establish a reliable communication. For instance, in Figure 2.29, the M-BS is allowed to communicate with M-UE 1 and M-UE 4 through relays M-UE 2 and M-UE 3, respectively. Furthermore, cooperative communication may permit to reduce the M-BS transmission power, which results in lower interference perceived at F-UEs and energy saving. Finally, the authors have proposed a RRM protocol that maximizes the aggregated throughput and includes routing strategies, power assignment, and channel allocation. Using stochastic optimization, non-linear integer programming problems are formulated. The proposed cognitive framework is one of the few RRM protocol that exploits the location dependency of spectrum opportunities to enhance the two-tier network performance. However, the high level of signalling and sensing overhead may result in low scalability.

Mustika *et al.* have proposed a game-theoretic approach to deal with the resource allocation in self-organizing closed access femtocells [128]. In the proposed scheme, the uplink interference scenario is considered where FAPs are affected by both co-tier and cross-tier interference. The resource allocation problem is modelled as a non-cooperative potential game where F-UEs is represented by the set of players, the selected Resource Blocks (RBs) is the associated strategy, and the utility function takes into account both the perceived and generated interference. Hence, each F-UE iteratively acquires information about its environment and distributively selects the most appropriate set of RBs that improve its utility function. The authors demonstrate that the proposed approach converges to a NE. In such state, no player has any advantages to deviate from the selected strategy [129]. However, according to the simulation results the number of iterations necessary to meet the NE is quite high. Therefore, such state may not be reach during the wireless channel coherence time and poor performance may be experience during the *long* iterative process. Finally, the proposed approach requires the knowledge of the link gains between F-UEs and nearby FAPs and M-BS, which is a hard task in the considered scenario.

2.4.3 Dynamic Spectrum Sharing

Spectrum Sharing functionalities aim to improve the coexistence of heterogeneous users accessing the radio resource. Three different cognitive transmission access paradigms are currently investigated in the literature [88]: *underlay*, *overlay*, and *interweave*. In underlay transmissions, cognitive users are allowed to operate in the band of the primary system while generated interference stays below a given threshold (see Figure 2.30).

In overlay transmissions, cognitive devices exploit some specific information to either cancel or mitigate perceived/generated interference on concurrent transmissions (see Figure 2.31).

In interweave transmissions, opportunistic users transmit only in spectrum holes; if during in-band sensing a opportunistic user detects a primary one, it vacates its channel to avoid harmful interference (see Figure 2.32).

To improve the coexistence between macrocell and femtocells, these schemes have been implemented also in cognitive-based two-tier networks.

Cheng *et al.* have investigated the theoretical downlink capacity of a two-tier network, for each of the above-mentioned approaches [130]. The authors have shown that underlay and overlay approaches can result in better spectral reuse than the interweave scheme. However, former mechanisms require a better awareness of the network state and higher level information (e.g., the position of neighbour licensee users, scheduling information, and channel gains).

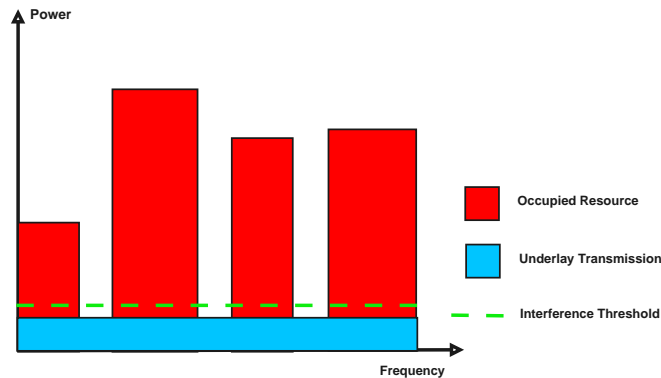


Figure 2.30: Underlay transmission scheme [88].

Underlay spectrum access

Galindo-Serrano *et al.* have proposed a distributed Q-learning based mechanism [131], which controls the aggregated femto-to-macro interference [132]. Femtocells distributively find a policy that ensure an optimal decision exploiting sensing outputs and periodic feedbacks transmitted by the M-BS. However, the successful implementation of the proposed mechanism in a broadband cellular network is constrained by the length of the learning process. Hence, the authors have introduced a novel cognitive concept, named *docition*, which permits FAPs to exchange their knowledge and experience. Femtocells are able to identify the most appropriated *teachers*. In fact, it is fundamental that cognitive terminals learn from *experts* that are in the same radio environment. This process increases the convergence speed and accuracy. Furthermore, the docitive approach may significantly reduce the sensing period resulting in energy saving and higher throughput. Depending on the cooperation degree, and thus the introduced overhead, two docitive schemes are investigated: in Startup Docition, cognitive femtocells share their policies only when a new node joins the network; in IQ-Driven Docition, cognitive femtocells periodically share their knowledge. However, further overhead and complexity are introduced by coordination with the macro network, which periodically feedbacks the interference perceived at the M-UEs.

Chandrasekhar *et al.* have discussed a different approach to limit the femto-to-macro interference [133]. The authors first investigate the consequences of the near-far effect, which may result in excessive cross-tier interference in two-tier cellular networks (see Figure 2.7). Simulation results show that, due to mutual interference, achieving high SINR in one tier constricts the achievable SINR in the other tier. To deal with this issue, a closed loop power control is implemented at femtocells. The proposed algorithm iteratively reduces the F-UE uplink power until SINR target at M-BSs is met. The authors have proposed that each node distributively adapts its power to maximize a utility function, which results in lower complexity and overhead. This function is made up of two components: a reward and a penalty. The reward describes the gain achieved by the F-UE as a function of the difference between the experienced link quality and the minimum SINR target. The penalty represents the cost that femto transmission implies for the macrocell network as a function of the interference perceived at the M-BS. The proposed power adaptation mechanism does not require explicit cooperation between macrocell and femtocell networks. Nevertheless, to evaluate the generated interference at the M-BS, each F-UE needs to estimate the channel gain characterizing its link to the M-BS. Moreover, the proposed power control scheme may not be sufficient to guarantee reliability of macrocell transmissions. In such cases, coordination is introduced, and based on periodic M-BS feedbacks, stronger femto interferers iteratively decrease their

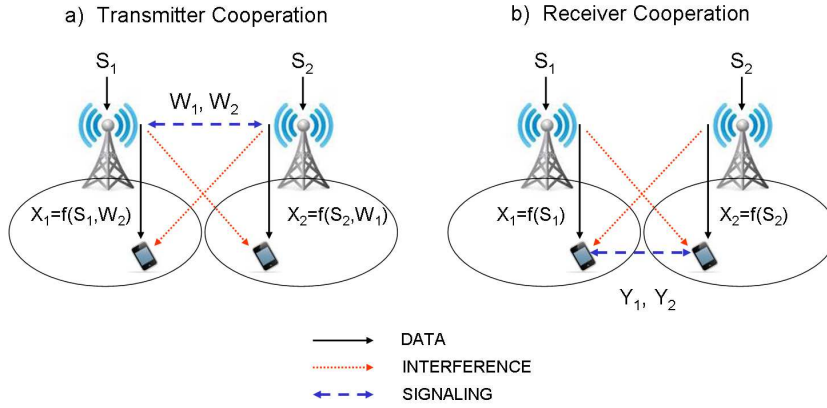


Figure 2.31: (a) Overlay transmission scheme in transmitter cooperation scenario: the two BSs exchange information to acquire a-priori knowledge about the concurrent transmissions. Such information is then exploited to either cancel or mitigate mutual interference [88]. (b) Overlay transmission scheme in receiver cooperation scenario: the two UEs jointly process received signals to correctly decode desired information.

SINR target until the generated interference is adequately lowered.

Interweave spectrum access

To allow distributed intercell spectrum access, da Costa *et al.* have proposed a Game-based Resource Allocation in Cognitive Environment (GRACE) [134]. In such an approach spectrum access is autonomously managed at each femtocell. Hence, intercell coordination is avoided, leading to a better scalability and SE. The aggregate femtocell strategy is modelled as a game $\Gamma = \langle \mathfrak{S}, (\Sigma_i)_{i \in \mathfrak{S}}, (\Pi_i)_{i \in \mathfrak{S}} \rangle$, where \mathfrak{S} is the set of femtocell players, Σ_i is the access strategy of the i th player, and Π_i is the utility function of the i th player. The utility function indicates the preferences of each player with respect to the possible access strategies. In GRACE, this function is constructed to jointly optimize capacity, load balance, and femto-to-femto interference. Simulation results show that GRACE achieves higher throughput than classic FR schemes especially at users that experience poorest performance. GRACE avoids inter-cell coordination, leading to high scalability and SE; however, this approach decreases the speed of the learning process and reduces the accuracy of the algorithm.

Garcia *et al.* have introduced a Self-Organizing Coalitions for Conflict Evaluation and Resolution (SOCCER) mechanism, which fairly distributes available resource between cognitive femtocells [5]. This approach is based on both graph and coalitional game theories and permits to avoid harmful femto-to-femto interference. Soccer is composed of two main phases (see Figure 2.33): in the first phase, FAPs, which join the network or seek for more band, detect the presence of possible conflicts.

In particular, based on the RSRP measured at F-UEs, each FAP estimates which neighbouring FAPs are currently strong interferers. In SOCCER, an interferer is strong, whenever, due to the mutual interference, an orthogonal access results to be more effective than a full reuse scheme. In the second phase, coalitions are formed and resource is distributed accordingly. The authors have shown through simulation that, even in high density deployment scenarios, the interference degree (i.e., the number of neighbour interferers) of a FAP is rarely higher than three. Thus, to

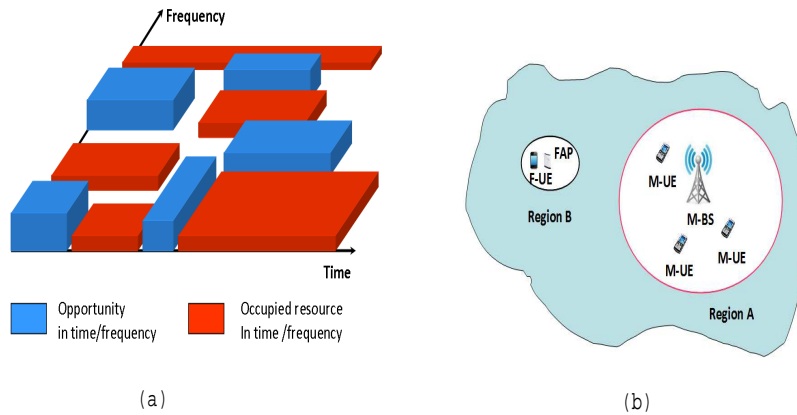


Figure 2.32: (a) Interweave transmission approach in time/frequency domain: FAPs are not allowed to transmit while M-BS is transmitting. (b) Interweave transmission approach in space domain: Some area around the M-BS (i.e., the Region A) can not be reused by FAP transmissions; however Region B can be used without interfering M-UEs.

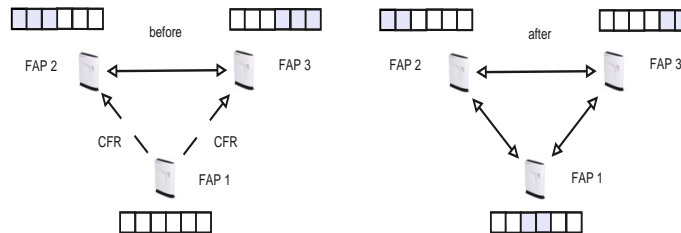


Figure 2.33: Dynamic Spectrum Sharing according to SOCCER [5].

limit the algorithm complexity and the network overhead, SOCCER considers the case in which a new entrant BS sends a Coalition Formation Request (CFR) at most two coalition candidates. After receiving the CFR message, coalition candidates fairly reorganize the available spectrum to avoid mutual interference. It is important to note that, interference towards the macrocell is not considered in the both the works of Costa and Garcia, which may result in poor performance at M-UEs.

On the contrary, Pantisano *et al.* have proposed a cooperative spectrum sharing approach, which may limit the effect of both cross-tier and co-tier interference [135]. In the proposed scheme FAPs opportunistically access the bandwidth used by the macrocell uplink transmissions to avoid interference towards nearby M-UEs (see Figure 2.34). Furthermore, neighbouring FAPs are able to form coalitions in which available frequency resources are cooperatively shared and femto-to-femto interference is limited. In fact, while isolated FAPs select their channels according to the perceived level of interference, FAPs in the same coalition use a Time Division Multiple Access (TDMA) scheme, which avoids that neighbour FAPs operating on the same channel transmit on the same time slot. However, co-tier interference is not fully eliminated because different coalitions generate mutual interference with one other. The proposed cooperation algorithm is divided

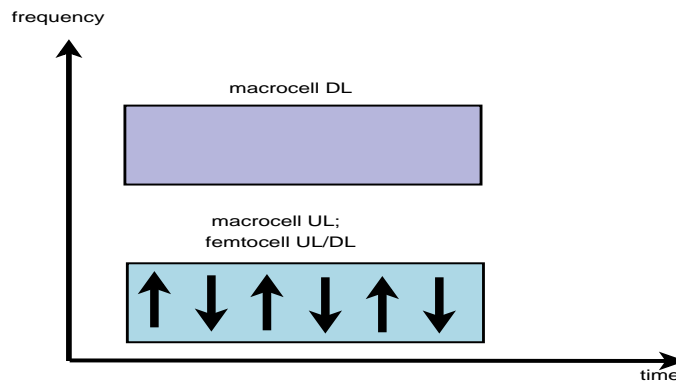


Figure 2.34: A Time Division Duplex transmission scheme for cross-tier interference mitigation.

into three main phases: neighbour discovery, recursive coalition formation, and coalition-level scheduling. During the first phase each FAP uses a neighbour discovery technique to identify potential coalition partners. The second step is iteratively performed: first each FAP find coalitions characterized by an acceptable cost. This cost is related to power consumption due to the signalling exchange amongst the coalition members and depends on spatial distribution of the coalition members. Then, each FAP joins the coalition that ensures the maximum payoff. The coalition payoff is related to the achieved throughput and corresponding power consumption. Finally, the coalition formation ends when a stable partition is reached (i.e., FAPs have no incentive to leave their belonging partition). In the third phase, FAPs within the same coalition, first exchange information about their scheduling preferences on a defined in-band common control channel; then, a graph-coloring based algorithm [136] is used in each coalition to schedule available RBs. The proposed approach may enable reliable co-channel deployment of femtocells and macrocells in the same geographic region. However, perfect sensing is supposed at FAPs, even though missing detection of the M-UE transmission can result in harmful macro-to-femto interference.

Overlay spectrum access

In sub-urban or low density urban deployment scenarios a femtocell generally operates in very high SINR regime. However, we can identify two scenarios in which macro-to-femto interference may affect the transmission reliability. In the first case, harmful downlink interference is experienced at F-UEs when the femtocell is very close to a M-BS. In the second case, an indoor M-UE that is far from its serving BS adapts its transmission power using fractional power control [137]. This mechanism may generate harmful interference at neighbouring FAPs. However, in both cases, the harmful transmission is generally characterized by both high power and low rate. Thus, with high probability, the receiver (i.e., the FAP or the F-UE) can process and cancel the perceived interference and subsequently correctly decode the useful message (a more detailed discussion on Interference Cancellation (IC) theory can be found in [138]). The general assumption of overlay transmission schemes is that the cognitive network possesses the necessary information (such as the channel gain related to the interferer transmission) to either cancel or mitigate interference.

The amount of signalling and coordination classically required in overlay access schemes may result in excessive complexity and overhead. Therefore, Rangan have investigated an overlay approach that limits cooperation within two-tier networks [139]. The proposed method assumes Fractional Frequency Reuse (FFR) at macrocells. The overall band is divided in four contiguous

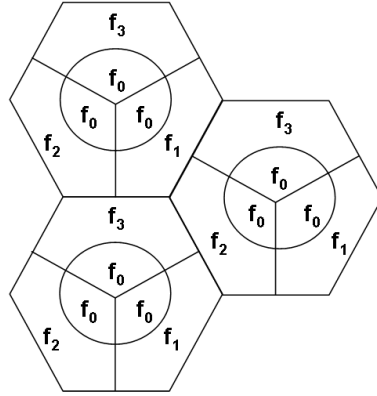


Figure 2.35: A FFR scheme for two-tier cellular networks [139].

bands (f_0 , f_1 , f_2 , and f_3) as shown in Figure 2.35.

Each cell site is three way sectorized, and each of this sectors is referred to as a cell. Each cell is further divided in two regions, an inner region and an outer region. Subband f_0 is reused in all cells and it is allotted to M-UEs that are closer to the M-BS. However, remaining bands are used in only one cell per cell site and are allocated to cell edge M-UEs. Although this scheme reduces the system SE, it limits both the macro-to-macro and the femto-to-macro interference. The subband partitioning permits femtocells, regardless of their positions, to access a part of the spectrum where the generated cross-tier interference is minimal. To effectively reduce femto-to-macro interference, joint femtocell channel selection and power allocation is based on a load spillage power control method. This method avoids femtocells to operate in bands either where the operating macro receiver is close, or high load traffic is transmitted. Signalling between macro and femto networks is required to allow each femtocell to be aware of the macro load factors. Furthermore, to successfully implement the load spillage power control, femto transmitters need to estimate channel gains that characterize the femto-to-macro links. Nevertheless, this scheme does not reduce the macro-to-femto interference experienced at F-UEs close to the M-BS. Thus, the author have proposed to implement the above-mentioned IC technique to jointly decode and cancel undesired signals. Femto-to-femto interference is not mitigated by the proposed approach, however, due to the geographic based frequency partition, this interference can strongly affect femtocell performance especially in dense deployment scenario.

On the contrary, Zubin *et al.* have proposed a dynamic resource partitioning scheme between femto and macro cells, which does not use IC [112]. In this scheme, M-UEs identify the cell IDs of interferers, by listening to the BCH of neighbour FAPs. Then, based on the corresponding RSRP, each M-UE identifies most interfering femtocells and feedbacks this information to its serving M-BS. Hence, the M-BS indicates to interfering FAPs the channels that they should refrain to allocate, to avoid cross-tier interference. This coordination message can be disseminated via X2 and S1 interfaces [140]. However, whenever the macrocell scheduling pattern changes, the M-BS should transmit new information to each interferer that is located in its region. The length of the scheduling period in modern cellular systems is related to the wireless channel coherence time. Hence, in medium/high density deployment scenarios, this scheme may result in excessive overhead, which limits the system scalability.

Kaimaletu *et al.* have extended the idea previously presented to the femto-to-femto interference scenario [141]. In this scheme, both M-BSs and FAPs schedule frequency resources by

considering the potential interference generated towards each other UEs. UEs classify interfering cells according to the strength of their RSRP. Therefore, they feedback this information to the serving cell, which forwards to neighbouring cells the number of victim UEs they create and the total number of its UEs. According to this information, macro/femtocells cooperatively block a subset of their frequency channels such as the victim UEs are protected. At the end of this iterative process, each cell uses a Proportional Fair (PF) scheduler [142] to serve its UE with minimum amount of perceived/generated interference. To realized the proposed scheme, the authors have assumed perfect synchronization between all cells in the system both in time and frequency. In the proposed scheme signalling exchange does not need to be performed in small time scale thus it results in lower overhead with respect to the Zubin's proposition [112]. However, in a dense deployment scenario sources of interference can frequently change. This may increases the need for coordination, reducing the system scalability and increasing overhead.

Pantisano *et al.* have introduced a cooperative framework for uplink transmissions, where F-UEs act as a relay for neighbouring M-UEs [143]. In this framework, each M-UEs can autonomously decide to lease part of its allotted bandwidth to a cooperative F-UE. The latter split these channels into two parts: the F-UE uses the first part of the received band to forward the M-UE's message to its serving FAP; on the contrary, the second part of the band represents a reward for the relaying F-UE, which can transmit its own traffic avoiding interference from neighbouring M-UEs. Cooperation can be beneficial for both M-UEs and FAPs, which may avoid excessive retransmissions (i.e., latency) and reduce the perceived cross-tier interference, respectively (see Figure 2.36). In fact, cell edge and indoor M-UEs likely experience poor performance, due to penetration and propagation losses; hence, they are expected to transmit with relative high power to avoid excessive outage events. Therefore, M-UEs' transmission result in strong interference at neighbouring FAPs (see Figure 2.7). To increase their throughput, F-UEs can decide to cooperate with a group of M-UEs forming a coalition, where transmission are managed at the F-UE and separated in time in a TDMA fashion. Each member of the coalition perceives a payoff that is measured as the ratio between the experienced capacity and related latency. Note that, such a payoff depends for both macro and femto users on the amount of power/band that the F-UE uses to relaying M-UEs messages and the remaining part that is used to transmit its own packets. At the best of our knowledge, this proposal is the first that consider device to device communication to enable cooperative transmission in two-tier cellular networks. However, two main challenges arises in this work: first, this kind a cooperation results in security problems due to the exchange of data amongst coalition partners; second, relaying through the FAP introduce additional latency, due to the transmission over the IP-based backhaul, that can results in poor performance at the M-UEs.

Cheng *et al.* have proposed a mixed transmission strategy, which enhances the femtocell SE [144]. In such strategy F-UEs access idle RBs (as in the interweave approach) and further exploit the opportunities that arise during M-BS retransmissions. In particular, each FAP overhears transmissions originated at the M-BS so that during the retransmissions, F-UEs can transmit their data and FAPs are able to eliminate or mitigate the perceived interference. To be aware of retransmission events, it is assumed perfect synchronization between femtocells and the macrocell; hence FAPs are able to detect the retransmission feedback sent by neighbouring M-UEs. Moreover, the authors have presumed that each F-UE knows the channel statistics of the links between M-BS and M-UE, between M-BS and itself, and between M-UE and itself.

The process of interference mitigation is divided into two stage as illustrated in Figure 2.37. In stage *S0*, a FAP overhears the data transmitted by the M-BS while its F-UE is idle. When M-UE does not correctly decode the received message, it sends a Negative Acknowledgement (NACK) to the M-BS requiring a retransmission. This NACK is received also at the FAP, which schedules

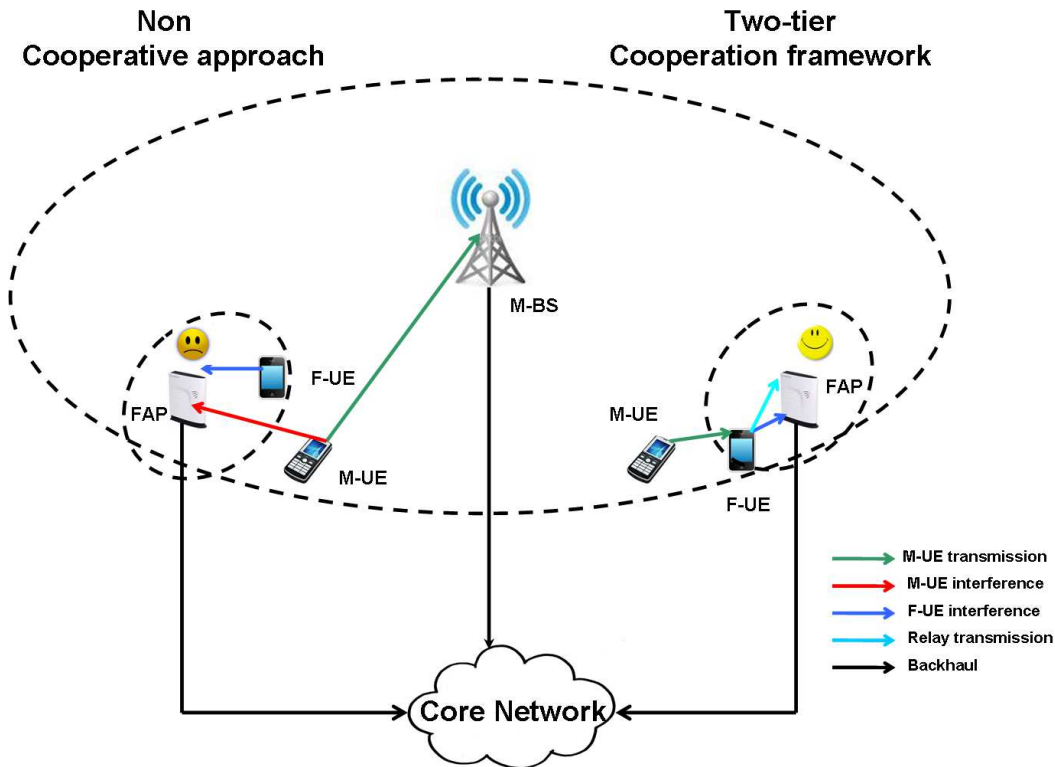


Figure 2.36: Two-tier network cooperation framework [143].

its F-UEs in the next slot. Thus, in stage $S1$ the M-BS and the F-UE transmit simultaneously. Furthermore, the FAP exploits the message received at the stage $S0$ to improve its decoding capability. Whenever it is able to correctly decode the M-BS message it completely eliminates the perceived interference, otherwise it optimally combines both the data received in $S0$ and $S1$ to maximize the experienced SINR.

Moreover, femtocells decide to access to retransmission slots according to a given probability p . The optimal value of p is numerically computed to maximize the femtocell SE. Furthermore, to limit the femto-to-macro interference during retransmissions, the transmission power at the F-UE is constrained by a maximum value. This power is computed such as the outage probability constraint at the M-UE is satisfied. The proposed strategy strongly ameliorates the SE achieved with the classic interweave approach, however its efficacy is related to the precision of synchrony between the macrocell and femtocells and the channel statistics awareness at FAPs. These are complex tasks, which require high overhead and may need signalling between the M-BS and FAPs.

Eventually, we resume in Table 2.4 the main features of the analysed interference mitigation/cancellation techniques. The first column indicates the bibliography reference of such reviewed schemes and the second column describes the investigated interference scenario. The third and the fourth columns indicate the cellular technology and the transmission scenario (i.e., uplink or downlink) in which the algorithm is implemented. The fifth and the sixth columns describe the FAP access type and the kind of cooperation that is exploited by the proposed strategy. A FAP can cooperate with the underlying M-BS as in [102], with neighbouring FAPs as in [105], or both type of coordination can be implemented as in [132]. Obviously, cooperation has a direct impact

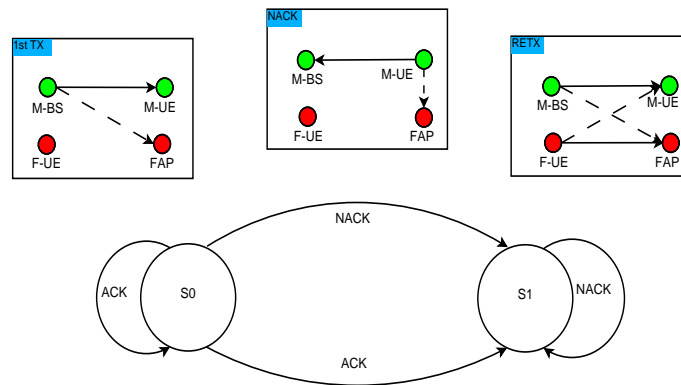


Figure 2.37: The overlay transmission scheme proposed by Cheng *et al.*[144].

on both the overhead and the system complexity, which are indicated in column seven and eight, respectively. Note that to give a qualitative description of the algorithm complexity we have taken into account also the number of transceivers required at the devices, the type of information (such as location of the M-UE, scheduling, channel gain) needed and the architecture (i.e., centralized or distributed) required.

Ref.	Interference	Tech.	Scenario	Access	Coop.	Overhead	Compl.
[127]	Cross-tier	WiMax	DL	Closed	No	High	High
[102]	Cross-tier	LTE	UL/DL	Closed	Macro	High	High
[105]	Co-tier	/	DL	Closed	Femto	Medium	High
[112]	Cross-tier	LTE	DL	Closed	Macro	High	High
[121, 122]	Cross-tier/co-tier	LTE	UL/DL	Closed	No	Low	Low
[126]	Cross-tier/co-tier	WiMax	UL/DL	Open	Macro	Average	High
[128]	Cross-tier/co-tier	LTE	UL	Closed	No	Low	High
[132]	Cross-tier	/	DL	Closed	Macro/femto	High	High
[133]	Cross-tier	/	UL	Closed	Macro	Medium	High
[134]	Co-tier	/	UL/DL	Closed	No	Low	Medium
[5]	Co-tier	LTE	UL/DL	Closed	Femto	Medium	Medium
[135]	Cross-tier/co-tier	/	UL/DL	Closed	Femto	High	High
[139]	Cross-tier	LTE	UL/DL	Closed	Macro	Medium	High
[144]	Cross-tier	LTE	UL	Closed	Macro	Medium	High
[145]	Co-tier	LTE	DL	Closed	No	Low	Low
[146]	Cross-tier/co-tier	LTE	DL	Closed	No	Low	Low
[143]	Cross-tier	/	UL	Closed	Macro	Medium	High

Table 2.4: Characteristics of analysed CR-based RRM schemes.

2.4.4 Green Agile Femtocell Networks

Femtocell networks have been proposed as an efficient and cost-effective approach to enhance cellular network capacity and coverage. Recent economical investigations claim that femtocell deployment might reduce both the Operational Expenditure (OPEX) and Capital Expenditure

(CAPEX) for cellular operators [147]. A recent study [148] shows that expenses scale from \$ 60000/year/macrocell to \$ 200/year/femtocell. However, according the ABI Research [4], by the end of 2012, more than 36 million of femtocells are expected to be sold worldwide with 150 million of customers. Cellular network energy consumption might be drastically increased by the dense and unplanned deployment of additional BSs. The growth of energy consumption will cause an increase in the global CO_2 emissions and impose more and more challenging operational costs for operators.

Although the model presented in Section 2.2.2.3 permits to understand trade-offs related to the femtocell deployment, relationships between EE, service constraints, and deployment efficiency are not straightforward and reducing the overall energy consumption while adapting the target of SE to the actual load of the system and QoS emerges as a new challenge in wireless cellular networks.

Furthermore, most of the literature aims to underline how much energy gain is achievable by deploying femtocells in the macrocell region [149], few practical algorithms have been proposed to enhance the two-tier network EE.

A general classification of such energy-aware mechanisms can be realized according to the temporal scale in which they operate (cf. Figure 2.4). Deployment of additional femtocells, which offload the neighbouring macrocell and improve the network EE, is realized in a long-time scale (such as weeks). Due to the static characteristic of the indoor femtocell deployment scenarios, mechanisms that depend on the cell load, such as dynamic cell switch-off [150] and cell zooming [151] operate in mid-time scale (e.g., hours). Finally, energy-aware resource allocation schemes are implemented in short-time scale (e.g., the system scheduling period).

López-Pérez *et al.* have investigated a short-time scale scheme, where self-organizing femtocells independently assign MCS, RBs and transmission power levels to UEs, while minimizing the cell RF output power and meeting QoS constraints [145]. In such scenario, FAPs are aware of the spectrum usage at nearby femtocells and tend to allocate less power to those UEs that are located in the proximity of the serving FAP or have low data rate requirements. Subsequently, nearby FAPs allocate UEs with bad channel condition or high data rate constraints on those RBs characterized by low interference. Thus, in the proposed algorithm, neighboring femtocells dynamically control inter-cell interference without any coordination or static frequency planning. However, the authors have not considered the impact of the proposed scheme in terms of femto-to-macro interference. M-UEs are affected by the aggregate interference produced by nearby FAPs. As shown in Figure 2.38, the discussed approach creates spikes of interference, which may corrupt macrocell transmissions, especially in high density femtocells scenarios.

Cheng *et al.* have proposed a more effective power optimization strategy [146]. The authors have considered a scenario in which femtocell and macrocell are deployed on orthogonal bands to avoid cross-tier interference. Furthermore, the spectral reuse between femtocells is limited to control the co-tier interference. System EE is measured through the *green factor*, which is defined as

$$green\ factor = \frac{W(rT_m + (1-r)N_f r_f T_f)}{P_{system}^T} \quad (2.11)$$

where W is the cellular bandwidth, r is the ratio between the number of channel dedicate at the macrocell and the total available channel, T_m is the macrocell downlink throughput, N_f is the number of deployed FAPs, r_f is the spectral reuse factor at femtocells, T_f is the femtocell downlink throughput, and P_{system}^T is the aggregate system power consumption of both macro and femtocells. Therefore, the proposed strategy aims to efficiently share the spectrum between M-BSs and FAPs to maximize the green factor while guaranteeing a certain SE at both M-UEs and F-UEs. However, even though the proposed approach results in limited interference and low complexity it may

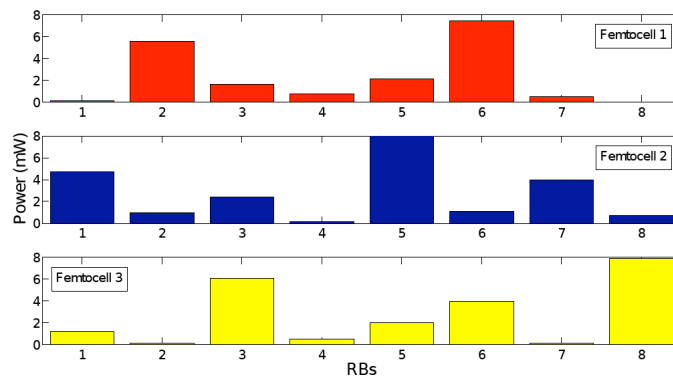


Figure 2.38: RB and power allocation of three neighbouring FAPs according to the scheme proposed by López-Pérez *et al.* [145].

not be suitable in realistic scenarios, where SE constraints of different UEs can strongly vary. Furthermore, due to the orthogonal bandwidth deployment, it can result in low SE performance for both M-UEs and F-UEs, especially in deployment scenarios characterized by a high density of femtocells.

Higher EE can be achieved by dynamically switching off those FAPs that are not serving active users. Idle FAPs disable pilot transmission and associated radio processing that represent the strongest contribution to the femtocell system power consumption. Dynamic femtocell switch on/off is capturing the attention of both operators and researchers because it can introduce an important energy gain without seriously affecting UEs performance. In fact, in this scenario, cellular coverage is guaranteed by the active macrocell, while femtocells dynamically create high capacity zones adapting their activity status to the UE deployment.

Ashraf *et al.* have proposed to equip FAPs with an energy detector that permits to *sniff* the presence of a nearby M-UEs [150]. As previously discussed, an indoor UE, which is served by the M-BS, likely transmits with high power; hence it is easy to detect. Detection threshold is computed at femtocell by estimating the path loss to the M-BS, such that UEs located at the femtocell edge can be correctly detected (see Figure 2.39). Henceforth, when an UE is detected, the FAP switches in active mode and whether the UE has the right to access the femtocell, the handover process is initiated. Otherwise, the FAP reverts to the deactivated mode. Simulation results have shown the proposed approach can lead to high energy gain. However, in high density scenarios the aggregate energy received from different sources of interference can cause false alarm events that affect the detection reliability.

To avoid additional hardware at FAPs, the authors extend the energy detector based proposal introducing two novel algorithms to control the femtocell activity [8]. In the first scheme, the femtocell status is managed by the core network, which is in charge to transmit a specific message via the backhaul that control FAPs activation/deactivation. The core network exploits the knowledge about the UE position to find FAPs to which the UE is able to connect. Therefore, this solution has the advantage to distinguish between registered UEs that can be served by CSG FAPs and unregistered UEs that can be served only by open/hybrid access femtocells. Furthermore, this approach permits also to take a centralized decision that consider the a global knowledge of the network status. In the second scheme the femtocell activity is controlled directly by the UE. Two approach are feasible: in the first case, a UE served by the M-BS periodically broadcast a wake-up message to find idle FAPs in its range. In the second case, a reactive scheme is followed: UEs send the wake-

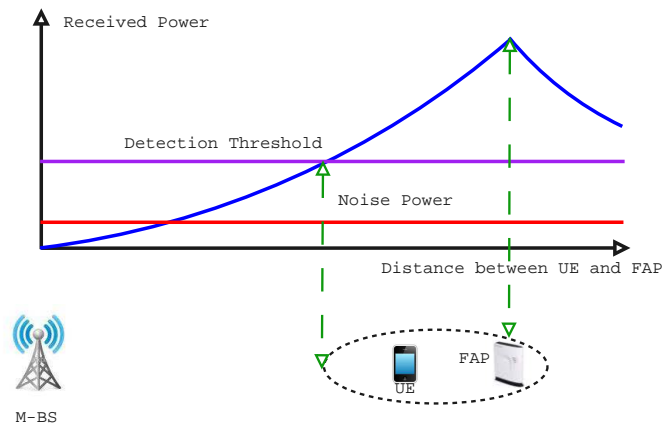


Figure 2.39: UE detection scheme in cell switch-off strategy [150].

up message either when they experience poor performance from the M-BS or when they require higher data rate. In both the scheme FAPs are required to be able to detect the wake-up message during the sleep mode. This message could include identification information such that closed access femtocell wake up only for registered UEs. The UE controlled scheme suffers mainly by two drawbacks: first it increases the UE battery consumption, especially in the proactive version. Furthermore, it requires the specification a robust physical/logical wireless control channel where UE can send the wake-up message.

An alternative solution is proposed by Telefonica [152], where the UE detection is based on usage of a Short Range Radio (SRR) interface, such as Bluetooth Low Power. Furthermore, to reduce the power consumption, the SRR interface is maintained in stand-by as much as possible, and it is activated only when the UE is located nearby its serving FAP. In fact, UEs store a database, named as femto-overlapping macrocells list, which includes the IDs of M-BSs located in the serving FAP neighbourhood. A UE camping in any of these M-BSs activates its SRR interface (passing from stand-by mode to initiating mode) and starts searching for advertising packets broadcast by its FAP. Subsequently, whether the UE is allowed to access the FAP, the two SRR change in connect status, and after the connection is created the FAP switch on its RF apparatus. This method is reliable because it is based on a point-to-point connection between the FAP and its UE; however, the main drawback is that currently there are no practical solutions to pass the FAPs from the stand-by mode to the advertising mode. Hence, FAPs should always maintain their SRRs activated, decreasing the system EE and increasing interference in the already overcrowded ISM bands.

Dynamic cell switch off mechanisms are inherent to FAPs that are not serving active UEs; however, cell DTX [2] has been recently proposed to enhance EE of lightly loaded systems.

Cell DTX is implemented on a fast-time scale and allows the BS to immediately switch off cell specific signalling during subframes where there are no user data transmissions. Such a fast adaptation mechanism may allow a great energy saving especially in low traffic scenarios. However, connectivity issues arise as UEs may not be able to detect a cell in DTX mode. Therefore, this mechanism may result in excessive handover latency and packet loss.

2.5 Conclusions

Femtocells have been proposed as a cost-effective solution to uniformly offer high data rate services in cellular networks. However, in this scenario, novel challenges arise due to the unplanned and dense deployment of additional BSs, which operate in uncoordinated way. Including cognitive principles in two-tier networks can allow to dynamically manage the femtocell activity and also to mitigate generated/perceived interference. Henceforth, the design of efficient and robust cognitive-aware strategies for two-tier networks is an interesting research field. Here, we aim to underline some open issues on the domain that we are tackling in the following chapters:

- Classically, researchers have tried to develop spectrally efficient systems to enable heterogeneous networks to coexist within the same spectrum. Nevertheless, recent studies showed how spectrum scarcity is almost due to static resource allocation strategies and that CR can notably improve the spectrum usage. However, the femtocell deployment requires a new paradigm because of two main reasons. First, F-UEs can benefit from a high quality down-link signal enabled by short range communications characterizing femtocell deployments. Second, only few users locally compete for a large amount of frequency resources in a femtocell. Therefore, a femtocell may benefit from a huge amount of available spectral/power resources. In this context, novel *green* agile mechanisms can be investigated to save power consumption, reduce interference, and improve battery life of customer's devices.
- Most of the work proposed in the literature does not jointly investigate both co-tier and cross-tier interference (see Table 2.4). To justify this lack often researchers either consider an orthogonal spectrum sharing approach or claim that femto-to-femto interference is negligible. However, orthogonal spectrum sharing strongly limits the network capacity and due to the massive deployment of femtocell expected in the near future, co-tier interference can strongly affect users' performance. Therefore, novel interference management are necessary to ameliorate femto and macro transmission robustness.
- Amongst the discussed studies, only one paper [126], has considered the Open Access Femtocell case. However, this is a very promising scenario in both terms of SE (due to the less perceived/generated interference) and EE (due to the increased macrocell offloading). Cognitive algorithms can represent a powerful instrument to deal with the problem inherent to this scenario such as the frequency of handover and femto-to-femto interference.
- As mentioned in the previous section, most of the contribution in the field attempt to investigate the amount of energy that can be saved through the femtocell deployment. In fact, the research community has proposed few work to improve the femtocell network energy efficiency. Investigations on dynamic cell switch off avoid energy wastage at femtocells in absence of active users. However, novel agile mechanisms are required to manage the femtocell activity when neighbouring users are active, both in lightly loaded and in highly loaded scenarios.

Chapter 3

Green Ghost Femtocells

The femtocell deployment in cellular networks sets new challenges to interference mitigation techniques and radio resource management. In this chapter, we propose a novel paradigm that achieves effective spectral reuse between macrocells and femtocells while guaranteeing the performance of users served by both macro and femto base stations. In particular, our proposal exploits the characteristics of the femtocell deployment to limit the overall interference per chunk generated outside the coverage range of a femtocell while reducing the irradiated power in each resource block. We introduce two algorithms that implement such a strategy in both networked and stand-alone femtocell scenarios. Simulation results show that the proposed schemes enhance the energy efficiency of femtocells and improve both the macrocell and femtocell transmission robustness.

The chapter is organized as follows: In Section 3.1, we introduce the motivation for this study, related work, and our contribution. Then, in Section 3.2, we present the system model and related assumptions that are adopted in this chapter. In Section 3.4, we first detail the ghost femtocell paradigm and then, we introduce two radio resource management algorithms for stand-alone and networked femtocell. In Section 3.5, we analyse the performance of the proposed schemes and finally, in Section 3.6, we conclude the chapter.

3.1 Introduction

3.1.1 Motivation

Femtocell networks have recently gained attention as a technical solution to offer uniform broadband wireless service in indoor environment. F-UEs likely experience larger coverage, high quality link, and prolonged battery life. These advantages are mainly due the reduced distance between the user terminal and the FAP, the limited number of UEs served by a FAP, and reduced interference due to penetration and propagation losses. Moreover, cellular network offloading by femtocell deployment may enable a notable reduction of the OPEX at mobile operators.

However, as already mentioned in Chapter 2, such a novel architecture sets new challenges to interference mitigation techniques and RRM schemes.

In fact, macrocells and femtocells likely share the same spectrum in a given geographic region. Thus, M-UEs located nearby to FAPs can experience harmful femto-to-macro interference that can drastically corrupt the reliability of communication (see Figure 2.7). Similarly, neighbouring femtocells belonging to the same operator may also interfere with each other thus creating femto-to-femto interference (see Figure 2.8).

Moreover, CSG femtocell deployment introduces new challenges with respect to classic cellular network, where the usage of the X2 interface can enable ICIC through direct cooperation amongst neighbouring BSs. Therefore, femtocells need to be autonomous and self-adaptive to limit the undesired effects of interference at neighbouring cells.

3.1.2 Related Work

Most of the literature does not consider joint mitigation of co-tier interference and cross-tier interference (see Table 2.4) in co-channel femtocell deployment. Some authors, consider static or dynamic orthogonal resource allocation amongst femtocells and macrocells to avoid cross-tier interference; however, this approach limits the cellular network capacity [130].

For instance, Chandrasekhar *et al.* propose to split the available bandwidth such that resource partitioning is optimized with respect to both macrocell and femtocell users' rate constraints [23]. Moreover, the authors defined a *blind round-robin* scheduler to limit femto-to-femto interference. Other proposals suppose perfect spectrum sensing at femtocell and subsequently investigate only femto-to-femto interference [135]. Finally, some studies consider direct cooperation between M-BSs and FAPs [102, 112] to reduce the effect of the femto-to-macro interference; however, due to complexity and limited backhaul capacity, such coordination is infeasible in the current cellular systems.

Classically, researchers tried to develop spectral efficient systems to enable heterogeneous networks to coexist in the same bandwidth. However, femtocells require a different paradigm because of two main reasons. First, F-UEs can benefit from a high quality downlink signal due to the short range communication characterizing femtocell deployments. Second, only few UEs locally compete for a large amount of resource in a femtocell. Therefore, a femtocell benefits from a huge amount of transmission resources. In our vision, there is a need for designing novel low-complexity approaches for reducing interference, improving spectrum reuse and communications robustness in two-tier cellular networks.

3.1.3 Contribution

In this chapter, we focus on interference mitigation techniques based on resource allocation management. More precisely, we concentrate on both co-tier interference and cross-tier interference in LTE downlink scenarios.

We present a simple and effective method that improves the performance of macro and femto users in co-channel deployment. In particular, we apply techniques based on modulation and coding scaling to trade-off energy for frequency resources [153]. In this way, we can reduce the downlink transmission power per RB that is required to obtain a target bit rate in femtocells and subsequently decrease the overall generated interference.

Hence, we propose two schemes that exploit such an approach in both residential stand-alone and networked enterprise femtocell deployments. In the first scheme, referred to as *Ghost*_{SAF}, FAPs are not able to cooperatively mitigate the generated interference and they selfishly attempt to maximize the spectrum reuse. In the latter scheme, named as *Ghost*_{NF}, first we introduce a distributed method for estimating how neighbouring FAPs affect each other transmission reliability. Then, we define a femtocell controller that uses this information to locally coordinate the access of neighbouring femtocells and manage the FR amongst nearby FAPs.

The novelty of this chapter is based on a patent [P1], a journal paper [J1], and four conference papers [C1], [C2], [C3], and [C4].

3.2 System Model

We consider a two-tier wireless cellular network in which mobile terminals and BSs implement an Orthogonal Frequency Division Multiple Access (OFDMA) air interface based on 3GPP/LTE downlink specifications [154]. Orthogonal Frequency Division Multiplexing (OFDM) symbols are organized into a number of physical RBs consisting of 12 contiguous sub-carriers for 7 consecutive OFDM symbols. With a bandwidth W of 10 MHz, 50 RBs are available for data transmission.

Each user is allocated one or several RBs in two consecutive slots, i.e., the Transmission Time Interval (TTI) is equal to two slots and its duration T is 1 ms.

The overall channel gain \mathbf{g} is composed of the antenna gain, a fixed distance dependent path loss, a slowly varying component modeled by lognormal shadowing, and Rayleigh fast fading with unit power.

We assume that femtocells are deployed in a block of 10 m x 10 m apartments according to the 3GPP grid urban deployment model [31]. In such a scenario each FAP can simultaneously serve up to to 4 users. The block of apartments belongs to the same region of a macrocell, which share the same bandwidth of the neighbouring femtocells. Moreover, we assume that 6 additional M-BSs surround the central macrocell generating additive interference for both macro and femto users.

Further details on the femtocell deployment and related signal propagation models are presented in Section 2.2.2.1.

Table 3.1 shows key model parameters including shadowing, fast fading, the macrocell antenna gain, and the transmission power.

Theoretic Limits in Non-Ergodic Block Fading Channels

We can characterize many delay-constrained communication systems such as OFDM systems as instances of a block fading channel. Since the momentary instance of the wireless channel has a finite number of states, the channel is not-ergodic and it admits a null Shannon capacity [155].

Parameter	value
Carrier frequency	2.0 GHz
Carrier bandwidth	$W=10.0$ MHz
Total number of Resource Blocks	$N_{RB}=50$
Inter-site distance	500 m
M-BS Tx power	40W
M-BS antenna gain after cable loss	13 dB
FAP antenna gain after cable loss	0 dB
Maximum number of UE served by a single FAP	$N_{max} = 4$
Shadowing distribution	Log-normal
Shadowing standard deviation	8 dB
Autocorrelation distance of shadowing	50 m
Fast fading distribution	Rayleigh
Thermal noise density	$N_0=-174$ dBm/Hz

Table 3.1: Main system model parameters.

The information theoretical limit is established by defining an outage probability $P_r(\text{out})$ such as the probability that the instantaneous mutual information for a given fading instance is smaller than the nominal SE η associated with the transmitted packet:

$$P_r(\text{out}) = P_r(I(\gamma, \alpha) < \eta),$$

where $I(\gamma, \alpha)$ is a random variable representing the instantaneous mutual information for a given fading instance α and γ is the instantaneous SINR. For an infinitely large block length, $P_r(\text{out})$ is the lowest error probability that can be achieved by a channel encoder and decoder pair. Therefore, when an outage occurs, the correct packet decoding is not possible, hence $P_r(\text{out})$ is an information theoretical bound on the packet error rate. To obtain $P_r(\text{out})$, it is necessary to compute $I(\gamma, \alpha)$ associated with the current channel measurement on each group of RBs (M OFDM symbols x N subcarriers):

$$I(\gamma, \alpha) = \frac{1}{M \cdot N} \sum_{i=1}^M \sum_{j=1}^N I_{ij} \left(|\alpha_{i,k}|^2, \sigma_k^2 \right)$$

where

$$I_{ij} \left(|\alpha_{i,k}|^2, \sigma_k^2 \right) = \log_2(A) - \frac{1}{A} \sum_{k=1}^A E_z \left[\log_2 \left(\sum_{q=1}^A A_{i,j,k,q} \right) \right] \quad (3.1)$$

and

$$A_{i,j,k,q} = \exp \left[- \frac{|\alpha_{ij} a_k + z - \alpha_{ij} a_q|^2 - |z|^2}{2\sigma^2} \right]$$

Note that Eq. (3.1) is derived from the work of Ungerboeck [156], where A is the size of the M-QAM modulation alphabet, \mathbf{a} is the real or complex discrete signal transmitted vector, and \mathbf{z} are the Gaussian noise samples with variance σ^2 .

3.3 Energy per Bit versus Spectral Efficiency

SE has been classically considered as the main criterion to optimize performance in communication systems. Recently, energy consumption is rising as an important design metric to achieve *green* communications in future cellular networks. Preliminary results on the relation between Energy per information bit (E_b) and SE are based on seminal work of Shannon in [157], from which Golay in [158] derived the minimum amount of received energy per bit of information (E_b^r) to reliably communicate over AWGN channels:

$$E_b^r = N_0 \log_e 2 \quad (3.2)$$

where N_0 is the one-sided noise spectral level. This result can be obtained only at cost of infinite bandwidth and therefore null SE [159]. In realistic scenarios, the required E_b of information is strictly greater than the value achieved when Shannon capacity is considered [159]. Moreover, it is important to note that, considering only RF irradiated power, as in [159, 160], can lead to misleading conclusions. In such a model, irradiated E_b monotonically increases with the SE (see the star-marked curves in figure 3.1). Therefore, using the lowest order of MCS, which limits the SE, may be assumed to be the best strategy to minimize energy consumption [160].

On the contrary, when a more realistic model, which includes the energy consumption due the various components of the BS transceiver, is considered, the relation between E_b and SE is given by

$$E_b = \frac{P_0}{W \cdot \eta} + \frac{\Delta_p \cdot (2^\eta - 1)}{\gamma_0 \cdot W \cdot \eta} \quad (3.3)$$

where P_0 and Δ_p are parameters defined in the power consumption model discussed in Section 2.2.2.3, W is the channel bandwidth, and γ_0 is the normalized SINR experienced at the receiver. Therefore, a joint optimization of SE and energy consumption can allow more efficient communication [161]. In particular, assigning higher orders of MCS to those UEs that experience high SINR (e.g., UEs that are close to the serving BS) may enable greater energy savings (see the solid curves in Fig. 3.1).

Nevertheless, trading-off bandwidth for irradiated power has also been proposed to improve two-tier network capacity by exploiting under-utilized frequency resources at femtocells. In particular, Guvenc and Kozat analysed the benefits of such approach on the capacity of two neighbouring femtocells [162]. We extended such investigation considering the presence of a co-channel M-BS located nearby a dense femtocell network [163]. Moreover, we underlined as the joint implementation of MCS scaling and power control may limit co-channel interference and increase transmission robustness. However, these works attempted to see how much throughput gain can be achieved rather than developing algorithms that can be implemented in practice.

3.4 Green Ghost Femtocells: the Proposed Interference Mitigation Paradigm

3.4.1 Problem Statement

Consider a region where macrocells ($\mathcal{M} = \{1, \dots, N_M\}$) are overlaid by a set of femtocells $\mathcal{F} = \{1, \dots, N_F\}$ deployed in a block of apartments as described in Section 3.2. Each M-BS serves outdoor UEs and indoor UEs ($\mathcal{M} \mathcal{U} \mathcal{E} = \{1, \dots, N_{MUE}\}$) that can not be served by active FAPs. Femtocells operate in the same bandwidth of macrocells and offer service to indoor UEs ($\mathcal{F} \mathcal{U} \mathcal{E} =$

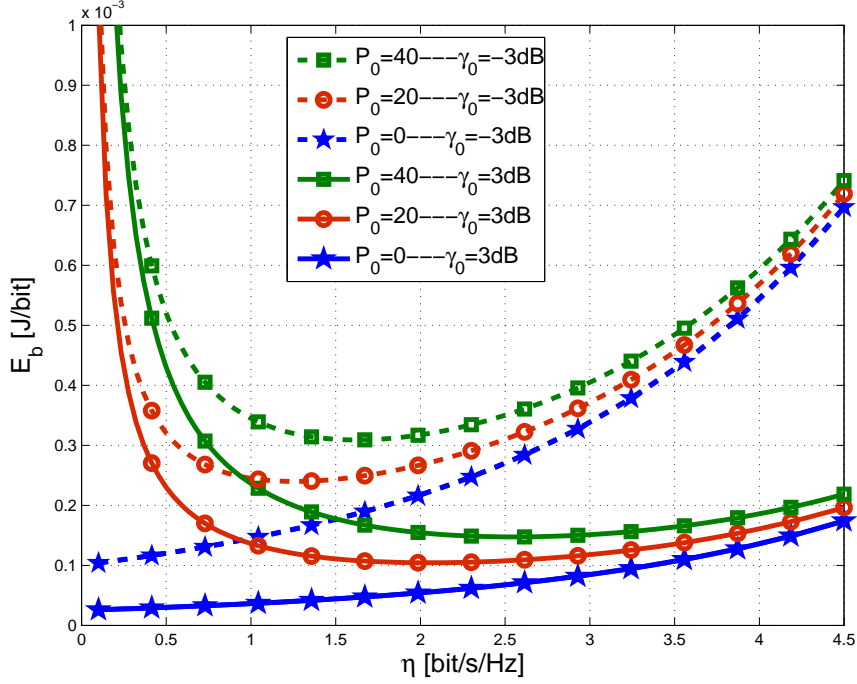


Figure 3.1: Energy per bit versus Spectral Efficiency trade-off. Star-marked, circle-marked, and square-marked curves respectively correspond to scenarios in which the BS minimum power consumption P_0 is equal to 0W, 20W, and 40W. Dashed and solid curves respectively correspond to results obtained for scenarios with normalized SINR γ_0 equals to -3dB and 3dB.

$\{1, \dots, N_{\text{FUE}}\}$ that are located in their coverage areas. Therefore, indoor M-UEs locate in the proximity of deployed FAPs likely experience poor performance due to interference and propagation losses.

The instantaneous SINR can measure such a performance for each M-UE/RB pair $(n,k) \in \mathcal{MUE} \times C_h$

$$\gamma_{l,n,k} = \frac{|g_{l,n,k}|^2 P_{l,k}^{\text{RF}}}{\sum_{m \in M \setminus l} |g_{m,n,k}|^2 P_{m,k}^{\text{RF}} + \sum_{f \in F} |g_{f,n,k}|^2 P_{f,k}^{\text{RF}} + \sigma^2}, \quad (3.4)$$

where $C_h = \{1, \dots, N_{\text{RB}}\}$ is the set of available RBs and $g_{l,n,k}$, $g_{m,n,k}$, and $g_{f,n,k}$ represent the channel gain on the RB k between the M-UE n and the associated M-BS l , the interfering M-BS m , and the interfering FAP f , respectively.

Accordingly, the instantaneous SINR can measure the performance for each F-UE/RB pair $(j,k) \in \mathcal{FUE} \times C_h$

$$\gamma_{i,j,k} = \frac{|g_{i,j,k}|^2 P_{i,k}^{\text{RF}}}{\sum_{m \in M} |g_{m,j,k}|^2 P_{m,k}^{\text{RF}} + \sum_{f \in F \setminus i} |g_{f,j,k}|^2 P_{f,k}^{\text{RF}} + \sigma^2} \quad (3.5)$$

where $g_{i,j,k}$, $g_{m,j,k}$, and $g_{f,j,k}$ represent the channel gain on the RB k between the F-UE j and the associated FAP i , the interfering M-BS m , and the interfering FAP f , respectively.

FAPs are generally not aware of the M-BS scheduling pattern and can hardly estimate the RBs that they should refrain to allocate. Therefore, we take advantage of the unusual communication context of femtocells for which few users compete for a large amount of transmission resources. We aim to limit peaks of irradiated power at FAPs to underlay macrocell transmissions while exploiting under-utilized frequency resources and satisfying QoS constraints of F-UEs.

This optimization problem can be expressed as

$$\min \max_{k \in C_h} P_i^{\text{RF}} \quad \forall i \in \mathcal{F}$$

s.t.

$$\sum_{k \in C_h} P_{i,k}^{\text{RF}} \leq P_{\max}^{\text{RF}} \quad \forall i \in \mathcal{F} \quad (3.6)$$

$$\sum_{k \in C_h} R_{k,j} \geq T_{\text{tg}} \quad \forall j \in \mathcal{F} \mathcal{UE} \quad (3.7)$$

$$\sum_{j \in \mathcal{F} \mathcal{UE}^i} S_{j,k}^{\text{Ch}} \leq 1 \quad \forall k \in C_h, \quad (3.8)$$

where $\mathcal{F} \mathcal{UE}^i = \{1, \dots, N_i\}$ is the set of F-UEs associated to the FAP i and S^{Ch} is the RB allocation matrix of size $[N_i \times N_{\text{RB}}]$.

Eq. 3.6 indicates that the overall irradiated power P^{RF} is constrained by the maximum RF output power P_{\max}^{RF} , Eq. 3.7 points out that, at each F-UE, the aggregate throughput R has to satisfy the QoS constraint T_{tg} , and Eq. 3.8 indicates that the same RB can not be allocated to different UEs that belong to the same cell.

To achieve such goal we propose a heuristic RRM approach that jointly exploits

1. a *matrix-based* scheduler [164] that iteratively picks the best user-RB pair to find the minimum amount of frequency resources necessary to satisfy the user rate constraints;
2. a spreading scheme that allocates to each scheduled UEs additional RBs lowering the MCS order associated to each transmission;
3. a power scaling algorithm that adjusts the power irradiated in each RB to meet the SINR threshold given by the target Packet Error Rate (PER) and the selected MCS.

In the following, we describe the implementation details of these main steps in both stand-alone and networked femtocell scenarios.

3.4.2 The Proposed Ghost_{SAF} for Green Stand-Along Femtocells

In stand-alone case, FAPs are not able to exchange information to coordinate their access to the radio medium. Each F-UE periodically feedbacks Channel Quality Indicator (CQI) at its serving FAPs. Note that the frequency and the amount of sent CQI values determine the reliability of Channel State Information (CSI) at the FAP side; therefore, there is a trade-off between the undesired overhead and the CSI effectiveness.

Each TTI, according to the selected scheduling algorithm and CSI measurements, the FAP i computes the scheduling metric

$$\lambda_{j,k} = \gamma_{i,j,k} \quad \forall (j,k) \in \mathcal{F} \mathcal{UE}^i \times C_h \quad (3.9)$$

where $\gamma_{i,j,k}$ represents the instantaneous SINR perceived on the RB k at the UE $j \in \mathcal{F} \mathcal{UE}^i$ (cf. Eq. 3.5).

Note that $\gamma_{i,j,k}$ is computed according to Eq. 3.5 and considering a flat RF power allocation such that

$$P_{i,k}^{\text{RF}} = \frac{P_{\text{max}}^{\text{F}}}{N_{\text{RB}}} \quad \forall (i,k) \in \mathcal{F} \times \mathcal{C}_h \quad (3.10)$$

Although any conventional scheduler is suitable, here we consider a PF-based scheduler [142], hence, during the scheduling process λ is iteratively update as

$$\lambda_{j,k} = \frac{\gamma_{i,j,k}}{\sum_l^K \gamma_{i,j,l}}, \quad (3.11)$$

where $\sum_l^K \gamma_{i,j,l}$ is the sum of SINR of K RBs that have been allotted to the user j .

Therefore, our algorithm uses the metric λ to construct the scheduling matrices \mathbf{M}^{Tx} and \mathbf{M}^{Sp} of dimension $[N_i \times N_{\text{RB}}] \forall i \in \mathcal{F}$.

Based on \mathbf{M}^{Tx} the scheduler allocates to each active user the minimum number of RBs necessary to satisfy power (Eq. 3.6) and QoS (Eq. 3.7) constraints. However, the matrix \mathbf{M}^{Sp} is used in the spreading process to allocate further RBs to each scheduled UE and reduce irradiated power at FAPs.

First, the algorithm finds the best user-RB pair that maximizes the scheduling matrix \mathbf{M}^{Tx} . Second, according to the SINR thresholds indicated into a pre-defined Look-Up-Table (LUT), named as $\mathbf{SINR}^{\text{th}}$, the algorithm associates to the selected user-RB pair the highest possible MCS (see Table 3.2). Then, the algorithm updates the user throughput \mathbf{R} according to the vector \mathbf{PS} , which indicates the number of data bits that can be transmitted in a RB with a given MCS. If the aggregate rate satisfies QoS constraints the UE is successfully served. This process ends either when all UEs have been scheduled or if all RBs have been allotted.

Algorithms 1 and 2 give a detailed description of the first step of the scheduling process.

MCS mode	$\mathbf{SINR}^{\text{th}}$ [dB]	Modulation	Coding	η	Packet Size (\mathbf{PS}) [bits]
1	-0.46	QPSK	1/3	2/3	96
2	1.84	QPSK	1/2	1	144
3	3.95	QPSK	2/3	4/3	192
4	4.27	16-QAM	1/3	4/3	192
5	4.88	QPSK	3/4	3/2	216
6	6.97	16-QAM	1/2	2	288
7	7.82	64-QAM	1/3	2	288
8	9.67	16-QAM	2/3	8/3	384
9	10.89	16-QAM	3/4	3	432
10	11.16	64-QAM	1/2	3	432
11	14.44	64-QAM	2/3	4	576
12	16.05	64-QAM	3/4	9/2	648

Table 3.2: Packet Size and Spectral Efficiency for MCS.

It should be noted that the matrix \mathbf{M}^{Sp} indicates the RBs available after the first scheduling process. Subsequently, our scheme associates to served UEs additional available RBs where the original message is spread.

The goal of the spreading function is threefold. First, it increases transmission robustness of each allocated RB. Second, it permits to reduce the associated RF power. Third, it also limits the

Algorithm 1 Main

```

1: for all  $i \in \mathcal{F}$  do
2:    $\mathbf{S}^{\text{Ch}} = 0_{N_i, N_{\text{RB}}}$ 
3:    $\mathcal{S}^{\text{UE}} = \{\emptyset\}$ 
4:    $\mathbf{R} = 0_{N_{\text{RB}}, N_i}$ 
5:    $\text{MCS}^* = 0_{N_i, 1}$ 
6:    $\mathcal{X}_j = \{\emptyset\} \quad \forall j \in \mathcal{F}^{\text{UE}^i}$ 
7:    $\lambda_{j,k} = \gamma_{i,j,k} \quad \forall (j,k) \in \mathcal{F}^{\text{UE}^i} \times \mathcal{C}_i$  {see Eq. 3.9}
8:    $\mathbf{M}^{\text{Tx}} = \boldsymbol{\lambda}$ 
9:    $\mathbf{M}^{\text{Sp}} = \boldsymbol{\lambda}$ 
10:  while ANY( $\mathbf{M}^{\text{Tx}}$ ) do {see note below}
11:    Algorithm 2 {Scheduling}
12:  end while
13:  Algorithm 3 {Spreading}
14:  Algorithm 4 {Power Control}
15: end for

```

{line 10: **ANY**(\mathbf{v}) = TRUE **IF** $\exists 0 < i \leq |\mathbf{v}|$ s.t. $v_i \neq 0$ }

padding thus improving the SE. Algorithm 3 gives a describes the MCS scaling process in the proposed $\text{Ghost}_{\text{SAF}}$ RRM algorithm.

Finally, each FAP i estimates the SINR perceived at the served UE j and subsequently adjusts the allocated transmission power to meet the SINR threshold ($\text{SINR}_{\text{MCS}_j^*}^{\text{th}}$) given by the target PER and the selected MCS (MCS_j^*).

$$P_{i,k}^{\text{RF}} = \frac{\text{SINR}_{\text{MCS}_j^*}^{\text{th}} P_{\text{max}}^{\text{F}}}{\gamma_{i,j,k} N_{\text{RB}}} + \delta_{\text{M}} \quad \forall k \in \mathcal{X}_j, \quad (3.12)$$

where \mathcal{X}_j is the set of RBs allocated to the UE j and δ_{M} is a margin that takes into account CSI reliability.

Figure 3.2 represents main functionalities of the proposed $\text{Ghost}_{\text{SAF}}$.

3.4.3 The Proposed Ghost_{NF} for Green Networked Femtocells

Although the discussed ghost algorithm attempts to limit interference by limiting irradiated power per RB at FAPs, uncoordinated access of neighbouring femtocells to the same RBs can still lead to peaks of harmful interference for both M-UEs and F-UEs. However, as already mentioned, in networked femtocells scenario the availability of the X2 interface may enable direct cooperation amongst interconnected FAPs. Moreover, a local femtocell gateway characterized by additional functionalities can act as a FCS, which allows centralized coordination and inter-cell interference mitigation (see Figure 3.3).

In particular, our proposal is the following:

1. **Step 1** : Femtocells autonomously implement a distributed scheme for estimating how neighbour interferers may impact transmission reliability at each femtocell;

Algorithm 2 Algorithm that finds the active F-UEs that can be successfully served (\mathcal{S}^{UE}); it also associates to these F-UEs the RBs and related MCS to meet QoS and power constraints

- 1: $(j^*, k^*) = \operatorname{argmax}_{j,k} \mathbf{M}^{\text{Tx}}$
- 2: $\mathcal{K}_{j^*} = \mathcal{K}_{j^*} \cup \{k^*\}$
- 3: $\mathcal{L} = \{\lambda_{j^*,k} \mid k \in \mathcal{K}_{j^*}\}$
- 4: $\tilde{\lambda} = \mathbf{MAP}(\mathcal{L})$ {see note below}
- 5: $MCS = \max_s \{s \mid \tilde{\lambda} \geq SINR_s^{\text{th}}\}$
- 6: **if** $MCS \geq 1$ **then**
- 7: $S_{j^*,k^*}^{\text{Ch}} = 1$
- 8: $R_{k^*,j^*} = PS_{MCS}$
- 9: $\lambda_{j^*,k} = \frac{\gamma_{j,k}}{\sum_{l \in \mathcal{K}_{j^*}} \gamma_{j,l}} \quad \forall k \in \mathcal{C}_h$ {see Eq. 3.11}
- 10: **if** $\sum_{k \in \mathcal{C}_h} R_{k,j^*} \geq T_{\text{tg}}$ **then**
- 11: $M_{j^*,k}^{\text{Tx}} = 0 \quad \forall k \in \mathcal{C}_h$
- 12: $\mathcal{S}^{UE} = \mathcal{S}^{UE} \cup \{j^*\}$
- 13: $MCS_{j^*}^* = MCS$
- 14: **else**
- 15: $M_{j^*,k^*}^{\text{Tx}} = 0$
- 16: $M_{j^*,k}^{\text{Tx}} = \lambda_{j^*,k} \quad \forall k \in \mathcal{C}_h \setminus k^*$
- 17: **end if**
- 18: $M_{j,k^*}^{\text{Tx}} = 0 \quad \forall j \in \mathcal{F}^{UE^i} \setminus j^*$
- 19: $M_{j,k^*}^{\text{Sp}} = 0 \quad \forall j \in \mathcal{F}^{UE^i}$
- 20: $M_{j^*,k}^{\text{Sp}} = \lambda_{j^*,k} \quad \forall k \in \mathcal{C}_h$
- 21: **else**
- 22: $M_{j^*,k}^{\text{Tx}} = 0 \quad \forall k \in \mathcal{C}_h$
- 23: $M_{j^*,k}^{\text{Sp}} = 0 \quad \forall k \in \mathcal{C}_h$
- 24: **end if**

{line 4: $\mathbf{MAP}(\cdot)$ maps the SINR values of different allotted RBs to a Link Quality Metric (LQM) that predicts performance of an OFDMA system. Either the Exponential Effective SINR Mapping (EESM) [165] or the Mutual Information based Effective SINR Mapping (MIESM) [166] can be used here}

Algorithm 3 Spreading Algorithm

```

1: while ANY( $\mathbf{M}^{\text{Sp}}$ ) do {see note below}
2:    $(j^*, k^*) = \underset{j,k}{\text{argmax}} \mathbf{M}^{\text{Sp}}$ 
3:    $\mathcal{K}_{j^*} = \mathcal{K}_{j^*} \cup \{k^*\}$ 
4:    $\mathcal{L} = \{\lambda_{j^*,k} \mid k \in \mathcal{K}_{j^*}\}$ 
5:    $\tilde{\lambda} = \text{MAP}(\mathcal{L})$  {see note below}
6:    $MCS = \min_s \{s \mid \tilde{\lambda} \geq SINR_s^{\text{th}} \ \& \ |\mathcal{K}_{j^*}| \cdot PS_s \geq T_{\text{tg}}\}$ 
7:   if  $MCS \geq 1$  then
8:      $S_{j^*,k^*}^{\text{Ch}} = 1$ 
9:      $M_{j^*,k^*}^{\text{Sp}} = 0 \quad \forall j \in \mathcal{F} \ \mathcal{UE}^i$ 
10:     $MCS_{j^*}^* = MCS$ 
11:    if  $MCS = 1$  then
12:       $M_{j^*,k}^{\text{Sp}} = 0 \quad \forall k \in \mathcal{C}_h$ 
13:    else
14:       $\lambda_{j^*,k} = \frac{\gamma_{j,k}}{\sum_{l \in \mathcal{K}_{j^*}} \gamma_{j,l}} \quad \forall k \in \mathcal{C}_h$  {see Eq. 3.11}
15:       $M_{j^*,k}^{\text{Sp}} = \lambda_{j^*,k} \quad \forall k \in \mathcal{C}_h$ 
16:    end if
17:  else
18:     $M_{j^*,k}^{\text{Sp}} = 0 \quad \forall k \in \mathcal{C}_h$ 
19:  end if
20: end while

```

{line 1: ANY(\mathbf{v}) = TRUE **IF** $\exists 0 < i \leq |\mathbf{v}|$ s.t. $v_i \neq 0$ }

{line 5: MAP(\cdot) maps the SINR values of different allotted RBs to a LQM that predicts performance of an OFDMA system. Either the EESM [165] or the MIESM [166] can be used here}

Algorithm 4 Power Control

```

1: for all  $j \in \mathcal{S}^{\text{UE}}$  do
2:    $P_{i,k}^{\text{RF}} = \frac{SINR_{MCS_j^*}^{\text{th}} \cdot P_{\text{max}}^{\text{F}}}{\gamma_{i,j,k} \cdot N_{\text{RB}}} + \delta_{\text{M}} \quad \forall k \in \mathcal{K}_j$ 
3: end for

```

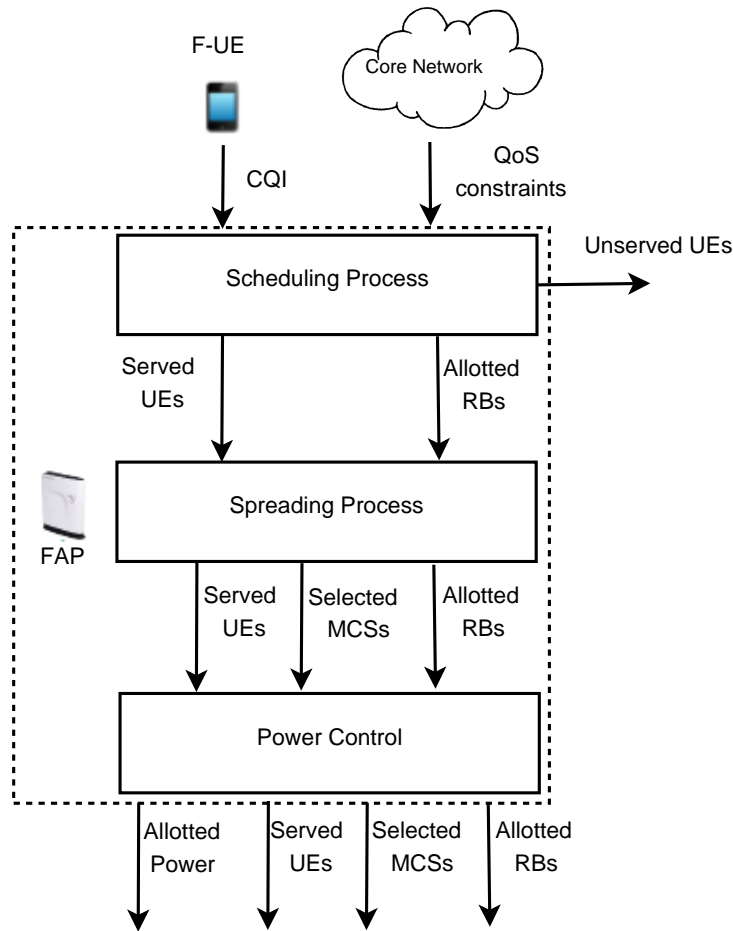


Figure 3.2: *Ghost_{SAF}*: proposed RRM algorithm for stand-alone femtocells.

2. **Step 2** : FAPs provide this information to a local FCS that allocates transmission resource in the coverage area of controlled FAPs;
3. **Step 3** : The FCS manages the access of neighbouring F-UEs and decides on FR amongst femtocells for which the estimated interference does not harm. In this way, the controller avoids peaks of interference while improving the spectrum reuse with respect to the orthogonal frequency resource allocation schemes;
4. **Step 4** : Finally, as discussed in the residential femtocell scenario, we apply techniques based on modulation and coding scaling to trade-off transmission energy for frequency resources. Such an approach allows reducing the downlink transmission power to obtain a given target bit rate in femtocells and it also limits the aggregate generated interference.

Although the latter step, which is composed of both MCS scaling and power control, has already been discussed in the previous paragraph, the former three steps represent the main novelty of the *Ghost_{NF}* and required further explanations.

In a cellular network, to support mobility, UEs use to continuously implement *cell search* mechanisms i.e., search for, synchronize to, and evaluate the reception quality of signals from neighbouring APs [167]. These functionalities enable to compare the signal received from the

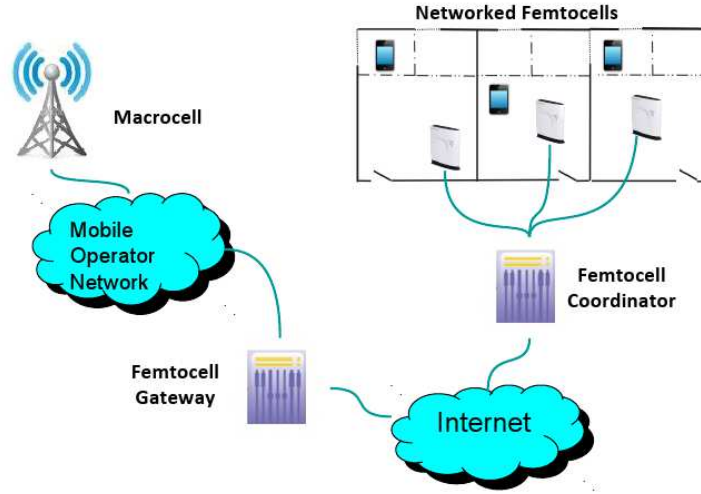


Figure 3.3: Proposed architecture for networked Ghost femtocells.

current serving AP with the signals of others cells and therefore decide whenever a *handover* or *cell reselection* processes have to be realized.

To allow cell search, two dedicated signals are transmitted by each AP on all component carriers, the Primary Synchronization Signal (PSS) and the Secondary Synchronization Signal (SSS).

In our work we do not deal with UE mobility, nevertheless, such functionalities allow each F-UEs to estimate and identify which neighbour FAPs are currently *strong* interferers. An interferer is strong if the related RSRP is larger than a predefined threshold; moreover, interferer identification is possible by jointly detection and identification of PSS and SSS, which carry the cell ID.

Hence, in the proposed scheme, each UE periodically sends to its serving FAP the cell ID of the strong interfering FAPs jointly with CQI reports. Subsequently, each FAP transfers this information to the FCS that constructs the interfering set \mathcal{V}_i of each served FAP i . Each scheduling period, the FCS uses the received feedback to implement a multi-cell scheduler, which manages the resource allocation in the femtocell network and limits the spectrum reuse amongst neighbouring FAPs. In fact, during this process, whenever a RB k is allotted to a given user $j \in \mathcal{F} \mathcal{U} \mathcal{E}^i$, the FCS eliminates k from the set of available RBs of all UEs that belong $\mathcal{F} \mathcal{U} \mathcal{E}^j$, where $j \in \mathcal{V}_i$. Note that, to avoid intra-cell interference, \mathcal{V}_i include also the UEs that belong to the same cell of UE j . Figure 3.4 represents the main functionalities of the proposed $Ghost_{NF}$. Further details on the $Ghost_{NF}$ are available in the Appendix A.

3.4.4 Complexity and Overhead of the RRM Ghost Algorithms

RRM Ghost algorithms can potentially enable the coexistence of a high number of femtocells in the macrocell region. Moreover, the proposed $Ghost_{NF}$ exploits femtocell coordination to limit inter-cell FR and therefore reduce both cross-tier and co-tier interference. However, such a scheme results in higher overhead and complexity with respect to $Ghost_{SAF}$.

The overhead is mainly due to the signaling exchange between FAPs and the FCS. Each

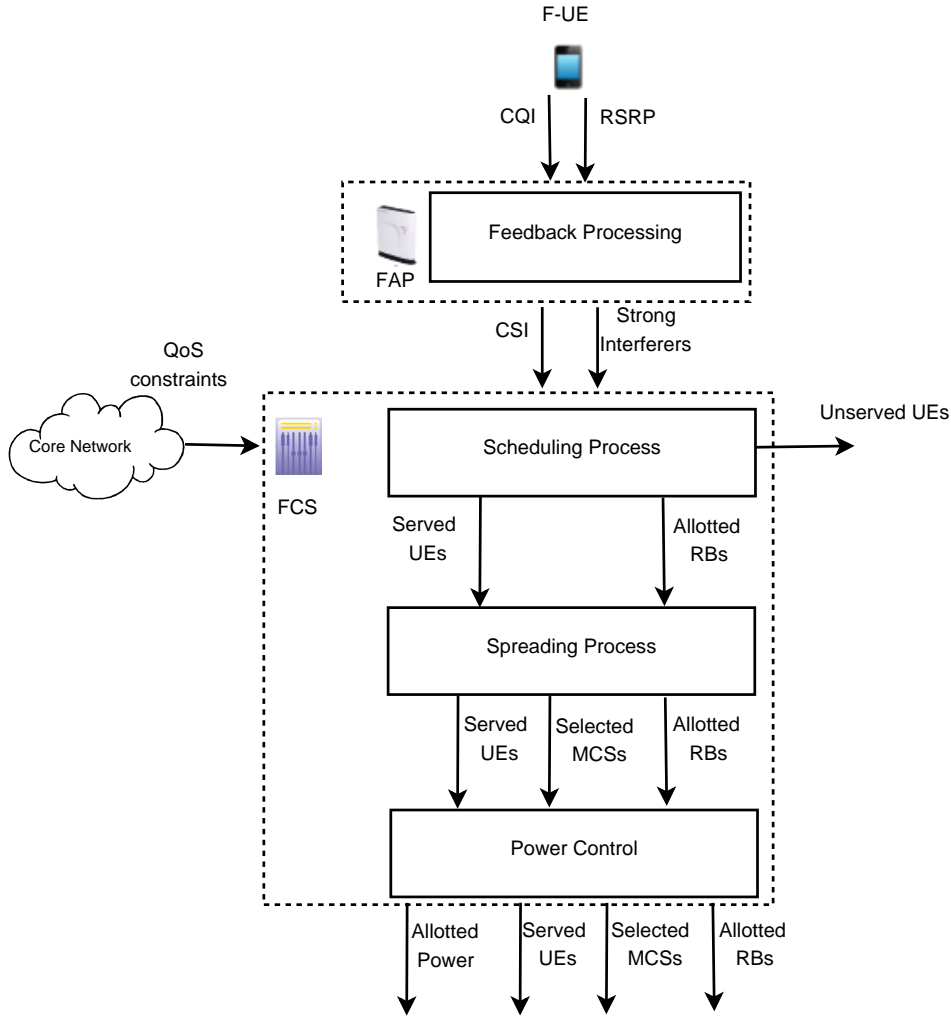


Figure 3.4: $Ghost_{NF}$: proposed RRM algorithm for networked femtocells.

scheduling period (i.e., N TTIs), first FAPs report to the network controller their CSI, then according to the RRM algorithm, the FCS feedbacks the decided scheduling pattern to each FAP. Furthermore, each M TTIs, FAPs in the network transmit to their controller the ID of the neighbouring FAPs, which are classified as strong interferers. Interference relationships amongst neighbouring FAPs depend on both the users' mobility and FAP activity status (on, off, sleep mode). Therefore, these sets slowly change during the time, and the frequency of related feedback is generally much lower than the scheduling period (i.e., $M \gg N$). For each femtocell network, such overhead can be expressed as follow

$$O_H = \frac{B \sum_{i=1}^{N_F} |\mathcal{V}_i| + \beta \cdot N_i \cdot N_{RB} (M + 1)}{M \cdot T} \left[\frac{bit}{s} \right], \quad (3.13)$$

where

$$M = \beta \cdot N,$$

B is the number of bytes used to represent the information, and T is the duration of one TTI. A further drawback of the centralized approach is its dependency on the FCS reliability,

which may result in low scalability in dense femtocell deployment. A distributed version of the discussed scheme, where signalling and computation costs are shared amongst neighbouring FAPs, is feasible. However, this solution would result in higher overhead and latency.

Due to the lack of inter-cell coordination, the proposed $Ghost_{SAF}$ is, on the contrary, characterized by limited overhead and complexity. Furthermore, it does not limit the spectrum reuse at FAPs. However, it may result in harmful interference, especially in dense femtocell deployment scenarios. In the next section, we aim at evaluating the impact of this interference by investigating the impact of the proposed algorithm at both M-UEs and F-UEs.

3.5 Simulation Results

In this section, we assess the effectiveness of the proposed $Ghost_{NF}$ and $Ghost_{SAF}$ by comparing their performance with a reference algorithm (RRM_{SOA}). The main differences between these schemes are the following:

1. In both $Ghost_{SAF}$ and RRM_{SOA} , there is no coordination within the femtocell network. Hence, FAPs are not aware of the presence and allocation strategy of neighbouring FAPs;
2. RRM_{SOA} aims at maximizing the SE of femtocells while minimizing the probability that users that belong to different cells access to same RBs. Thus, the RRM_{SOA} attempts to limit the number of RBs allotted to each F-UE;
3. RRM_{SOA} does not implement MCS and Power scaling (see Algorithms 3 and 4, respectively).

It is important to mention that RRM_{SOA} is also used at the M-BS in each investigated scenario.

We present simulation results for the system model and its parameters presented in Section 3.2. RRM algorithms are compared in terms of the following energy cost metric, which measures the average amount of irradiated energy required to transmit a bit of information:

$$\Gamma_i^F = \sum_{k \in C_h} \frac{P_{k,i}^{RF}}{\sum_{j \in \mathcal{F}} \mathcal{U}E^i R_{k,j}^*} \left[\frac{J}{bit} \right] \quad \forall i \in \mathcal{F} \quad (3.14)$$

and

$$\Gamma_n^M = \sum_{k \in C_h} \frac{P_{k,n}^{RF}}{\sum_{j \in \mathcal{M}} \mathcal{U}E^n R_{k,j}^*} \left[\frac{J}{bit} \right] \quad \forall n \in \mathcal{M}, \quad (3.15)$$

where Γ^M and Γ^F measure performance at the M-BS and neighbouring FAPs, respectively.

Note that the introduced metric considers only irradiated energy, to better highlight the effect of the power control mechanism and co-channel interference.

Results are averaged over 50 independent runs. We simulate 10^3 independent TTIs during each run and update channel fading instances at each TTI. At the beginning of each run, we randomly place one block of apartments in which FAPs, F-UEs, and M-UEs are randomly deployed. Moreover, in the presented simulations, we consider that all deployed FAPs are active ($\rho_a = 1$) with four F-UEs per FAP. Finally, indoor M-UEs are randomly distributed in the apartments where FAPs are not deployed.

In our simulations, solid, dashed, and dotted-dashed lines correspond to the performance of RRM_{SOA} , $Ghost_{SAF}$, and $Ghost_{NF}$ schemes, respectively.

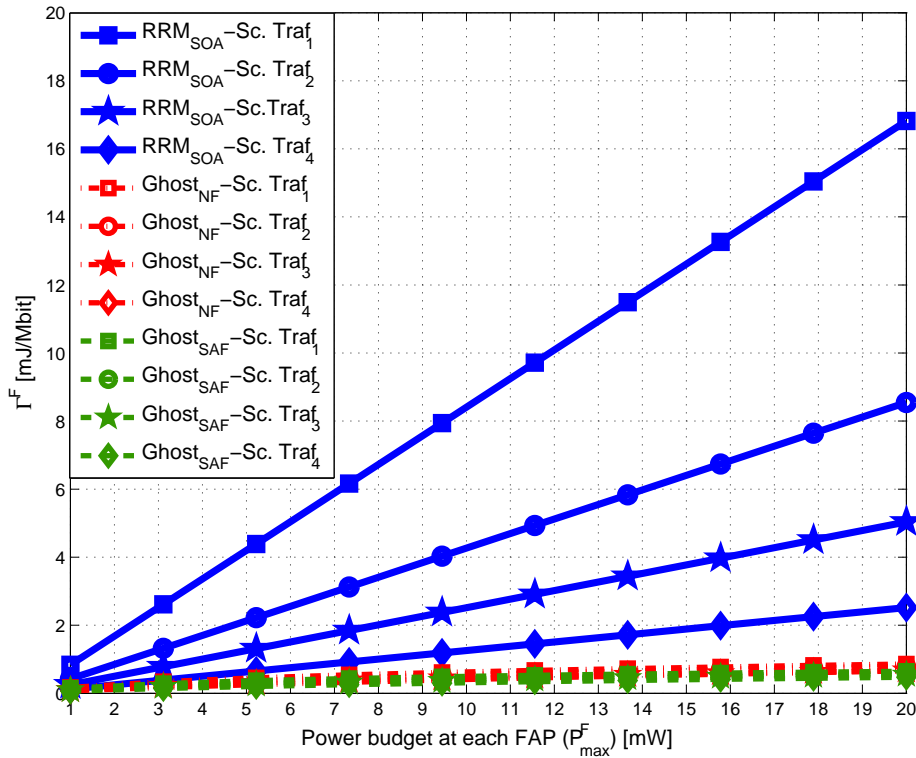


Figure 3.5: Average Γ^F as a function of the power budget P_{max}^F at each FAP in different traffic scenarios.

Discussion on femto users' performance

Figure 3.5 shows the femtocell performance as Γ^F versus the power budget P_{max}^F at each FAP. We have set ρ_d equal to 0.3 and considered four different traffic scenarios:

1. **Scenario Traf.1:** F-UE throughput target $T_{tg} = 300$ kbit/s, square marked curves.
2. **Scenario Traf.2:** F-UE throughput target $T_{tg} = 600$ kbit/s, circle marked curves.
3. **Scenario Traf.3:** F-UE throughput target $T_{tg} = 1$ Mbit/s, star marked curves.
4. **Scenario Traf.4:** F-UE throughput target $T_{tg} = 2$ Mbit/s, diamond marked curves.

We can observe that both the proposed $Ghost_{NF}$ and $Ghost_{SAF}$ improve the femtocell performance with respect to RRM_{SOA} . For instance, considering a FAP power budget equal to 10 mW, the proposed $Ghost_{NF}$ and $Ghost_{SAF}$ gain up to 95% with respect to RRM_{SOA} in Scenario *Traf.1*, up to 90% in Scenario *Traf.2*, up to 85% in Scenario *Traf.3*, and up to 75% in Scenario *Traf.4*. Moreover, results outline that performance gain increases in lightly loaded scenarios (Scenario *Traf.1* and Scenario *Traf.2*) where our algorithms permit to strongly reduce the transmission power by lowering the selected MCS. In this cases, our schemes takes advantage of the lower throughput targets to decrease the downlink irradiated power and spreading over RBs. On the contrary, in highly loaded scenarios the achieved gain is limited. This comes from some concurrent effects. With higher T_{tg} , a larger number of RBs and/or a higher MCS are needed for each

user to meet QoS constraints. This translates in either larger interference generated to neighbouring cells on some RBs and/or a need to transmit on the same number of RBs, but with a higher order of MCS. Transmission is thus more sensitive to both noise and interference generated by close interferers. Finally, we can observe that $Ghost_{SAF}$ slightly improves the femtocell performance compared to $Ghost_{NF}$. Even though coordination between neighbour FAPs permits to limit femto-to-femto interference, $Ghost_{SAF}$ increases the FR and exploits the available resources to further improve the energy saving at each cell. Furthermore, as discussed in Section 3.4.4, $Ghost_{NF}$ results in higher complexity and overhead due to signalling between FAPs and the FCS. Therefore, we can conclude that the proposed $Ghost_{SAF}$ outperforms the $Ghost_{NF}$ from the femtocell perspective.

Discussion on macro users' performance

Figure 3.6 and Figure 3.7 show the improvement in M-UE performance under $Ghost_{NF}$ and $Ghost_{SAF}$.

In the co-channel femtocell deployment, indoor M-UE performance is limited by femto-to-macro interference.

In absence of coordination amongst the M-BS and the neighbouring FAPs, the macrocell scheduler is not aware of the RBs exploited by the interfering FAPs. When the M-BS assigns to an indoor user a RB that is used by a nearby FAP, this M-UE can be exposed to a high level of interference. We aim to evaluate the effect of this interference at M-UEs when femtocells use the reference RRM_{SOA} and the proposed $Ghost_{NF}$ and $Ghost_{SAF}$ schemes.

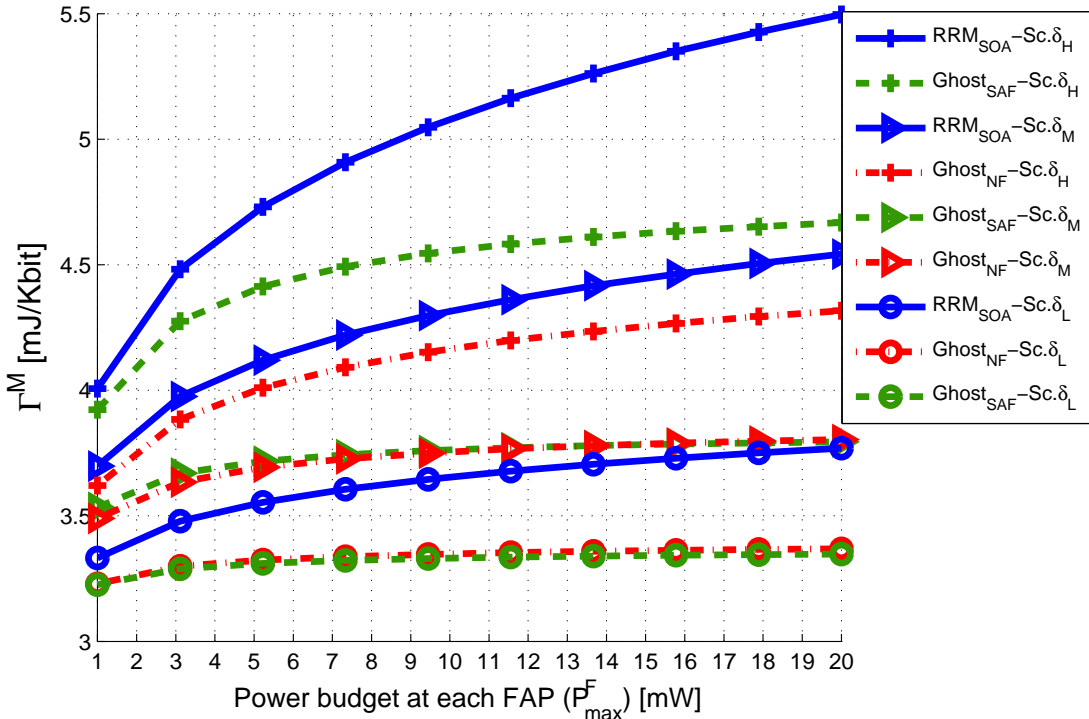


Figure 3.6: Average Γ^M measured at M-UEs as a function of the power budget at each FAP P_{max}^F in different traffic scenarios.

To compare these algorithms, we have set the M-UE throughput target (T_{tg}^M) equals to 300

kbit/s, the F-UE throughput target (T_{tg}^{F}) equal to 600 kbit/s and considered three different femtocell deployment scenarios:

1. **Scenario δ_L** : low density— $\rho_d = 0.3$, circle marked curves.
2. **Scenario δ_M** : medium density— $\rho_d = 0.5$, triangle marked curves.
3. **Scenario δ_H** : high density— $\rho_d = 0.8$, plus marked curves.

On Figure 3.6, we show the macrocell performance as Γ^{M} versus the power budget $P_{\text{max}}^{\text{F}}$ at each FAP. Results indicate that Ghost_{NF} and $\text{Ghost}_{\text{SAF}}$ permit to limit the impact of the femto-to-macro interference in all considered scenarios. This improvement only comes from the femtocell behaviour; in fact, the M-BS uses a fixed RF power in each allotted RB. On the other side, MCS scaling, spreading, and power control mechanisms permit to reduce the FAP downlink power transmission in each RB and mitigate interference. For instance, considering $P_{\text{max}}^{\text{F}}$ equal to 20 mW, the proposed $\text{Ghost}_{\text{SAF}}$ gains up to 11%, 16%, and 15% with respect to RRM_{SOA} in Scenarios δ_L , δ_M , and δ_H . Moreover, the proposed Ghost_{NF} gains up to 11%, 16%, and 22% with respect to RRM_{SOA} in Scenarios δ_L , δ_M , and δ_H . While in Scenario δ_L and Scenario δ_M the $\text{Ghost}_{\text{SAF}}$ slightly improves the performance achieved by the Ghost_{NF} , in Scenario δ_H the Ghost_{NF} outperforms the $\text{Ghost}_{\text{SAF}}$. In fact, the probability that several neighbour FAPs access to same RBs increases with the femtocell density, hence, in Scenario δ_H , M-UEs may experience high peaks of *cross-tier interference*. In Ghost_{NF} , the FCS coordinates the access of neighbouring femtocells limiting the overall interference perceived at M-UEs.

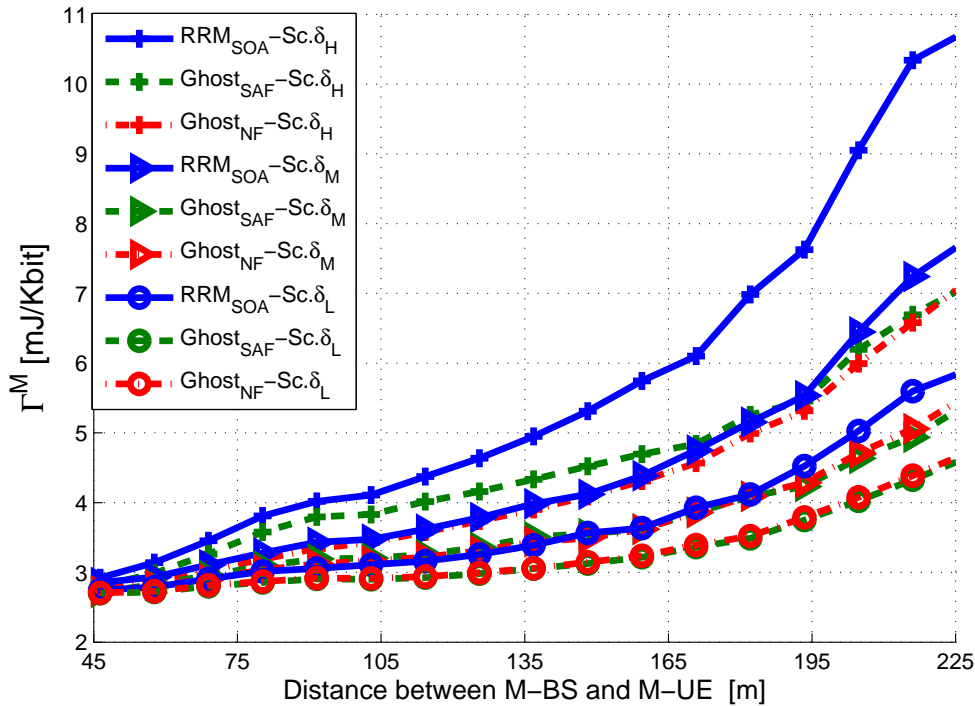


Figure 3.7: Average Γ^{M} measured at macro cells as a function of the distance between the end-user and the M-BS

Figure 3.7 shows the macrocell performance in function of the distance between the M-UE and the M-BS for different femtocell deployment scenarios and for P_{\max}^F equal to 20mW. M-UEs that are located far away from the M-BS perceive low average SINR due to propagation loss and interference generated by surrounding M-BSs and FAPs. Hence, it is fundamental to limit the femto-to-macro interference to satisfy these users' QoS constraints. Simulation results show that proposed algorithms can strongly enhance the performance of M-UEs placed at the border of the cell. Furthermore, we can note as the observed benefit increases with respect to femtocell density and distance between the M-UEs and the serving M-BS.

In Scenario δ_L , under RRM_{SOA} , the M-BS needs 5.8 mJ/Kbit to serve a M-UE placed at 225 meters far away, while 4.6 mJ/Kbit are necessary with the proposed $Ghost_{NF}$ and $Ghost_{SAF}$, respectively. In Scenario δ_M , under RRM_{SOA} , the M-BS needs 7.7 mJ/Kbit to serve a M-UE placed at 225 meters far away, while 5.5 mJ/Kbit and 5.4 mJ/Kbit are necessary with the proposed $Ghost_{NF}$ and $Ghost_{SAF}$, respectively. In Scenario δ_H , under RRM_{SOA} , the M-BS needs 10.9 mJ/Kbit to serve a M-UE placed at 225 meters far away, while 7.1 mJ/Kbit are necessary with both the proposed $Ghost_{NF}$ and $Ghost_{SAF}$.

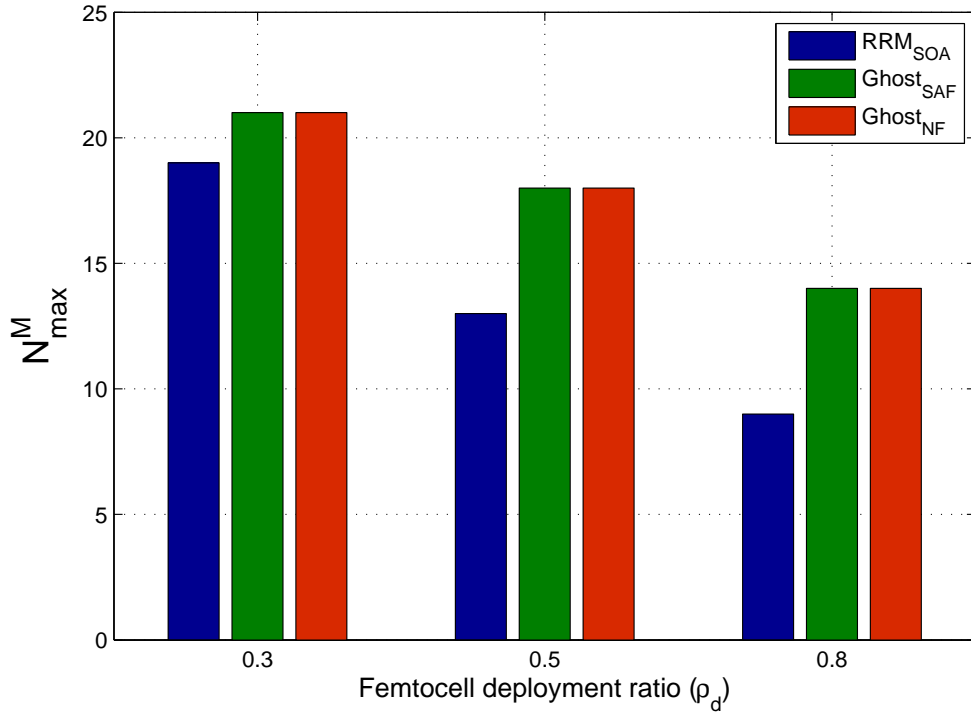


Figure 3.8: Maximum number of cell edge M-UEs that can be contemporarily served by the M-BS in different femtocell deployment scenarios

This improvements result in higher macrocell coverage and capacity. The average number of cell edge M-UEs that can be contemporarily served by the M-BS is

$$N_{\max}^M = \frac{P_{\max}^F}{\Gamma^M \cdot T_{\text{tg}}^M} \quad (3.16)$$

Figure 3.8 shows the values of N_{\max}^M in different femtocell deployment scenarios.

3.6 Conclusion

The future 3GPP/LTE femtocells deployment is expected to be dense: a large population of potential interferers will need to share scarce common frequency resources while indoor femtocell users will benefit of high quality links. Classical resource allocation and interference mitigation techniques cannot address the challenge of limiting interference between neighbouring femtocells and maintaining a high level of reliability for macro UE communications.

The femtocell deployment requires a new paradigm because of two main reasons. First, femtocell users can benefit from a high quality downlink signal enabled by short range communications characterizing femtocell deployments. Second, only few users locally compete for a large amount of frequency resources in a femtocell. Therefore, a femtocell benefits from a huge amount of spectral/power resources.

Such observations have led to the design of a novel transmission paradigm for femtocell networks, which trade-off irradiated power for frequency resources. Moreover, we have proposed two RRM algorithms, named as $Ghost_{SAF}$ and $Ghost_{NF}$, which can be implemented in stand-alone and networked femtocell scenarios, respectively. In this chapter, we have discussed the effectiveness of these algorithms in a two-tier network in terms of complexity, overhead, and performance at both M-UEs and F-UEs. The proposed algorithms limit the undesired effects of interference by reducing the irradiated power per RB required at femtocells to meet target QoS constraints.

Simulation results have shown that the proposed algorithms outperform the classic RRM strategies. Moreover, $Ghost_{NF}$ can allow higher performance at M-UEs with respect the $Ghost_{SAF}$ by limiting spectrum reuse in dense femtocell deployment scenarios. However, such an improvement comes at the cost of higher complexity and overhead. Eventually, it is worth to underline that the irradiated power slightly impacts on the overall power consumption at femtocells; however, in the future, femtocell PAs will be likely designed to scale their energy consumption with irradiated power [168]. In such scenario, the Ghost paradigm can drive to notable *greening* effect and enabling the cost-effective femtocell deployment in two-tier cellular networks.

Chapter 4

Dynamic Activation for Open Access Femtocell Networks

The exponential increase in high rate traffic driven by a new generation of wireless devices is expected to overload cellular network capacity in the near future. Femtocells have recently been proposed as an efficient and cost-effective approach to enhance cellular network capacity and coverage. However, dense and unplanned deployment of additional access points and their uncoordinated operation may increase the system power consumption. Thus, efficient schemes are essential for managing femtocells activity and improving the system performance. In this chapter, we investigate the effect of femtocell deployment on the cellular network energy efficiency. The goal is twofold: first, we aim to analyse how classic femtocell access schemes affect the system energy efficiency; second, inspired by the Double Hopping algorithm presented in Section 2.3.3, we propose a novel cell selection scheme for open access femtocells; the proposed mechanism allows the effective deployment of femtocells in the cellular network reducing power consumption and limiting the effect of interference.

The chapter is organized as follows: In Section 4.1, we introduce the motivation for this study, related work, and our contribution. Then, in Section 4.2, we present the system model and related assumptions that are adopted in this chapter. In Section 4.3, we mathematically describe the investigated problem and then, in Section 4.4, we detail the proposed femtocell network management scheme. In Section 4.5 we analyse the performance of the proposed scheme and finally, in Section 4.6, we conclude the chapter.

4.1 Introduction

4.1.1 Motivation

In earlier studies, FAPs have been considered as an instrument to enhance the indoor coverage of the macro-centric cellular network. More recently, femtocell deployment has been investigated as a cost-effective way of offloading data traffic from the macrocell network. Data offloading reduces the traffic carried over the MSP's radio and backhaul networks, thereby increasing available capacity and avoiding congestion in the overcrowded macrocell. To maximize benefits due to this new architecture, a dense deployment of low-power low-cost FAPs is required. However, as already discussed in Section 2.2.1 and Chapter 3, this strategy leads to cross-tier and co-tier interference, which may notably corrupt the communication in the cellular network and increase congestion due to the excessive number of retransmissions.

Moreover, the massive roll out of additional BSs may drastically increase the cellular network energy consumption, which in turn will cause an increase in the global CO_2 emissions and impose more and more challenging operational costs for operators.

Integrating femtocells in the classic cellular networks is fundamental to satisfy high data rate and coverage requirements of future mobile systems; however, in the same time, agile mechanisms have to be also introduced in this novel architecture to enable sustainable and effective broadband wireless communications.

4.1.2 Related Work

Several studies related to the EE of two-tier cellular networks have been recently proposed. Nevertheless, most of them attempted to see how much energy saving can be achieved rather than developing algorithms that can be implemented in practice.

Cao and Fan [149] investigated the trade-off between EE and user performance in two-tier networks. However, they only considered the irradiated RF power in the analysis. Other works have proposed an EE comparison between different size cells [169, 170]. Chen et al. studied how the density of small cells affects the system EE [171]. In a recent magazine [172], the authors have analysed the energy saving achievable in macrocell networks by switching off those BSs that are characterized by low traffic. Other researchers have investigated centralized and distributed energy saving procedures that allow FAPs to completely switch off radio transmissions and associated processing when not involved in active calls [8, 152]. Son et al. studied the problem of finding the minimum number of micro BSs to deploy in the macrocell region to support high rate traffic scenarios while minimizing energy consumption [173]. They also investigated the trade-off between flow-level performance and cellular network EE [174]. However, the BS/UE association and BSs activity have to be jointly optimized to improve system EE while guaranteeing UEs coverage and QoS constraints. Shou et al. considered a macrocell scenario and solved the BS-UE association problem: UEs are concentrated on the M-BSs with relatively high load [175]. However, the latter approach does not guarantee the coverage neither to all active UEs nor to further incoming users in the regions where M-BSs are idle. Cell zooming adaptively adjusts the cell size according to traffic load, user requirements, and channel conditions [151]. Therefore, M-BSs under light load self-deactivate to reduce the network energy consumption; subsequently their UEs have to connect to the nearby macrocell. Hence, such a method requires that activated M-BSs increase their irradiated power to guarantee coverage and avoid outage events.

Further work investigated the trade-off between open access and closed access femtocells [176, 177] and the benefits of macrocell offloading in terms of system capacity [125].

4.1.3 Contribution

In this chapter, we investigate the impact of macrocell offloading via femtocell deployment in terms of cellular network energy consumption and users' performance. Advantages and drawback of open access and closed access schemes are critically discussed from an EE perspective. Moreover, the integration of femtocell switch-off capability is considered in the analysed two-tier cellular network. Finally, we propose a network management scheme, which permits open/hybrid femtocell networks to self adapt offered capacity to the traffic demand, dynamically reducing the number of active FAPs and limiting the network power consumption. We discuss the implementation of the proposed scheme in both networked and stand-alone femtocell scenarios from performance, overhead, and complexity perspectives. Finally, we underline that there is a trade-off between the energy saving at the operator and benefits at customers' side; to compensate consumers' expenditure, operators should introduce a business model that rewards (for instance in terms of capacity or service cost) those customers that open the access of their femtocells.

The novelty of this chapter is based on a patent [P2] and a conference paper [C5].

4.2 System Model

We consider a two-tier wireless cellular network in which mobile terminals and BSs implement an OFDMA air interface based on 3GPP/LTE downlink specifications [154]. OFDM symbols are organized into a number of physical RBs consisting of 12 contiguous sub-carriers for 7 consecutive OFDM symbols. With a bandwidth W of 10 MHz, 50 RBs are available for data transmission.

Each user is allocated one or several RBs in two consecutive slots, i.e., the TTI is equal to two slots and its duration T is 1 ms.

The RF power budget at FAPs (P_{\max}^F) is set equal to 10 dBm. The overall channel gain \mathbf{g} is composed of the antenna gain, a fixed distance dependent path loss, a slowly varying component modeled by lognormal shadowing, and Rayleigh fast fading with unit power.

We assume that femtocells are deployed in a block of 10 m x 10 m apartments according to the 3GPP grid urban deployment model [31]. In such a scenario each FAP can simultaneously serve up to to 4 users. The block of apartments belongs to the same region of a macrocell, which share the same bandwidth of the neighbouring femtocells. Moreover, we assume that 6 additional M-BSs surround the central macrocell generating additive interference for both macro and femto users.

Further details on the femtocell deployment and related signal propagation models are presented in Section 2.2.2.1. Finally, our investigation is based on the EARTH E^3F power consumption model [17], which provides an accurate estimation of the BS power consumption considering the different components of the radio equipment such as antenna interface, PA, baseband interface, and cooling. Chapter 2.2.2.3 gives a description of the EARTH E^3F framework.

In this chapter, we use the same model parameters of Chapter 3; more details can be found in Table 3.1.

4.3 Problem Statement

Consider a macrocell region overlaid by a set of femtocells $\mathcal{F} = \{1, \dots, N_F\}$ deployed in a block of apartments such as described in Section 4.2. Femtocells operate in the same bandwidth of the macrocell and offer service to indoor UEs located in their coverage area. The M-BS serves outdoor UEs and indoor UEs that can not be served by active FAPs. Femtocell deployment has

great potential to improve the cellular network EE, however the overall energy consumption might be drastically increased by the massive and unplanned roll out of FAPs, operating in lightly load scenarios.

To optimize the aggregate power consumption, we aim at finding the subset of F of minimum size able to serve the indoor UEs ($\mathcal{F} \mathcal{UE} = \{1, \dots, N_{\text{FUE}}\}$) located in its coverage area. Therefore, deployed FAPs that do not have users to serve can be dynamically switched off. Hence, limiting the number of simultaneously activated FAPs our approach can improve the system EE and reduce co-channel interference (cf. Figure 4.1).

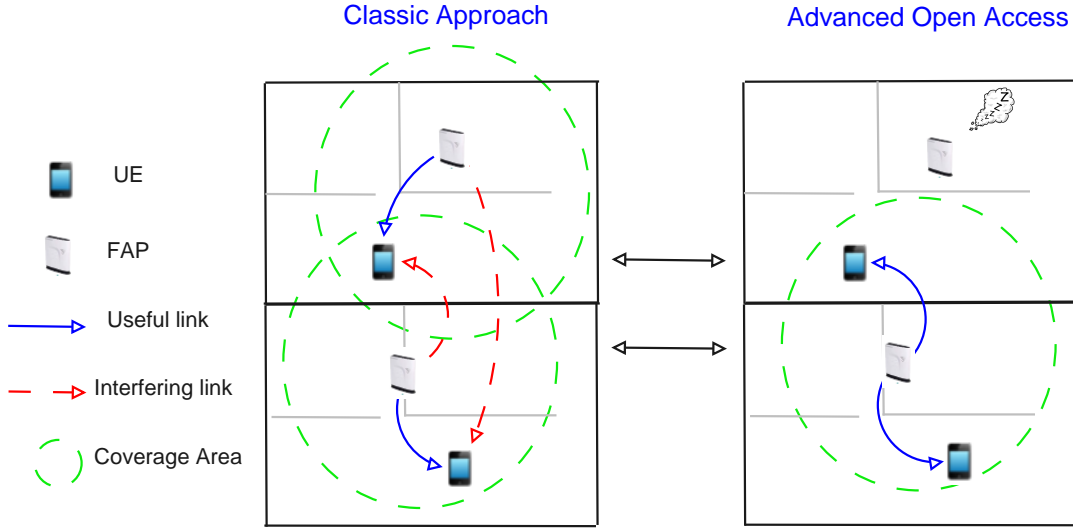


Figure 4.1: Classic approach vs. our Advanced Open Access scheme.

This optimization problem can be expressed as

$$\min \sum_{i \in \mathcal{F}} a_i$$

subject to

$$\sum_{j \in \mathcal{F} \mathcal{UE}} X_{j,i} \leq N_{\max} \quad \forall i \in \mathcal{F} \quad (4.1)$$

$$\sum_{i \in \mathcal{F}^j} a_i X_{j,i} = 1 \quad \forall j \in \mathcal{F} \mathcal{UE}, \quad \mathcal{F}^j \subseteq \mathcal{F} \quad (4.2)$$

$$a_i \in \{0, 1\} \quad \forall i \in \mathcal{F}$$

$$X_{j,i} \in \{0, 1\} \quad \forall (i, j) \in \mathcal{F} \times \mathcal{F} \mathcal{UE}$$

where \mathbf{a} is a vector whose elements indicate active FAPs and C_h is the set of available RBs. Element $X_{j,i}$ of the service matrix \mathbf{X} indicates whether i th UE is served by FAP j (i.e., $X_{j,i}=1$). Eq. (4.1) indicates that the maximum number of UEs that can be simultaneously served by a FAP is limited to N_{\max} . Eq. (4.2) underlines that the j -th UE can be served only by one of the FAPs that belong to its active set \mathcal{F}^j .

The above formulation corresponds to a combinatorial problem that can hardly be solved especially in dense urban scenarios. Furthermore, we can compute an optimal solution only having the complete knowledge of all activity sets, which requires coordination amongst neighbouring FAPs.

Hence, to find a near-optimal solution, we propose a heuristic approach, named as Advanced Open Access, that can be easily implemented in both networked and stand-alone femtocell deployment scenarios (cf. Figure 4.2).

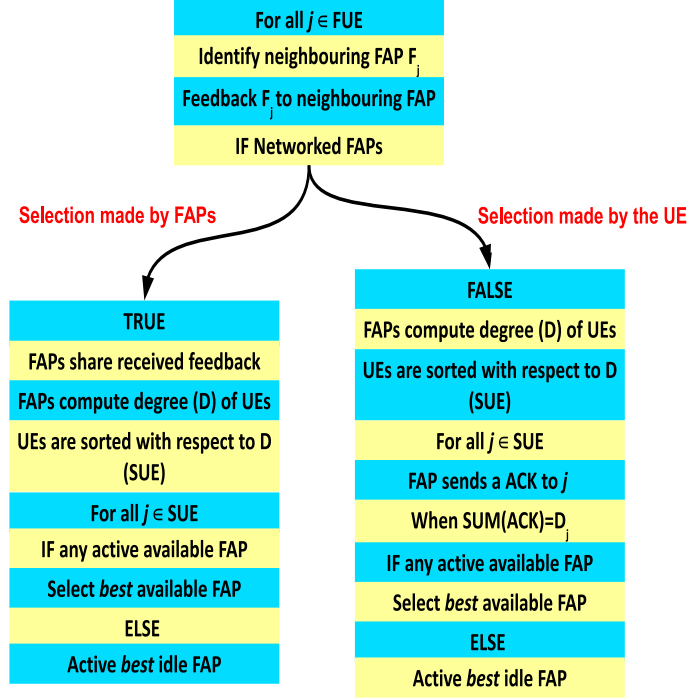


Figure 4.2: Proposed Advanced Open Access algorithms for networked and stand-alone femto-cells.

4.4 Proposed Advanced Open Access Algorithms

In our scheme, each UE j identifies its active set \mathcal{F}^j comparing the strength of the RSRP with a predefined threshold. We indicate the length of active set \mathcal{F}^j as D_j (i.e., the degree of UE j). The main issue in solving the problem presented in the previous section is to decide the order in which associate UEs FAPs. Inspired by the Double Hopping algorithm presented in Section 2.3.3, we propose a strategy that sorts UEs according to their degree and then selects the UE with the lowest degree first. The rationale behind this approach is to permit also to those UEs with few neighbouring FAPs to be successfully served.

UEs are ordered by the femtocells, thus each user has to feedback its active set to neighboring FAPs. The Algorithm 5 describe the identification of the active set at each UE and the signalling exchange amongst UEs and neighbouring FAPs.

Then, in the networked femtocell scenario, FAPs are directly connected and able to share the received information (see Algorithm 6). Hence, sorting UEs according to their degree is straightforward. Subsequently, our algorithm picks up the unserved UE with the lowest degree and associates it with the active cell that maximizes a predefined EE metric (see Algorithm 7). If there are not available active FAPs, the "best" idle cell is activated.

Algorithm 5 Identification of the active sets and feedback exchange amongst FAPs and UEs

```

1: for all  $j \in \mathcal{FUE}$  do
2:    $cont = 0$  { $cont$  is used only in the stand-alone scenario}
3:    $\mathcal{F}^j = \{i \in \mathcal{F} \mid RSRP_i \geq T_h\}$ 
4:   for all  $i \in \mathcal{F}^j$  do
5:     SEND( $i, \mathcal{F}^j$ ) {SEND transfers to the FAP  $i$  the active set of the UE  $j$  ( $\mathcal{F}^j$ )}
6:   end for
7: end for

```

Algorithm 6 FAPs exchange of the received active set

```

1: for all  $i \in \mathcal{F}$  do
2:    $\mathcal{FUE}^i = \{j \in \mathcal{FUE} \mid i \in \mathcal{F}^j\}$ 
3:   for all  $j \in \mathcal{FUE}^i$  do
4:     for all  $k \in \mathcal{F} \setminus \mathcal{F}^j$  do
5:       SEND( $k, \mathcal{F}^j$ ) {SEND transfers to the FAP  $k$  the active set of the UE  $j$  ( $\mathcal{F}^j$ )}
6:     end for
7:   end for
8: end for

```

Algorithm 7 Algorithm to implement the UE/FAP association

```

1: for all  $i \in \mathcal{F}$  do
2:    $\mathbf{X} = 0_{N_{FUE}, N_F}$ 
3:    $\mathbf{D} = 0_{N_{FUE}, 1}$ 
4:    $\mathbf{a} = 0_{N_F, 1}$ 
5:   for all  $j \in \mathcal{FUE}$  do
6:      $D_j = |\mathcal{F}^j|$ 
7:   end for
8:    $SUE = \mathbf{SORT}(\mathbf{D}, \mathcal{FUE})$  {SORT sorts UEs  $\in \mathcal{FUE}$  according to their degree}
9:   for all  $j \in SUE$  do
10:     $i^* = \mathbf{ASSO}(\mathcal{F}^j, \mathbf{a}, \mathbf{X})$  {ASSO( $\cdot$ ) selects the serving FAP  $i^*$  of the UE  $j$ }
11:     $X_{j, i^*} = 1$ 
12:    if  $a_{i^*}^* = 0$  then
13:       $a_{i^*}^* = 1$ 
14:    end if
15:   end for
16: end for

```

Note that Algorithm 6 and Algorithm 7 refer to a distributed implementation of the proposed Advanced Open Access in networked femtocell deployment. However, a centralized scheme, which results in limited overhead and computational costs, is feasible. In the centralized case, FAPs transfer the received active sets directly to the femtocell coordinator, which is in charge to associate active UEs and FAPs. Then, the central unit sends the output of the association process to the selected FAPs. Finally, FAPs, which have not received any feedback from the coordinator, self-deactivate.

In the stand-alone scenario, each FAP knows only the active sets of the UEs that are located in its coverage area. Thus, our algorithm distributively sorts UEs without any signalling exchange amongst neighbouring FAPs.

Each FAP orders its neighbouring UEs and iteratively sends a feedback to the unserved UE with the lowest degree (see Algorithm 8). Note that this message also indicates the number of UEs that are currently served by the FAP. When an UE has received the feedbacks from all FAPs that belong to its active set, it can make its cell selection without colliding with some other user's choice (see Algorithm 9). Then, it feedbacks its selection to each FAPs in its vicinity that subsequently pick up the following unserved UE.

Algorithm 8 FAPs manage the activity according to the received feedback

```

1: for all  $i \in \mathcal{F}$  do
2:    $n_i = 0$ 
3:    $\mathcal{F}^{UE^i} = \{j \in \mathcal{F}^{UE} \mid i \in \mathcal{F}^j\}$ 
4:    $\mathbf{D} = 0_{|\mathcal{F}^{UE^i}|, 1}$ 
5:   for all  $j \in \mathcal{F}^{UE^i}$  do
6:      $D_j = |\mathcal{F}^j|$ 
7:   end for
8:    $S^{UE} = \text{SORT}(\mathbf{D}, \mathcal{F}^{UE^i})$  {SORT sorts UEs  $\in \mathcal{F}^{UE^i}$  according to their degree}
9:   for all  $j \in S^{UE}$  do
10:     $X_{j,i} = \text{FDBK}(j, n_i)$  {call the Algorithm 9}
11:    if  $X_{j,i} = 1$  then
12:       $n_i = n_i + 1$ 
13:      if  $a_i = 0$  then
14:         $a_i = 1$ 
15:      end if
16:    end if
17:   end for
18: end for

```

Due to the static characteristic of the indoor femtocell deployment scenarios, the active sets do not change at fast time scale. Thus, the frequency of the reconfiguration process and the generated overhead is low. However, when incoming UEs are detected by the femtocell network or some UEs leave the network, idle FAPs have to be activated and the UE-FAP association has to be updated accordingly. As already mentioned, the cellular coverage for these UEs, which can not be served by active FAPs, have to be guaranteed by the closer macrocell. Note that in such a scenario, it is easy to detect incoming/outgoing UEs that are attached to the M-BS, because they likely transmit with high power due to the experienced attenuation (composed mainly by path loss

Algorithm 9 The UE replies to the received feedback signalling whether FAP j has been selected

```

1:  $cont = cont + 1$ 
2: if  $cont = |\mathcal{F}^j|$  then
3:    $\tilde{X} = 0_{|\mathcal{F}^j|}$ 
4:    $i^* = \text{ASSO}(\mathcal{F}^j, n_i)$  {ASSO( $\cdot$ ) selects the serving FAP  $i^*$  of the UE  $j$ }
5:    $\tilde{X}_{i^*} = 1$ 
6:   for all  $i \in \mathcal{F}^j$  do
7:     SEND( $i, \tilde{X}_i$ ) {SEND transfers  $\tilde{X}_i$  to the FAP  $i$ }
8:   end for
9: end if

```

and wall losses).

4.5 Simulation Results

In this section, we assess the effectiveness of the proposed Advanced Open Access scheme by comparing its performance with the reference closed access and open access approaches. The main differences between these schemes are the following:

1. In the closed access femtocells deployment, a UE can be served by a FAP only if that the access point is placed in the user apartment.
2. In the open access femtocells deployment, UEs can be in the coverage area of several femtocells. Hence, each user selects the available FAP associated with the best RSRP.

In these schemes, dynamic switching off can be implemented to disable femtocells that are not serving neighbouring UEs. In our analysis, switched off FAPs do not impact the aggregate power consumption. However, note that some hardware components have to be always active in to dynamically activate/deactivate FAPs when necessary (see Section 2.4.4).

We consider a scenario in which 30 cellular users are deployed in the macrocell area. In line with recent studies [19], we assume that 70% of the traffic is generated by indoor UEs. The results are averaged over 50 independent runs. We simulate 10^3 independent TTIs during each run and update channel fading instances at each TTI. At the beginning of each run, FAPs and indoor UEs are randomly deployed in the block of apartments placed at the macrocell edge. Outdoor UEs are randomly deployed in the macrocell region. The traffic generated by cellular users is modeled as a constant bit rate traffic and the throughput target T_{tg} is set equal to 150 Kbit/s. A PF-based scheduler [142] is used at both the macrocell and femtocells. Finally, link adaptation is implemented in downlink transmissions for which MCSs are selected according to momentary feedback transmitted by the served UE.

In our simulations, triangle marked lines, circled marked lines, squared marked lines, diamond marked lines, and star marked lines respectively correspond to the closed access, closed access plus cell switch off, open access, open access plus cell switch off, and Advanced Open Access plus cell switch off.

Analysis on energy consumption

First, we aim at comparing these strategies in terms of the femtocell Energy Consumption Gain (ECG) [178]. This metric permits to efficiently compare performance achieved by implementing the investigated approaches. In fact, it is simply the ratio between the energy consumed by the baseline and the scheme under test. In Fig. 4.3, closed access and open access schemes are considered as the reference approaches. The difference between these two schemes is related to the number of UEs served by FAPs (i.e., the load of the femtocell network): in the open access deployment the probability that a UE can be served by a FAP is higher than in the closed access deployment. However, as previously mentioned (see Section 2.2.2.3), the FAP system power consumption slightly depends on the load, thus open access and closed access schemes result in the same performance in the femtocell network (see the squared marked and triangle marked lines). On the contrary, when cell switching off is implemented, a high number of closed access FAPs can be deactivated and the power consumption of closed access femtocells is lower than in the open access case, especially for the low values of ρ_d . Clearly, if all 25 apartments in the block are equipped with a femtocell (i.e., $\rho_d = 1$), both the strategies serve all indoor users, and the performance of these two strategies are coincident. In our simulations, up to 16% of the gain can be achieved by implementing cell switching off with respect to the reference approaches. However, adapting the femtocell activity to the traffic load can introduce a much higher gain. In fact, the proposed Advanced Open Access strongly lowers the femtocell network energy consumption achieving up to 60% of the energy saving with respect to the reference schemes.

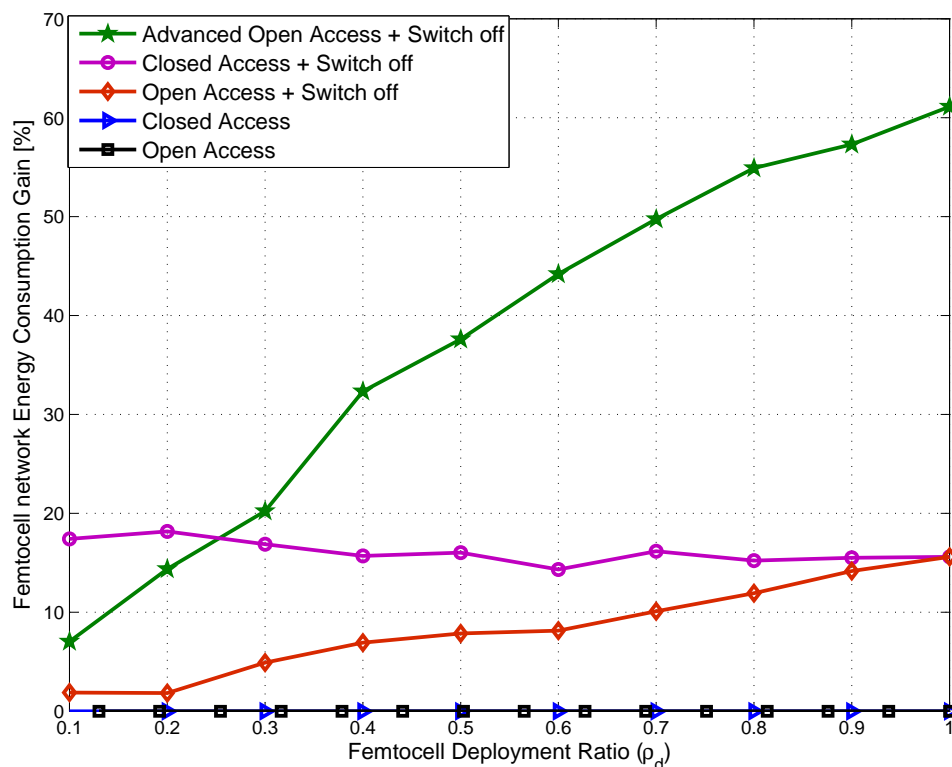


Figure 4.3: Femtocell network Energy Consumption Gain with respect to the femtocell deployment ratio ρ_d .

In Figure 4.4, we show the aggregate ECG of the investigated approaches with respect to the femtocell deployment ratio. This gain accounts for both the macrocell and femtocell system energy consumption and is computed considering the closed access scheme as the reference approach. Both open access and closed access schemes improve the system EE via the macrocell offloading. However, the former scheme further increases the macrocell offloading and reduces the system energy consumption. Simulation results show that open access achieves up to 10% of the gain with respect to the closed access approach. Therefore, while open access femtocells may consume more power than closed access femtocells (see Fig. 4.3), the former are more energy efficient from the overall cellular network perspective. Nevertheless, when the number of active FAPs is greater than a certain value (i.e., $\rho_d \geq 0.4$), the aggregate capacity of open access femtocells exceeds the service request and the EE gain decreases. The system performance can be further enhanced switching off those FAPs that are not serving active UEs.

In our simulations, up to 4% of the gain can be achieved by implementing cell switching off. Finally, the proposed Advanced Open Access Scheme gains up to 10% and 14% with respect to the classic strategies with and without cell switching off.

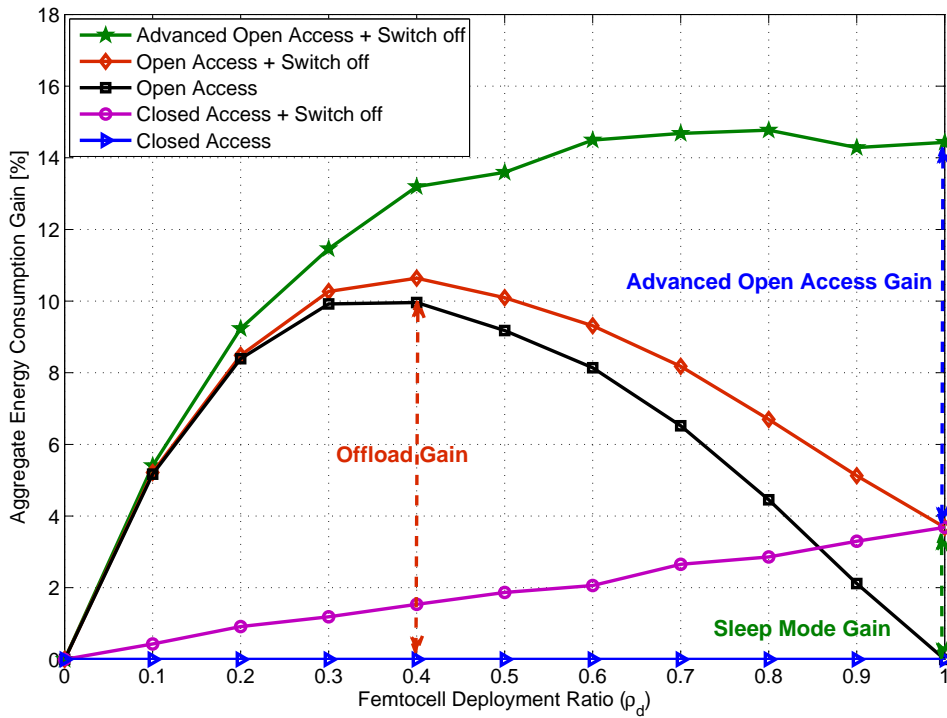


Figure 4.4: Aggregate Energy Consumption Gain with respect to the femtocell deployment ratio ρ_d .

Discussion on users' performance

Our proposed algorithm does not permit UEs to select the FAP associated with the *best* RSRP. Hence, we may expect that user performance decreases when using Advanced Open Access femtocells. In Figure 4.5, we present the impact of the proposed scheme on the performance perceived

by cellular users (both macro and femto users). We show the average normalized Throughput experienced by end-users with respect to the femtocell deployment ratio for different access schemes. Cell switching off does not impact user performance, thus we compare the performance achieved in the closed access, open access, and Advanced Open Access femtocell deployment. In the closed access case, only a restricted set of UEs has the right to access femtocells, thus in low/medium density femtocell scenarios several indoor users are constrained to be served by the far-away M-BS. Furthermore, femto-to-macro interference decreases the performance of these users. In higher density femtocell scenarios ($\rho_d \geq 0.5$), the probability that an indoor UE may be served by a FAP increases, thus users experience better performance. In both open and Advanced Open Access schemes, there is a high probability that an indoor user can be served by a FAP even in low density femtocell deployment scenarios. Therefore, these schemes perform in the fairly same way. However, UEs experience better performance compared to the Closed Access case (up to 7% of the gain) due to the reduced distance between the end-user terminal and its AP and limited effect of interference.

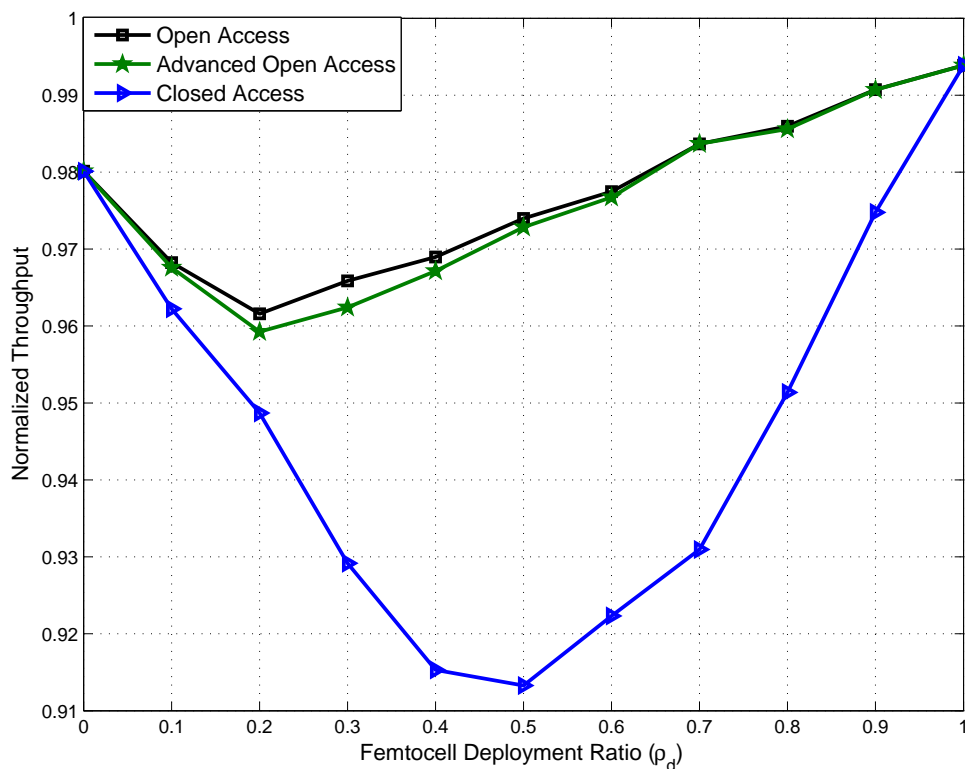


Figure 4.5: Performance experienced by cellular users with respect to the femtocell deployment ratio ρ_d .

4.6 Conclusions

The future 3GPP/LTE femtocell deployment is expected to be dense: the deployment of additional BSs and their uncoordinated operation may raise both the level of interference and the aggregate power consumption of the cellular network. Nowadays, the energy consumption of cellular base stations (i.e, local APs) is mainly due to keep them activated and guarantee coverage also in lightly loaded scenarios. On the contrary, the impact of the cell load on the BS power consumption is fairly limited. This scenario is very inefficient and its drawbacks are even more important in the small cell deployment. Therefore, cost-effective strategies are essential to dynamically limit energy wastage while satisfying QoS of cellular users.

Investigations presented in this chapter indicate that while open access femtocells are characterized by a higher average power consumption with respect to closed access femtocells, they are more energy efficient from the overall cellular network perspective. Moreover, cell switch off mechanisms can further increase the energy saving adapting the AP activity to the presence of neighbouring end-users.

Furthermore, we have proposed the Advanced Open Access scheme, which permits neighbouring femtocells to cooperatively coordinate the cell activation/deactivation and the association amongst users and deployed APs. This mechanism adapts the network capacity to traffic scenarios, dynamically reducing the number of active FAPs and limiting the cellular network power consumption.

Simulation results show that the proposed strategy strongly enhances the system EE without affecting users' QoS. Adaptation comes at cost of higher network overhead and complexity required to efficiently select the serving APs. The frequency of the proposed activity management mechanism is related to changes in the femtocell network topology (for instance users that join or leave the network). Hence, due to the reduce mobility in indoor environment, the impact of the overhead is limited. Eventually, the proposed Advanced Open Access algorithm can be investigated as an enabling technique in multi-operator scenarios in which different operators may decide to pool their APs together to further improve energy saving in cellular networks.

Chapter 5

Dynamic Traffic Management for Green Open Access Femtocell Networks

The additional deployment of local access points can offload the macrocell network and reduce operational costs at mobile operators. However, the dense and chaotic deployment of femtocells can result in low energy efficiency; moreover, uncoordinated femtocell operations result in harmful co-channel interference. Thus, context-aware schemes are essential to dynamically match network capacity and service demand avoiding energy wastage and outage events. Classical cell switch off and discontinuous transmission algorithms aim at improving the network energy efficiency in lightly loaded scenarios. In this chapter, we propose a novel multi-cell architecture for open access femtocell networks, which also enables energy saving at medium and high loads without compromising the end-user performance.

The chapter is organized as follows: In Section 5.1, we present the motivation for this study, related work, and our contribution. Then, in Section 5.2, we discuss the system model adopted in this chapter. In Section 5.3 we recall strategies based on discontinuous transmissions. In Section 5.4, we mathematically present the investigated problem and then, in Section 5.5 we describe the proposed multi-cell activity management scheme. In Section 5.6 we analyse the performance of our proposition and Section 5.7 concludes the chapter.

5.1 Introduction

5.1.1 Motivation

Femtocell deployment in future cellular wireless network is expected to be dense. This technical solution is necessary to satisfy the increasing demand of high data rate services and offer uniform coverage to both indoor and outdoor users. Moreover, femtocells allow macrocell offloading, which reduces OPEX at the mobile operator and enhance the macrocell capacity. Nevertheless, in such a scenario, uncoordinated operations of neighbouring FAPs may result in excessive co-channel interference. Moreover, a high number of femtocells operating in lightly load status leads to a notable wastage of energy. The growth of wireless service demand imposes more and more challenging operational and capital costs for operators.

As discussed in Chapter 2.1.3, network optimization schemes, which operates in mid/long time scale, adapt the network characteristics (such as topology and cell activation) to the traffic statistical behaviour. However, fast adaptation mechanisms are also required to dynamically match the capacity offered by the two-tier network and service demand. These approaches enable further energy saving while ensuring users' QoS and coverage.

5.1.2 Related Work

As shown in Figure 2.4, RRM and system level mechanisms for achieving energy saving in cellular networks, can be classified with respect to the time scale in which they operate. In Chapter 3, we have proposed the *Ghost Femtocells* algorithm that lowers the FAPs irradiated power and reduces interference, trading off transmission energy for frequency resources while meeting users' QoS. López-Pérez et al. proposed a similar approach in [145], in which self organizing femtocells exploit a distributed resource allocation scheme that minimizes the cell RF output power. Calvanese Strinati and Greco introduced a RRM scheme that discriminates traffic according to the delay constraints and then reduces the BS irradiated power by trading-off delay of non-urgent packets for energy consumption [180]. However, in small cell deployment, power consumption slightly depends on the irradiated power, then, energy saving achieved with RRM algorithm is usually limited. On the contrary, Frenger et al. proposed Cell DTX [2] to allow M-BSs to switch off radio in subframes where there are no user data transmissions. Such a fast adaptation mechanism allows a great energy saving especially in low traffic scenarios. Gupta and Calvanese Strinati investigated the delay-energy consumption trade-off in the frame of cell DTX [181].

Other researchers have investigated centralized and distributed energy saving procedures that allow FAPs to completely switch off radio transmissions and associated processing in absence of end-users [8, 152]. Cell zooming adaptively adjusts the cell size according to traffic load, user requirements, and channel conditions [151]. Therefore, M-BSs under light load self-deactivate to reduce the network energy consumption; subsequently their UEs have to connect to the nearby macrocell. Hence, such a method requires that activated M-BSs increase their irradiated power to guarantee coverage and avoid outage events. To avoid outage and improving the network energy efficiency, Conte et al. proposed cell wilting and blooming mechanisms, which enable soft BSs deactivation and activation, respectively [182].

5.1.3 Contribution

Most of the work in the past has focused on improving the EE of BSs at low load or in the absence of end-users. However, in this chapter, we propose a novel architecture that improves system EE

even at moderate load scenarios. In particular, we introduce a novel algorithm for multi-cell traffic management that dynamically distributes user data amongst neighboring femtocells and adaptively controls the FAPs activity. The proposed approach exploits the knowledge of the local network topology, the traffic characteristics, and the link quality to dynamically activate/deactivate neighbouring FAPs reducing the femtocell network power consumption and also limiting co-channel interference. These gains come at the expense of an increasing packet delay, which is acceptable if it stays within the application QoS requirements. We also present a centralized architecture, where the multi-cell algorithm is implemented, and we discuss advantages and drawbacks of the selected network design strategy.

The novelty of this chapter is based on a patent [P3] and a conference paper [C6].

5.2 System Model

We consider a two-tier wireless cellular network in which mobile terminals and BSs implement an OFDMA air interface based on 3GPP/LTE downlink specifications [154]. OFDM symbols are organized into a number of physical RBs consisting of 12 contiguous sub-carriers for 7 consecutive OFDM symbols. With a bandwidth W of 10 MHz, 50 RBs are available for data transmission.

Each user is allocated one or several RBs in two consecutive slots, i.e., the TTI is equal to two slots and its duration T is 1 ms.

The RF power budget at FAPs (P_{\max}^F) is set equal to 10 dBm. The overall channel gain \mathbf{g} is composed of the antenna gain, a fixed distance dependent path loss, a slowly varying component modeled by lognormal shadowing, and Rayleigh fast fading with unit power.

We assume that femtocells are deployed in a block of 10 m x 10 m apartments according to the 3GPP grid urban deployment model [31]. In such a scenario each FAP can simultaneously serve up to 4 users. The block of apartments belongs to the same region of a macrocell, which share the same bandwidth of the neighbouring femtocells. Moreover, we assume that 6 additional M-BSs surround the central macrocell generating additive interference for both macro and femto users.

Further details on the femtocell deployment and related signal propagation models are presented in Section 2.2.2.1. Finally, our investigation is based on the EARTH E^3F power consumption model [17], which provides an accurate estimation of the BS power consumption considering the different components of the radio equipment such as antenna interface, PA, baseband interface, and cooling. Chapter 2.2.2.3 gives a description of the EARTH E^3F framework.

In this chapter, we use the same model parameters of Chapter 3; more details can be found in Table 3.1.

5.3 Classic DTX scheme and further improvements

We now briefly introduce the classical cell DTX and an extended version of this scheme, which we refer as cell E-DTX (see Figure 5.1). Cell DTX allows BSs to avoid radio operations whenever there is no user data transmitted in the cell. While in the classic approach the BS tries to serve its UEs within the shortest delay, in E-DTX it buffers received data and transmits as much as possible during the *transmit intervals*. Therefore, the BS efficiently exploits available frequency resources and introduces longer *silent intervals* at the cost of higher delay experienced by the application layer. Due to the limited number of UEs that can be simultaneously served by a FAP and the short distance between the AP and the user terminal, spectrum resource is often under-utilized at

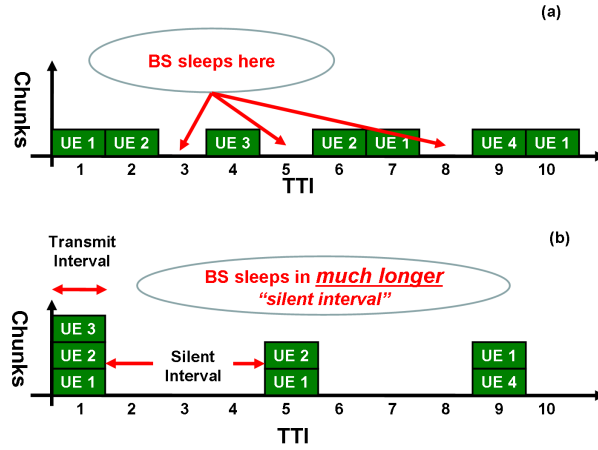


Figure 5.1: (a) Classic DTX and (b) E-DTX schemes.

femtocells. Hence, E-DTX is a very promising approach in femtocell deployment, however, it is important to limit the introduced additional delay due to buffering to comply with the application QoS constraints.

5.4 Problem Statement

Consider a macrocell region overlaid by a set of femtocells $\mathcal{F} = \{1, \dots, N_F\}$ deployed in a block of apartments as described in Section 5.2. The M-BS serves outdoor UEs and indoor UEs that can not be served by active FAPs. Femtocells operate in the same bandwidth of the macrocell and offer service to indoor UEs ($\mathcal{F} \mathcal{UE} = \{1, \dots, N_{FUE}\}$) that are located in their coverage areas. Each UE j identifies the set of closest femtocells (i.e., $\mathcal{F}^j \subseteq \mathcal{F}$) comparing the strength of the RSRP with a predefined threshold.

Therefore, we aim at dynamically associating UEs and FAPs to minimize the femtocell network energy consumption (within the observed TTIs $\mathcal{T} = \{1, \dots, N_{TTI}\}$) while meeting QoS (latency and throughput) constraints.

This optimization problem can be expressed as

$$\min \sum_{k \in \mathcal{T}} \sum_{i \in \mathcal{F}} P_i^*(k)$$

s.t.

$$n_i(k) \leq N_{\max} \quad \forall i \in \mathcal{F}, \quad \forall k \in \mathcal{T} \quad (5.1)$$

$$\sum_{i \in \mathcal{F}^j} a_i(k) X_{j,i}(k) \leq 1 \quad \forall j \in \mathcal{UE}, \quad \forall k \in \mathcal{T} \quad (5.2)$$

$$\sum_{p=k}^{k+d} \sum_{i \in \mathcal{F}^j} R_{j,i}(p) a_i(p) X_{j,i}(p) \geq PQ_{j,d}(k) \quad \forall j \in \mathcal{UE}, \quad \forall k \in \mathcal{T} \quad (5.3)$$

$$a_i(k) \in \{0, 1\} \quad \forall i \in \mathcal{F}, \quad \forall k \in \mathcal{T}$$

$$X_{j,i}(k) \in \{0, 1\} \quad \forall (i, j) \in \mathbf{X}, \quad \forall k \in \mathcal{T}$$

where P_i^* is the power consumption of the i -th FAP (see Eq. 2.3), n_i is the number of UEs served by the i -th FAP, \mathbf{a} is a vector whose elements indicate active FAPs, and the element $X_{j,i}$ of the service matrix \mathbf{X} indicates whether i th UE is served by FAP j (i.e., $X_{j,i}=1$). Moreover, R_{ji} is the useful data allocated to j -th UE by the i -th FAP and PQ_{jd} is the packet size for the user j and delay tolerance d . Eq. (5.1) indicates that the maximum number of UEs that can be simultaneously served by a FAP is limited by N_{\max} . Eq. (5.2) underlines that the j -th UE can be served only by one of the FAPs that belong to the set F^j . Finally, Eq. (5.3) points out that each packet that arrives in the queue of the j -th UE at TTI k has to be scheduled within its delay tolerance d . This ensures that QoS constraints of femtocell users are satisfied.

The above formulation corresponds to a combinatorial problem with high computational complexity especially in dense urban scenarios. Hence, to find a suboptimal solution, we propose a heuristic algorithm that can be implemented in networked femtocells deployment scenarios with a limited amount of signalling overhead.

5.5 Multi-cell architecture for dynamic cell DTX and traffic management

Here we discuss the proposed architecture for implementing Multi-Cell DTX (MC-DTX) in a femtocell network. In such an architecture, the femtocell network is characterized by a local femtocell coordinator, indicated as FCS. The FCS dynamically manages the activity of FAPs to limit the network power consumption while meeting traffic constraints. We should note here that the FCS is connected to FAPs via high speed low latency backhaul, which allows the implementation of fast adaptation mechanisms without affecting communications reliability. The FCS is responsible for three main functionalities:

1. Traffic management;
2. Dynamic UE/FAP association;
3. FAP activation.

The FCS receives from the core network the data related to the set of UEs attached to its femtocell network (cf. Figure 5.2). Therefore, it is able to classify the received traffic according to the delay constraint. High priority traffic needs to be sent within the next few TTIs, before the packet will be dropped by the user application; on the contrary, low priority traffic is characterized by less stringent constraints. This classification is realized comparing the packet delay tolerance with a delay threshold (D_{th}). D_{th} is a system parameter that depends on the time necessary to activate idle FAPs and permit to these femtocells to acquire CQI for data transmissions.

Algorithm 10 describes the selection of the set of FAPs ($\hat{\mathcal{F}} \subseteq \mathcal{F}$), which is in charge to serve UEs with high priority traffic ($\mathcal{F} \mathcal{U} \mathcal{E}^L \subseteq \mathcal{F} \mathcal{U} \mathcal{E}$). The coordinator activates serving femtocells exploiting stored average CQI (\mathbf{CQI}^*), which indicates the status of the links amongst femtocells \mathcal{F} and neighboring users $\mathcal{F} \mathcal{U} \mathcal{E}$. We recall that such an assignment is represented by the service matrix \mathbf{X} , which indicates whether UE j is served by FAP i .

Then, the FCS uses \mathbf{CQI}^* to define the set $\mathcal{F} \mathcal{U} \mathcal{E}^H \subseteq \mathcal{F} \mathcal{U} \mathcal{E}$; This is the set of the UEs characterized by only low priority traffic that are located in the vicinity of the activated FAPs $\hat{\mathcal{F}}$. Therefore, FCS assigns part of these UEs to the set $\hat{\mathcal{F}}$ such that available frequency resources at the activated FAPs can be used to transmit additional data packets.

Spectrum resource is often under utilized at femtocells, however, increasing the load of active FAPs we improve the femtocell EE. Furthermore, the more data is transmitted during the *activated*

Algorithm 10 Algorithm to select the set of priority users \mathcal{UE}^H and serving FAPs $\hat{\mathcal{F}}$

- 1: $\mathcal{FUE}^H \leftarrow \{j\} \in \mathcal{FUE} \text{ s.t. } PQ_{j,d} > 0, d \leq D_{th}$
 - 2: $\mathbf{X} = 0_{N_{FUE}, N_F}$
 - 3: $\hat{\mathcal{F}} = \{\emptyset\}$
 - 4: **for all** $j \in \mathcal{FUE}^H$ **do**
 - 5: $i^* = \operatorname{argmax}_i CQI_{j,i}^*$
 - 6: $\hat{\mathcal{F}} = \hat{\mathcal{F}} \cup \{i^*\}$
 - 7: $X_{j,i^*} = 1$
 - 8: **end for**
 - 9: $\mathbf{n} = 0_{1, N_F}$
 - 10: $n_i = \sum_{j \in \mathcal{FUE}^H} X_{j,i} \forall i \in \hat{\mathcal{F}}$
-

TTIs, higher the possibility of introducing sleep modes in future TTIs. Finally, the FCS routes the traffic of selected UEs to their associated FAPs and subsequently buffers the traffic that will not be scheduled in following TTIs. It should be noted here that the FCS is not in charge for the RRM scheduling, which is independently implemented at activated femtocells.

Algorithm 11 describes the approach that assigns low priority users to the set ($\hat{\mathcal{F}}$). Note that D_{Max} is the queue length at the FCS and the rationale behind using the metric \mathbf{M} is to ensure that the maximum amount of low priority traffic is allocated in the remaining resources of each FAP.

Algorithm 11 Algorithm to associate low priority users to the activated femtocells $\hat{\mathcal{F}}$

- 1: $\mathcal{FUE}^L \leftarrow \{j\} \in \mathcal{FUE} \text{ s.t. } PQ_{j,d} > 0, d > D_{th}$
 - 2: $\mathbf{PQ}^L \leftarrow PQ_{j,d} \text{ s.t. } j \in \mathcal{FUE}^L, d \leq D_{Max}$
 - 3: $\mathbf{CQI}^L \leftarrow CQI_{j,i}^* \text{ s.t. } j \in \mathcal{FUE}^L, i \in \hat{\mathcal{F}}$
 {line 2,3: extract data and CQI related to the set \mathcal{FUE}^L }
 - 4: $\mathbf{M} = 0_{|\mathcal{FUE}^L|, |\hat{\mathcal{F}}|}$
 - 5: $M_{j,i} = (\sum_{d=1}^{D_{max}} PQ_{j,d}^L) \cdot CQI_{j,i}^L$
 - 6: **while** $\mathbf{ANY}(\mathbf{M})$ & $\mathbf{ANY}(\mathbf{n} < N_{max})$ **do**
 - 7: $(j^*, i^*) = \operatorname{argmax}_{j,i} \mathbf{M}$
 - 8: $X_{j^*, i^*} = 1$
 - 9: $n_{i^*} = n_{i^*} + 1$
 - 10: $M_{j^*, i^*} = 0 \forall i \in \hat{\mathcal{F}}$
 - 11: **end while**
 {line 6: $\mathbf{ANY}(\mathbf{v}) = 1 \text{ IF } \exists 0 < i \leq \|\mathbf{v}\| \text{ s.t. } v_i \neq 0; \text{ ELSE } \mathbf{ANY}(\mathbf{v}) = 0$ }
-

We envision that the proposed coordination scheme can be realized within COMP framework where user data is available at multiple BSs and the transmitting BS may change from one sub-frame to another [183]. The main difference is due to the introduction of the FCS in the femtocell network architecture, which enables dynamic cell selection and FAP activity management without direct cooperation amongst neighboring FAPs. Furthermore, in our approach, FC routes user data only towards FAPs that are in charge of transmissions, which results in limited network overhead.

On the contrary, in a distributed implementation, the traffic related to the UE j has to be available in each FAP that belongs to its active set (i.e., the active set \mathcal{F}^j), which may lead to low scalability. The proposed scheme has an impact also on the LTE standard from the control signalling point of view; for example implementing cell DTX without losing UE/BS connectivity is currently a topic of investigation in the telecommunication community [2], however, it is beyond the scope of this thesis.

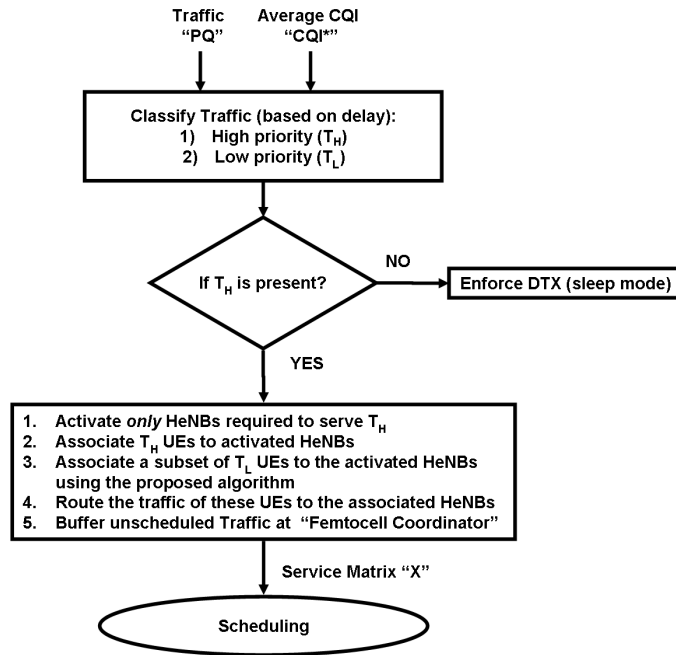


Figure 5.2: Proposed algorithm to dynamically associate traffic and FAPs at femtocell networks.

5.6 Simulation Results

In this section, we assess the effectiveness of the proposed MC-*DTX* scheme by comparing its performance with the E-*DTX* (see Section 5.3). Previous work has shown that E-*DTX* fairly outperforms the classic cell *DTX* [181]. Therefore, we consider E-*DTX* as the reference scheme. MC-*DTX* is based on open access femtocells, while E-*DTX* can be implemented in both closed access and open access schemes. Thus, with respect to the E-*DTX* scheme

- in the closed access Femtocells deployment, a UE can be served by a FAP only if that the access point is placed in the user apartment;
- in the open access Femtocells deployment, UEs can be in the coverage area of several femtocells. Hence, each user selects the available FAP associated with the best RSRP.

In both E-*DTX* and MC-*DTX* the system buffers UE data to allow as longer as possible silent interval at serving FAPs. However, MC-*DTX* exploits dynamic cell selection amongst neighboring FAPs to increase the amount of traffic sent by activated FAPs within their transmit interval. We consider that the FAP power consumption during sleep mode $P_{sleep} \ll P_0$ and we do not investigate its impact on both E-*DTX* and MC-*DTX* schemes. In fact, we expect that in close future

the research progress on agile hardware will permit dynamic and energy efficient FAPs activation/deactivation.

We consider a scenario in which 30 cellular users are deployed in the macrocell area. In line with recent studies [19], we assume that 70% of the traffic is generated by indoor UEs. The results are averaged over 60 independent runs. We simulate $15 \cdot 10^3$ independent TTIs during each run and update channel fading instances at each TTI. At the beginning of each run, FAPs and indoor UEs are randomly deployed in the block of apartments placed at the macrocell edge. Outdoor UEs are randomly deployed in the macrocell region. The traffic generated by cellular users is modeled as a Near Real Time Video (NRTV) traffic [184] with rate of 64 kbps and a deterministic inter-arrival time between the beginning of each frame equal to 100ms. Moreover, the mean and maximum packet sizes are respectively equal to 50 and 250 bytes. A PF-based scheduler [142] is used at both the macrocell and femtocells. Finally, link adaptation is implemented in downlink transmissions for which MCSs are selected according to momentary feedback transmitted by the served UE. In our simulations, triangle marked lines, squared marked lines, and diamond marked lines, respectively correspond to the E-DTX with closed access, E-DTX with open access, and MC-DTX with open access.

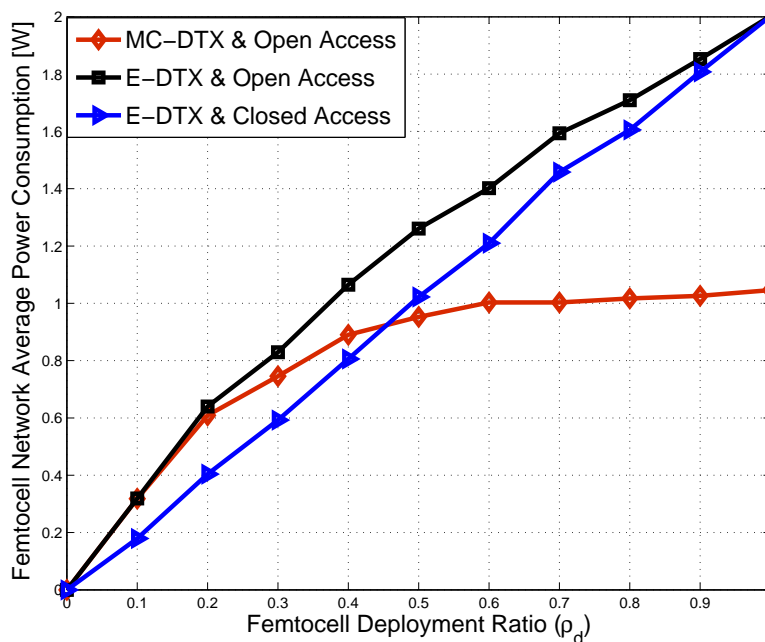


Figure 5.3: Femtocell network Average Power Consumption with respect to the femtocell deployment ratio (ρ_d).

First, we aim to discuss the impact of the analysed schemes in terms of femtocell power consumption. Figure 5.3 shows the average power consumption in the femtocell network with respect to the femtocell deployment ratio (ρ_d). The difference between open access and closed access schemes is related to the number of UEs served by FAPs (i.e., the load of the femtocell network): in the open access deployment the probability that a UE can be served by a FAP is higher than in the closed access deployment. Therefore, closed access results in longer silent intervals and lower power consumption at the femtocell network. Note that the gap between open access and closed access schemes is maximum for medium values of deployment ratio and decreases in

very dense deployment scenarios. In particular, when $\rho_d = 1$, all the apartments in the block are equipped with a femtocell, all indoor user can be served by the closest FAP, and the performance of these two strategies are coincident. However, while in E-DTX schemes power consumption fairly increases with the femtocell deployment ratio, MC-DTX power consumption slightly changes in medium/high femtocell density ($\rho_d \geq 0.4$) scenarios. In fact, in such a range of values the capacity of the femtocell network may exceed the service request and the MC-DTX avoids energy wastage adapting the femtocells activity to the network topology and load by implementing a dynamic UE-cell association. Simulation result shows that our proposal outperforms the reference approaches achieving up to the 50% of power saving.

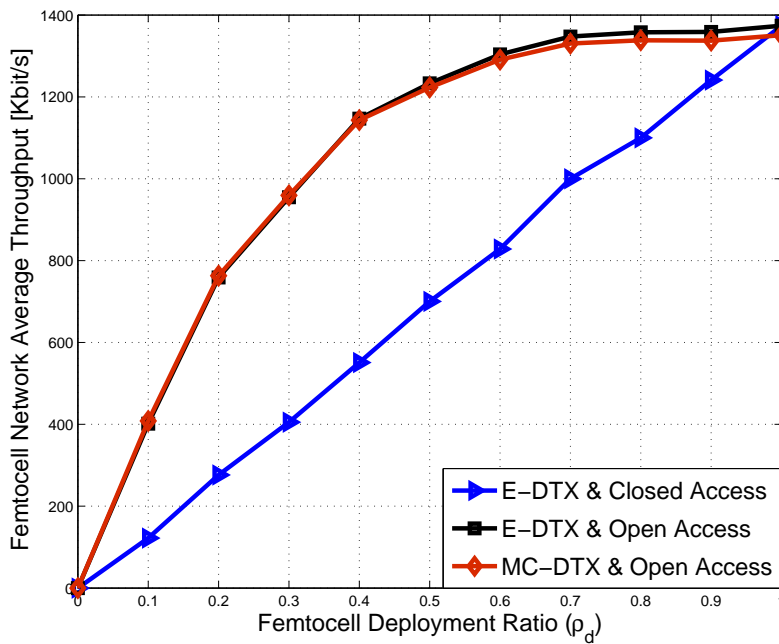


Figure 5.4: Femtocell network average aggregate Throughput with respect to the femtocell deployment ratio (ρ_d).

Our proposed algorithm does not permit UEs to select the FAP associated with the best RSRP. Hence, we may expect that user performance decreases when using MC-DTX. In Figure 5.4, we present the impact of the proposed scheme on the performance perceived by femto users. We show the average throughput at femtocell network with respect to the femtocell deployment ratio for the compared schemes. As previously mentioned, closed access scheme limits the macrocell offloading due to the femtocell deployment. This results in higher power consumption at the M-BS (see Figure 5.5) and lower throughput at the femtocell network. Simulation results in Figure 5.4 show that open access schemes lead to throughput increasing in the femtocell network up to the 136%. However, MC-DTX and E-DTX with open access femtocells perform in the fairly same way.

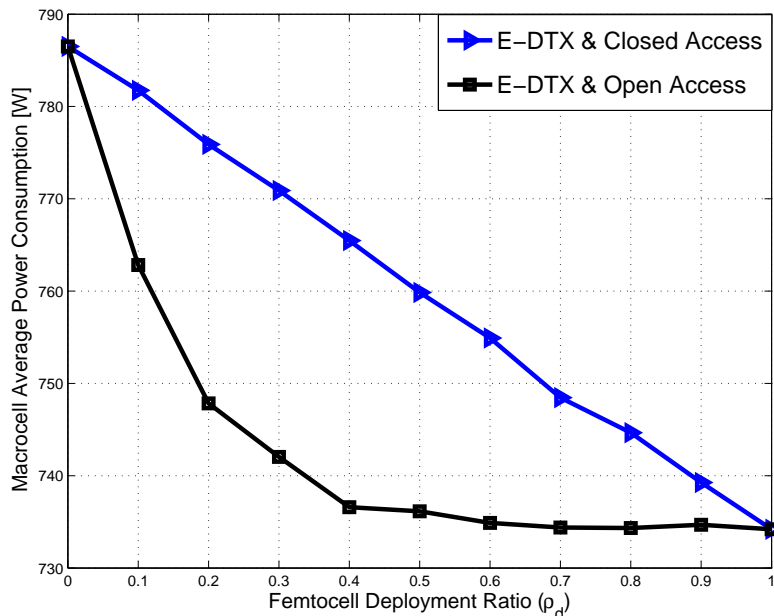


Figure 5.5: Macrocell average Power Consumption with respect to the femtocell deployment ratio (ρ_d).

5.7 Conclusions

Data traffic have recently surpassed voice and its volume in cellular network is growing exponentially. To satisfy users' expectation in terms of quality of experience cellular network are integrating FAPs, which offer high data rate services to indoor users.

However, the ad-hoc deployment of new APs and their uncoordinated operations may raise both the level of interference and the aggregate power consumption of cellular networks. Agile network mechanisms are required to manage this novel scenario in order to meet the end-user QoS requirements and improve the cellular network EE.

Most of the previous studies, propose mid/long time scale solutions that enable energy saving especially when the network is lightly loaded (i.e., the presence of active UEs is limited). However, these schemes do not exploit the traffic *diversity* that characterizes data and voice. In fact, although voice traffic is characterized by tight latency constraints, applications such as mails, video, and facebook notifications have less stringent constraints.

In this chapter, we have introduced a network management scheme that exploits the delay-energy trade-off locally buffering the traffic directed to active users and then, efficiently distributing packets amongst deployed APs according to latency requirements, network deployment characteristics, and link quality. The proposed approach for open access femtocells, named as MC-DTX, operates in a fast time scale (the scheduling period) and is effective also in moderated/high load scenarios. MC-DTX permits FAPs to cooperatively adapt their activity to the traffic scenarios, dynamically limiting the femtocell network power consumption. This advantages comes at cost of higher complexity and signalling overhead; to share these costs amongst the cooperating femtocell, a distributed implementation of MC-DTX is feasible, however, this approach further increases the network overhead.

Chapter 6

Conclusions and Future Work

6.1 Conclusions

Wireless cellular networks are tremendously successful, which results in wide proliferation and demand for ubiquitous heterogeneous broadband mobile wireless services. Mobile operators have observed an exponential growth of data traffic within their networks only over the last few months. To ensure the economic viability of cellular networks, the average revenue per user has to remain the same, although the user expectations are growing in terms of ubiquitous QoE, and data usage is becoming intensive due to the generalization of flat rates. This translates into the need to reduce both capital and operational expenditures and in the same time to enhance the cellular network infrastructure. In fact, both cell-edge and indoor users associated to the M-BS likely experience poor performance due to interference and propagation and penetration losses. Furthermore, network upgrades have to be smooth and exploit the already available infrastructure to take advantage of the previous investments and also to guarantee backward compatibility.

In Chapter 2 of this dissertation, we have first discussed main challenges and preliminary solutions to uniformly offer wireless broadband services in future cellular networks. Then, we have introduced the cognitive radio paradigm as an enabling technique for an agile cellular network. The advantages and drawbacks of femtocell networks have been investigated; moreover, we have presented some interesting solutions proposed in the literature to enable the cost-effective femtocells deployment and improve the coexistence of macrocells and femtocells in a given geographical region. Eventually, Chapter 2 has presented the Earth E^3F [17] power consumption model and some femtocell use cases proposed in the FP7 ICT BeFEMTO [32], which represent the baselines of the system model used throughout the thesis.

In Chapter 3, we have taken advantage of the resource management characteristics in the two-tier cellular networks deployment to propose a RRM paradigm, named as *Ghost* RRM, which jointly reduces co-channel interference and irradiated RF power at femtocells required to meet users' constraints. In fact, first, femtocell users likely benefit from a high SINR signal enabled by the limited propagation and penetration losses. Second, only few users are simultaneously served by a FAP, thus they locally compete for a large amount of resources. Therefore, we have exploited techniques based on MCS scaling and power control to trade-off transmission power for frequency

resources. Such an approach has been implemented in both stand-alone and networked femtocell deployment scenarios. In the former case, due to the latency of the IP-based backhaul, FAPs self-organize their access strategy; on the contrary, in the latter scenario, fast coordination is feasible and neighbouring FAPs cooperate to limit mutual interference. Simulation results have shown that both proposed RRM schemes enhance the performance perceived at macro and femto end-users. Moreover, our analysis has pointed out that femtocell cooperation leads to high benefits only in dense femtocell deployment scenarios.

In Chapter 4, we have proposed a femtocell activation management scheme to avoid resource wastage and uncoordinated operations in dense femtocell deployment scenarios. Our investigation has underlined the trade-off in terms of macrocell offloading and power consumption between the classic open access and closed access schemes. Then, we have presented the Advanced Open Access approach, which optimizes the association amongst deployed femtocells and neighbouring users leading to notable energy saving. This gain comes at the cost of higher overhead, which is limited by the reduced mobility in the indoor scenarios. Moreover, we have proposed two different schemes that enable the implementation of the Advanced Open Access in both networked and stand-alone cases. In the networked scenarios, the overhead and computational costs are shared at cooperative FAPs, although in stand-alone case, end-users contribute to the optimization process to cope with the absence of inter-cell coordination.

In Chapter 5, we have proposed MC-DTX, which permits femtocell networks to cooperatively adapt their activity to the traffic scenarios, dynamically limiting the network power consumption. Even though most of the previous studies have proposed mid/long time scale solutions to limit power consumption when the network is characterized by very low load (i.e., in absence of active UEs), we have introduced a network management scheme that operates within the scheduling period and is effective also in moderated/high load scenarios. In this scheme, a local coordinator is aware of the traffic characteristics, channel state information, and QoS constraints; it exploits such a consciousness to dynamically manage the traffic queues, UE/AP association, and APs activity to optimize the usage of available transmission resources and the network EE. Simulation results have shown that the proposed scheme is able to strongly reduce the femtocell network energy consumption without affecting end-users performance.

6.2 Future Work

Interference mitigation for small cells implementing cell DTX

Cell DTX technique [2] is a mechanism that enables to immediately switch off cell specific signalling during subframes where there is no user data transmission, thereby lowering the energy consumption as well as the Electro Magnetic Field (EMF) level. In Chapter 5, we have investigated the benefits related to this transmission technique and also proposed a network management scheme based on cell DTX, which is especially suitable for small cell deployment. However, in this scenario, an issue arises in the sense that the characteristics of the perceived interference in the cells change due to the discontinuous transmission of neighbouring BSs. In cell DTX, transmissions will likely to be realized in bursts, to increase the length of *silent periods*, then, interference becomes even more unpredictable and channel state information less reliable with respect to the classic cellular systems. Therefore, discontinuous transmissions result in local spikes of interference in the time frequency domain, which may be harmful for concurrent communications. Although in the indoor environment, penetration losses due to outdoor walls attenuate the effects of this problem, in outdoor environment cell-edge UEs may experience very poor performance. As a consequence, we aim at designing self-organizing techniques and inter-cell coordination al-

gorithms to improve the characterisation of interference patterns and permit reliable transmissions in the cells. Then, implementation of cell DTX in a robust manner will enable to reduce EMF exposure and energy consumption while limiting inter-cell interference.

Content and Context Aware Network Management

Emerging heterogeneous data services and UE/BS deployment create traffic asymmetry in space and time. Moreover, dense deployment of local APs, which is a tight requirement in cellular networks to offer ubiquitous broadband coverage, may result in excessive capacity and energy wastage. Network management schemes are a set of mechanisms that operates at system level to optimize the network behaviour, i.e., the energy consumption is reduced, co-channel interference is limited, and users' QoS constraints are guaranteed. Preliminary work attempts to manage the network characteristics (such as type of activated BSs, irradiated power, and used frequency bands) according to the statistical model of the traffic [185]. Nowadays, traffic load is mainly predicted according to long-term large-scale measurements, which allow to construct a daily traffic profile of a given geographical area (see Figure 6.1). However, predictions errors can lead to outage events

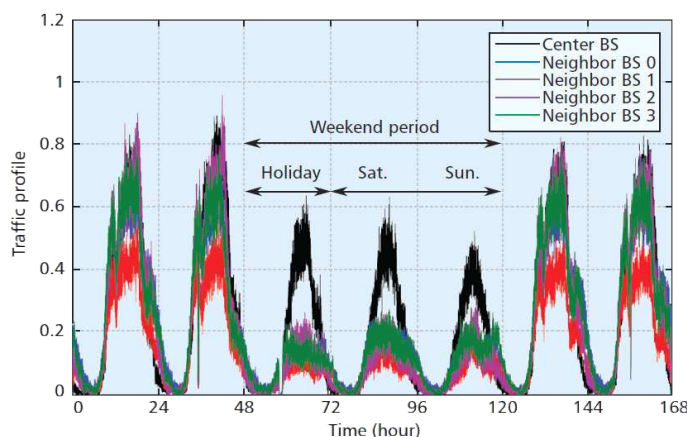


Figure 6.1: Traffic dynamics both in the time and space domains [172].

(when the traffic demand is underestimated) as well as to excessive energy consumption (when the traffic demand is overestimated) (see Figure 6.2).

On the contrary, a near-real time model that represents traffic characteristics in both space and time could lead to higher network performance.

Inspired by the Internet world, where the users' behaviour is continuously monitored, stored, and analysed to offer a higher QoE and also for commercial purposes, we aim at developing a framework in which specific informations on the content of the users' data are acquired and processed to construct a traffic map, which follows network load asymmetry. Moreover, information on the context where a given data traffic occurs might permit to better characterize the cell load behaviour and also to model the particular usage of each customer. Finally, estimated users' position and mobility characteristics could further enhance the reliability of such a framework.

We have also identified some preliminary strategies to acquire content information at the mobile operator:

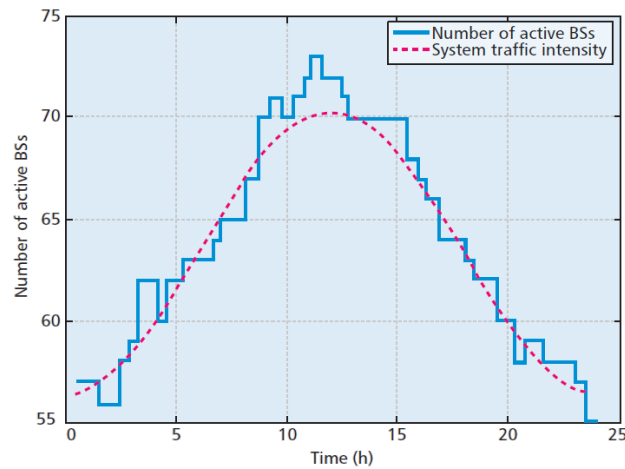


Figure 6.2: Dynamic BS sleep control and its effects [186].

- Information about traffic nature (i.e., the application) and characteristics (such as the length of a movie) is explicitly transmitted by the UE as part of control signalling; note that this approach requires standard modification.
- Install passive applications on UEs to gather content/context information.
- The operator tries to acquire content data awareness by characterizing the packet flow in the network using Deep Packet Inspection (DPI) technologies [187].

This network consciousness will enable to efficiently select management mechanisms to match the offered capacity with the future demands in traffic and minimize the effects of errors into the prediction process (see Figure 6.3).

Interference-aware Network Management in dense Heterogeneous Cellular Networks

Recent studies have attempted to characterize the aggregate interference generated/perceived in scenarios where nodes, which belong to different networks, uncoordinatedly share the same spectrum in a given geographical area [188, 189]. These models try to capture the uncertainty due to the unknown number of interferers, the unknown relative position between victim and interferer as well as the channel fading and other environment-dependent conditions (such as the presence of walls). Moreover, these studies consider a probabilistic process to represent the spatial distribution of neighbouring nodes. On the contrary, we aim at investigating a scenario where cellular users and BSs have peer-to-peer ranging capabilities, which enable cooperative positioning. Therefore, we will integrate in the prediction of aggregated interference levels some deterministic location information, to locally estimate the interference strength (depending on the actual network deployment) and optimize the network (in terms of APs activity, UEs and APs association, spectrum access), accordingly. However, such ranging mechanisms are affected by errors due to, for instance, interference and multipath. Then, we aim at enhancing performance of the proposed approach by considering the error characteristics in the constructed interference model.

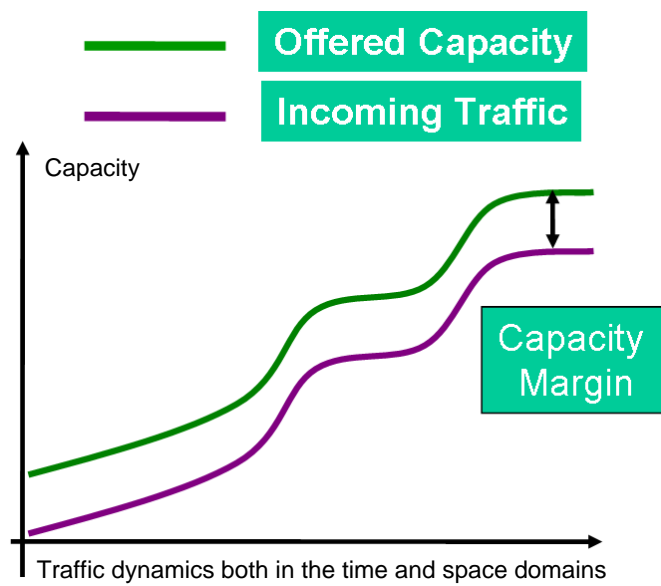


Figure 6.3: Capacity model of the proposed content/context aware framework.

Appendix A

Complements to Chapter 3: Green Ghost Femtocells

This appendix gives further implementation details for the proposed $Ghost_{NF}$ presented in Section 3.4.3. The main differences with respect to the $Ghost_{SAF}$, described in Section 3.4.2, are related to the presence of a central controller, which periodically manages resource allocation in the femtocell network. In particular, Algorithm 13 aims to find those active UEs that can be successfully served during the scheduling period. Algorithm 14 shares amongst the scheduled UEs those RBs that are still available after the first scheduling process in order to lower the MCS associated to their transmissions. Finally, the last step (Algorithm 15), takes advantage of the spreading process to adjust the irradiated power per RB in order to fulfil the QoS constraints and limit irradiated power.

Algorithm 12 Main

```

1: for all  $i \in \mathcal{F}$  do
2:    $\mathcal{V}_j = \{i^* \in \mathcal{F} \setminus i \mid RSRP_{i^*} \geq T_h\} \cup \{i\} \quad \forall j \in \mathcal{F} \cup \mathcal{E}^i$ 
3: end for
4:  $\mathbf{S}^{\text{Ch}} = \mathbf{0}_{N_{\text{FUE}}, N_{\text{RB}}}$ 
5:  $\mathcal{S}^{\mathcal{UE}} = \{\emptyset\}$ 
6:  $\mathbf{R} = \mathbf{0}_{N_{\text{RB}}, N_{\text{FUE}}}$ 
7:  $\mathbf{MCS}^* = \mathbf{0}_{N_{\text{FUE}}, 1}$ 
8:  $\mathcal{X}_j = \{\emptyset\} \quad \forall j \in \mathcal{F} \cup \mathcal{E}$ 
9: for all  $i \in \mathcal{F}$  do
10:   $\lambda_{j,k} = \gamma_{i,j,k} \quad \forall (j,k) \in \mathcal{F} \cup \mathcal{E}^i \times \mathcal{C}_h$  {see Eq. 3.9}
11: end for
12:  $\mathbf{M}^{\text{Tx}} = \boldsymbol{\lambda}$ 
13:  $\mathbf{M}^{\text{Sp}} = \boldsymbol{\lambda}$ 
14: while ANY( $\mathbf{M}^{\text{Tx}}$ ) do {see the note below}
15:   Algorithm 13 {Scheduling}
16: end while
17: Algorithm 14 {Spreading}
18: Algorithm 15 {Power Control}
    {line 14: ANY( $\mathbf{v}$ ) = TRUE IF  $\exists 0 < i \leq |\mathbf{v}|$  s.t.  $v_i \neq 0$ }

```

Algorithm 13 Algorithm that finds the active F-UEs that can be successfully served (\mathcal{S}^{UE}); it also associates to these F-UEs the RBs and related MCS to meet QoS and power constraints

- 1: $(j^*, k^*) = \underset{j,k}{\operatorname{argmax}} \mathbf{M}^{\text{Tx}}$
- 2: $\mathcal{K}_{j^*} = \mathcal{K}_{j^*} \cup \{k^*\}$
- 3: $\mathcal{L} = \{\lambda_{j^*,k} \mid k \in \mathcal{K}_{j^*}\}$
- 4: $\tilde{\lambda} = \mathbf{MAP}(\mathcal{L})$ {see the note below}
- 5: $MCS = \max_s \{s \mid \tilde{\lambda} \geq SINR_s^{\text{th}}\}$
- 6: **if** $MCS \geq 1$ **then**
- 7: $S_{j^*,k^*}^{\text{Ch}} = 1$
- 8: $R_{k^*,j^*} = PS_{MCS}$
- 9: $\lambda_{j^*,k} = \frac{\gamma_{j,k}}{\sum_{l \in \mathcal{K}_{j^*}} \gamma_{j,l}} \quad \forall k \in C_h$ {see Eq. 3.11}
- 10: **if** $\sum_{k \in C_h} R_{k,j^*} \geq T_{\text{tg}}$ **then**
- 11: $M_{j^*,k}^{\text{Tx}} = 0 \quad \forall k \in C_h$
- 12: $\mathcal{S}^{UE} = \mathcal{S}^{UE} \cup \{j^*\}$
- 13: $MCS_{j^*}^* = MCS$
- 14: **else**
- 15: $M_{j^*,k^*}^{\text{Tx}} = 0$
- 16: $M_{j^*,k}^{\text{Tx}} = \lambda_{j^*,k} \quad \forall k \in C_h \setminus k^*$
- 17: **end if**
- 18: **for all** $i \in \mathcal{V}_j^*$ **do**
- 19: $M_{j,k^*}^{\text{Tx}} = 0 \quad \forall j \in \mathcal{F}^{UE^i}$
- 20: $M_{j,k^*}^{\text{Sp}} = 0 \quad \forall j \in \mathcal{F}^{UE^i}$
- 21: **end for**
- 22: $M_{j^*,k}^{\text{Sp}} = \lambda_{j^*,k} \quad \forall k \in C_h$
- 23: **else**
- 24: $M_{j^*,k}^{\text{Tx}} = 0 \quad \forall k \in C_h$
- 25: $M_{j^*,k}^{\text{Sp}} = 0 \quad \forall k \in C_h$
- 26: **end if**

{line 4: $\mathbf{MAP}(\cdot)$ maps the SINR values of different allotted RBs to a LQM that predicts performance of an OFDMA system. Either the EESM [165] or the MIESM [166] can be used here}

Algorithm 14 Spreading Algorithm

```

1: while ANY( $\mathbf{M}^{\text{Sp}}$ ) do {see note below}
2:    $(j^*, k^*) = \text{argmax } \mathbf{M}^{\text{Sp}}$ 
3:    $\mathcal{K}_{j^*} = \mathcal{K}_{j^*} \cup \{k^*\}$ 
4:    $\mathcal{L} = \{\lambda_{j^*,k} \mid k \in \mathcal{K}_{j^*}\}$ 
5:    $\tilde{\lambda} = \text{MAP}(\mathcal{L})$  {see note below}
6:    $MCS = \min_s \{s \mid \tilde{\lambda} \geq SINR_s^{\text{th}} \ \& \ |\mathcal{K}_{j^*}| \cdot PS_s \geq T_{\text{tg}}\}$ 
7:   if  $MCS \geq 1$  then
8:      $S_{j^*,k^*}^{\text{Ch}} = 1$ 
9:     for all  $i \in \mathcal{V}_j^*$  do
10:       $M_{j^*,k^*}^{\text{Sp}} = 0 \ \forall j \in \mathcal{F} \cup \mathcal{E}^i$ 
11:    end for
12:     $MCS_{j^*}^* = MCS$ 
13:    if  $MCS = 1$  then
14:       $M_{j^*,k}^{\text{Sp}} = 0 \ \forall k \in \mathcal{C}_h$ 
15:    else
16:       $\lambda_{j^*,k} = \frac{\gamma_{j,k}}{\sum_{l \in \mathcal{K}_{j^*}} \gamma_{j,l}} \ \forall k \in \mathcal{C}_h$  {see Eq. 3.11}
17:       $M_{j^*,k}^{\text{Sp}} = \lambda_{j^*,k} \ \forall k \in \mathcal{C}_h$ 
18:    end if
19:    else
20:       $M_{j^*,k}^{\text{Sp}} = 0 \ \forall k \in \mathcal{C}_h$ 
21:    end if
22: end while

```

{line 1: ANY(\mathbf{v}) = TRUE IF $\exists 0 < i \leq |\mathbf{v}|$ s.t. $v_i \neq 0$ }

{line 5: MAP(\cdot) maps the SINR values of different allotted RBs to a LQM that predicts performance of an OFDMA system. Either the EESM [165] or the MIESM [166] can be used here}

Algorithm 15 Power Control

```

1: for all  $j \in \mathcal{S}^{UE}$  do
2:    $P_{i,k}^{\text{RF}} = \frac{SINR_{MCS_j^*}^{\text{th}} \cdot P_{\text{max}}^{\text{F}}}{\gamma_{i,j,k} \cdot N_{\text{RB}}} + \delta_{\text{M}} \ \forall k \in \mathcal{K}_j$ 
3: end for

```

Bibliography

- [1] V. Chandrasekhar, J. Andrews, and A. Gatherer, “Femtocell networks: a survey,” *IEEE Communications Magazine*, vol. 46, no. 9, pp. 59–67, September 2008.
- [2] P. Frenger, P. Moberg, J. Malmudin, Y. Jading, and I. Godor, “Reducing energy consumption in lte with cell dtx,” *IEEE 73rd Vehicular Technology Conference (VTC Spring 2011)*, pp. 1–5, May 2011.
- [3] I. F. Akyildiz, W-Y. Lee, and K. R. Chowdhury, “CRAHNS: Cognitive Radio Ad Hoc Networks,” *Ad Hoc Networks (Elsevier) Journal*, vol. 7, Issue 5, pp. 810–836, July 2009.
- [4] G. Gür and F. Alagöz, “Green wireless communications via cognitive dimension: an overview,” *IEEE Network*, vol. 25, no. 2, pp. 50–56, 2011.
- [5] L.G.U. Garcia, G.W.O. Costa, A.F. Cattoni, K.I. Pedersen, and P.E. Mogensen, “Self-organizing coalitions for conflict evaluation and resolution in femtocells,” in *IEEE Global Telecommunications Conference (GLOBECOM 2010)*, December 2010, pp. 1–6.
- [6] A. De Domenico, E. Calvanese Strinati, and M. G. Di Benedetto, “A Survey on MAC strategies for Cognitive Radio Networks,” *IEEE Communication Surveys and Tutorials*, 2012. Available at IEEEExplore.
- [7] C. Abgrall, E. Calvanese Strinati, and J.C. Belfiore, “Distributed power allocation for interference limited networks,” in *IEEE 21st International Symposium on Personal Indoor and Mobile Radio Communications (PIMRC 2010)*, 2010, pp. 1342–1347.
- [8] I. Ashraf, F. Boccardi, and L. Ho, “Sleep mode techniques for small cell deployments,” *IEEE Communications Magazine*, vol. 49, no. 8, pp. 72–79, August 2011.
- [9] Ericsson, “Mobile data traffic surpasses voice,” <http://www.ericsson.com/news>, March 2010.
- [10] Cisco, “Global Mobile Data Traffic Forecast Update, 2010-2015,” <http://www.cisco.com>, February 2011.
- [11] S. Mclaughlin, P.M. Grant, J.S. Thompson, H. Haas, D.I. Laurenson, C. Khirallah, Y. Hou, and R. Wang, “Techniques for improving cellular radio base station energy efficiency,” *IEEE Wireless Communications*, vol. 18, no. 5, pp. 10–17, 2011.
- [12] S. Landström, A. Furuskär, K. Johansson, L. Falconetti, and F. Kronstedt, “Heterogeneous networks-increasing cellular capacity,” *Ericsson Review*, February 2011.

- [13] Federal Communications Commission, "FCC, ET Docket No 03-222 Notice of proposed rule making and order," Tech. Rep., December 2003.
- [14] A.C. Stocker, "Small-cell mobile phone systems," *IEEE Transactions on Vehicular Technology*, vol. 33, no. 4, pp. 269–275, November 1984.
- [15] J. Shapira, "Microcell engineering in cdma cellular networks," *IEEE Transactions on Vehicular Technology*, vol. 43, no. 4, pp. 817–825, 1994.
- [16] A. Fehske, J. Malmodin, G. Biczók, and G. Fettweis, "The global footprint of mobile communications—the ecological and economic perspective," *IEEE Communications Magazine*, pp. 55–62, August 2011.
- [17] G. Auer, V. Giannini, C. Desset, I. Godor, P. Skillermark, M. Olsson, M.A. Imran, D. Sabella, M.J. Gonzalez, O. Blume, and A. Fehske, "How much energy is needed to run a wireless network?," *IEEE Wireless Communications*, vol. 18, no. 5, pp. 40–49, 2011.
- [18] Alcatel-Lucent, "Eco-sustainable Wireless Services," <http://www.alcatel-lucent-business-club.com/>, 2009.
- [19] Informa Telecoms & Media, "Mobile Broadband Access at Home," August 2008.
- [20] Informa Telecoms & Media, "Femtocell Market Status," www.femtoforum.org/fem2/resources.php, October 2011.
- [21] Alcatel-Lucent, "Metro Cells: A cost-effective option for meeting growing capacity demands," www.alcatel-lucent.com, 2011.
- [22] 3GPP TS 36.300 V10.5.0, "Evolved Universal Terrestrial Radio Access (E-UTRA) and Evolved Universal Terrestrial Radio Access Network (E-UTRAN): Overall Description," September 2011.
- [23] V. Chandrasekhar and J. Andrews, "Spectrum allocation in tiered cellular networks," *IEEE Transactions on Communications*, vol. 57, no. 10, pp. 3059–3068, October 2009.
- [24] G. de la Roche, A. Valcarce, D. Lopez-Perez, and Jie Zhang, "Access control mechanisms for femtocells," *IEEE Communications Magazine*, vol. 48, no. 1, pp. 33–39, January 2010.
- [25] S. Carlaw, "Ipr and the potential effect on femtocell markets," *FemtoCells Europe, ABIResearch*, 2008.
- [26] D. Knisely, T. Yoshizawa, and F. Favichia, "Standardization of femtocells in 3gpp," *IEEE Communications Magazine*, vol. 47, no. 9, pp. 68–75, September 2009.
- [27] E. Seidel and E. Saad, "LTE Home Node Bs and its enhancements in Release 9," in *Nomor Research*, 2010.
- [28] Broadband forum TR-196, "Femto Access Point Service Data Model," April 2009.
- [29] 3GPP2 X.S0059-000-0, "cdma2000 Femtocell Network: Overview, Version 1.0," January 2010.
- [30] WMF-T33-118-R016v01, "WiMAX Forum Network Architecture - Detailed Protocols and Procedures, Femtocells Core Specification," November 2010.

- [31] 3GPP TSG-RAN4#51, Alcatel-Lucent, picoChip Designs, and Vodafone, “R4-092042, Simulation assumptions and parameters for FDD HENB RF requirements,” May 2009.
- [32] M. Bennis, L. Giupponi, E.M. Diaz, M. Lalam, M. Maqbool, E.C. Strinati, A. De Domenico, and M. Latva-aho, “Interference management in self-organized femtocell networks: The befemto approach,” in *2nd International Conference on Wireless Communication, Vehicular Technology, Information Theory and Aerospace Electronic Systems Technology (Wireless VITAE 2011)*, March 2011, pp. 1–6.
- [33] 3GPP TSG RAN WG1 #61 bis, Nokia Siemens Networks, and Nokia, “R1-103822, Enhanced ICIC considerations for HetNet scenarios,” July 2010.
- [34] 3GPP TS 32.500 (release 11), “Telecommunication Management; Self-Organizing Networks (SON); Concepts and requirements,” June 2011.
- [35] G. de la Roche, A. Ladányi, D. López-Pérez, C.C. Chong, and J. Zhang, “Self-organization for lte enterprise femtocells,” in *IEEE GLOBECOM Workshops 2010*, December 2010, pp. 674–678.
- [36] D. Lopez-Perez, I. Guvenc, G. de la Roche, M. Kountouris, T.Q.S. Quek, and Jie Zhang, “Enhanced intercell interference coordination challenges in heterogeneous networks,” *IEEE Wireless Communications*, vol. 18, no. 3, pp. 22–30, June 2011.
- [37] 3GPP TSG RAN WG1 #60 and LG Electronics, “R1-101369, Considerations on interference coordination in heterogeneous networks,” February 2010.
- [38] S. Haykin, “Cognitive radio: brain-empowered wireless communications,” *IEEE Journal on Selected Areas in Communications*, vol. 23, pp. 201–220, February 2005.
- [39] I. F. Akyildiz, W. Y. Lee, M. C. Vuran, and S. Mohanty, “NeXt generation/ dynamic spectrum access / cognitive radio wireless networks: A survey,” *Computer Networks Journal (Elsevier)*, vol. 50, Issue 13, pp. 2127–2159, September 2006.
- [40] J. So and N. H. Vaidya, “Multi-channel MAC for ad hoc networks: handling multi-channel hidden terminals using a single transceiver,” in *Proceedings of the 5th ACM international symposium on Mobile ad hoc networking and computing*, Roppongi Hills, Tokyo, Japan, May 2004, pp. 222–233.
- [41] I. F. Akyildiz, W. Y. Lee, M. C. Vuran, and S. Mohanty, “A survey on spectrum management in cognitive radio networks,” *IEEE Communications Magazine*, vol. 46, no. 4, pp. 40–48, April 2008.
- [42] A. K. L. Yau, P. Komisarczuk, and P. D. Teal, “On Multi-Channel MAC Protocols in Cognitive Radio Networks,” in *Telecommunication Networks and Applications Conference ATNAC 2008. Australasian*, December 2008, pp. 300–305.
- [43] H. Wang, H. Qin, and L. Zhu, “A Survey on MAC Protocols for Opportunistic Spectrum Access in Cognitive Radio Networks,” in *International Conference on Computer Science and Software Engineering*, December 2008, vol. 1, pp. 214–218.
- [44] T. V. Krishna and A. Das, “A survey on MAC protocols in OSA networks,” *Computer Networks Journal (Elsevier)*, vol. 53, no. 9, pp. 1377–1394, 2009.

- [45] C. Cormio and K. R. Chowdhury, "A survey on MAC protocols for cognitive radio networks," *Ad Hoc Networks Journal (Elsevier)*, vol. 7, no. 7, pp. 1315–1329, 2009.
- [46] P. Pawelczak, S. Pollin, H. S. W. So, A. Bahai, R. V. Prasad, and R. Hekmat, "Performance Analysis of Multichannel Medium Access Control Algorithms for Opportunistic Spectrum Access," *IEEE Transactions on Vehicular Technology*, vol. 58, no. 6, pp. 3014–3031, July 2009.
- [47] J. Mo, H. S. W. So, and J. Walrand, "Comparison of multi-channel MAC protocols," *IEEE Transactions on Mobile Computing*, vol. 7, no. 1, pp. 50–65, January 2008.
- [48] Y. Xiao and F. Hu, "Cognitive Radio Network," *Taylor & Francis Group*, 2009.
- [49] J. Jia, Q. Zhang, and X. Shen, "HC-MAC: a hardware-constrained cognitive MAC for efficient spectrum management," *IEEE Journal on Selected Areas in Communications*, vol. 26 (1), 2008.
- [50] Hang Su and Xi Zhang, "Cross-Layer Based Opportunistic MAC Protocols for QoS Provisionings Over Cognitive Radio Wireless Networks," *Selected Areas in Communications, IEEE Journal on*, vol. 26, no. 1, pp. 118–129, January 2008.
- [51] M. M. Buddhikot, P. Kolodzy, S. Miller, K. Ryan, and J. Evans, "DIMSUMNet: New Directions in Wireless Networking Using Coordinated Dynamic Spectrum Access," in *Proceedings of the Sixth IEEE International Symposium on World of Wireless Mobile and Multimedia Networks (WOWMOM '05)*, 2005, pp. 78–85.
- [52] J. P. Romero, O. Sallent, R. Agustí, and L. Giupponi, "A novel on-demand cognitive pilot channel enabling dynamic spectrum allocation," in *2nd IEEE International Symposium on New Frontiers in Dynamic Spectrum Access Networks, (DySPAN'07)*, April 2007, pp. 46–54.
- [53] C. Cordeiro and K. Challapali, "C-MAC: A cognitive MAC protocol for multichannel wireless networks," in *Proceedings of the Symposium on Dynamic Spectrum Access Networks (DySPAN'07)*, April 2007, pp. 147–157.
- [54] K. Ghaboosi, M. Latva-aho, and Yang Xiao, "A distributed multi-channel cognitive mac protocol for iee 802.11s wireless mesh networks," in *3rd International Conference on Cognitive Radio Oriented Wireless Networks and Communications, (CrownCom'08)*, May 2008, pp. 1–8.
- [55] L. Ma, X. Han, and C.-C. Shen, "Dynamic open spectrum sharing MAC protocol for wireless ad hoc networks," in *Proceedings of the Symposium on Dynamic Spectrum Access Networks (DySPAN'05)*, Baltimore, MD, USA, November 2005, pp. 203–213.
- [56] T. Chen, H. Zhang, G. M. Maggio, and I. Chlamtac, "Cogmesh: A cluster-based cognitive radio network," in *Proceedings of the Symposium on Dynamic Spectrum Access Networks (DySPAN'07)*, Dublin, Ireland, November 2007, pp. 168–178.
- [57] J. Zhao and H. Zheng, "Distributed coordination in dynamic spectrum allocation networks," in *Proceedings of the Symposium on Dynamic Spectrum Access Networks (DySPAN'05)*, Baltimore, MD, USA, November 2005, pp. 259–268.

- [58] M. Timmers, S. Pollin, A. Dejonghe, L. Van der Perre, and F. Catthoor, "A Distributed Multichannel MAC Protocol for Multihop Cognitive Radio Networks," *IEEE Transactions on Vehicular Technology*, vol. 59, No. 1, pp. 446–459, January 2010.
- [59] C. M. Cordeiro, K. Challapali, and D. Birru, "IEEE 802.22: An Introduction to the First Wireless Standard based on Cognitive Radios," *Journal of communications, Special Issue from selected papers from DySPAN 2005*, vol. 1, No. 1, April 2006 (Invited Paper).
- [60] K. R. Chowdhury and I. F. Akyildiz, "Cognitive Wireless Mesh Networks with Dynamic Spectrum Access," *IEEE Journal on Selected Areas in Communications*, vol. 26, no. 1, pp. 168–181, January 2008.
- [61] W. Hu, D. Willkomm, L. Chu, M. Abusubaih, J. Grossand, G. Vlantis, M. Gerla, and A. Wolisz, "Dynamic Frequency Hopping Communities for Efficient IEEE 802.22 Operation," *IEEE Communications Magazine, Special Issue: "Cognitive Radios for Dynamic Spectrum Access"*, vol. 45, May 2007.
- [62] Y. R. Kondareddy and P. Agrawal, "Synchronized MAC Protocol for Multi-hop Cognitive Radio Networks," in *Proceedings of the IEEE International Conference on Communications (ICC'08)*, May 2008, pp. 3198–3202.
- [63] H.A.B. Salameh, M.M. Krunz, and O. Younis, "MAC Protocol for Opportunistic Cognitive Radio Networks with Soft Guarantees," *IEEE Transactions on Mobile Computing*, vol. 8, no. 10, pp. 1339–1352, October 2009.
- [64] B. Hamdaoui and K.G. Shin, "OS-MAC: An Efficient MAC Protocol for Spectrum-Agile Wireless Networks," *IEEE Transactions on Mobile Computing*, vol. 7, no. 8, August 2008.
- [65] M.Y. El Nainay, D.H. Friend, and A.B. MacKenzie, "Channel allocation & power control for dynamic spectrum cognitive networks using a localized island genetic algorithm," in *New Frontiers in Dynamic Spectrum Access Networks, 2008. DySPAN 2008. 3rd IEEE Symposium on*, October 2008, pp. 1–5.
- [66] H. Zheng and C. Peng, "Collaboration and fairness in opportunistic spectrum access," in *Proceedings of the IEEE International Conference on Communications (ICC'05)*, May 2005, vol. 5, pp. 3132–3136.
- [67] D. Willkomm, M. Bohge, D. Hollós, J. Gross, and A. Wolisz, "Double Hopping: A new Approach for Dynamic Frequency Hopping in Cognitive Radio Networks," in *Proceedings of the IEEE International Symposium on Personal, Indoor and Mobile Radio Communications, 2008 (PIMRC '08)*, September 2008, pp. 1–6.
- [68] F. Wang, O. Younis, and M. Krunz, "GMAC: A game-theoretic MAC protocol for mobile ad hoc networks," in *Proceedings of Modeling and Optimization in Mobile, Ad Hoc, and Wireless Networks 2006*, April 2006, pp. 1–9.
- [69] C. Zou and C. Chigan, "A Game Theoretic DSA-Driven MAC Framework for Cognitive Radio Networks," in *Proceedings of the IEEE International Conference on Communications (ICC'08)*, May 2008, pp. 4165–4169.
- [70] Q. Zhao, L. Tong, and A. Swami, "Decentralized cognitive mac for dynamic spectrum access," in *Proceedings of the Symposium on Dynamic Spectrum Access Networks (DySPAN'05)*, Baltimore, MD, USA, November 2005, pp. 224–232.

- [71] T. W. Rondeau, B. Le, C. J. Rieser, and C. W. Bostian, "Cognitive Radios with Genetic Algorithms: Intelligent Control of Software Defined Radios," in *SDR Forum Technical Conference*, Phoenix, AZ, USA, 2004, pp. C-3 – C-8.
- [72] B. Atakan and O.B. Akan, "Biologically-inspired spectrum sharing in cognitive radio networks," in *IEEE Wireless Communications and Networking Conference, (WCNC'07)*, March 2007, pp. 43–48.
- [73] H. Urkowitz, "Energy detection of unknown deterministic signals," *Proceedings of the IEEE*, vol. 55, pp. 523–531, April 1967.
- [74] T. Yücek and H. Arslan, "A survey of spectrum sensing algorithms for cognitive radio applications," *IEEE Communication Surveys & Tutorials*, vol. 11, no. 1, pp. 116–130, First Quarter 2009.
- [75] W. A. Gardner, "Signal Interception: A Unifying Theoretical Framework for Feature Detection," *IEEE Transactions on Communications*, vol. 36, pp. 897–906, August 1988.
- [76] E. Peh and Y.-C. Liang, "Optimization for cooperative sensing in cognitive radio networks," in *Proceedings of the IEEE Wireless Communications and Networking Conference (WCNC'07)*, Hong Kong, March 2007, pp. 27–32.
- [77] Y. S. Chow, H. Robbins, and D. Siegmund, "Great Expectations: The Theory of Optimal Stopping," *Houghton Mifflin Company*, 1971.
- [78] H. Kim and K. G. Shin, "Efficient Discovery of Spectrum Opportunities with MAC-Layer Sensing in Cognitive Radio Networks," *IEEE Transactions on Mobile Computing*, vol. 7, no. 5, pp. 533–545, May 2008.
- [79] Q. Zhao, L. Tong, A. Swami, and Y. Chen, "Decentralized cognitive MAC for opportunistic spectrum access in ad hoc networks: A POMDP framework," *IEEE Journal on Selected Areas in Communications*, vol. 25, no. 3, pp. 589–600, April 2007.
- [80] A. Ghasemi and E. S. Sousa, "Collaborative spectrum sensing for opportunistic access in fading environments," in *Proceedings of the Symposium on Dynamic Spectrum Access Networks (DySPAN'05)*, Baltimore, MD, USA, November 2005, pp. 131–136.
- [81] A. Ghasemi and E. S. Sousa, "Impact of user collaboration on the performance of sensing-based opportunistic spectrum access," in *Proceedings of the IEEE Vehicular Technology Conference (VTC Fall-06)*, Montreal, Canada, September 2006, pp. 1–6.
- [82] S. Mishra, A. Sahai, and R. Brodersen, "Cooperative sensing among cognitive radios," in *Proceedings of the IEEE International Conference on Communications (ICC'06)*, June 2006, vol. 4, pp. 1658–1663.
- [83] "IEEE Standard for Information Technology- Telecommunications and Information Exchange Between Systems- Local and Metropolitan Area Networks- Specific Requirements Part II: Wireless LAN Medium Access Control (MAC) and Physical Layer (PHY) Specifications," *IEEE Std 802.11g-2003* .
- [84] IEEE 802.11 WG, "Part 11:Wireless LAN Medium Access Control (MAC) and Physical Layer (PHY) Specification," in *IEEE Std 802.11-1999*, August 1999.

- [85] L. C. Wang and A. Chen, "Effects of Location Awareness on Concurrent Transmissions for Cognitive Ad Hoc Networks Overlaying Infrastructure- Based Systems," *IEEE Transactions on Mobile Computing*, vol. 8, no. 5, pp. 577–589, May 2009.
- [86] M. Kubale and L. Kuszner, "A better practical algorithm for distributed graph coloring," in *International Conference on Parallel Computing in Electrical Engineering, (PARELEC '02)*, September 2002, pp. 72–75.
- [87] D.H. Friend, M.Y. EINainay, Yongsheng Shi, and A.B. MacKenzie, "Architecture and performance of an island genetic algorithm-based cognitive network," in *5th IEEE Consumer Communications and Networking Conference, 2008 (CCNC'08)*, January 2008, pp. 993–997.
- [88] A. Goldsmith, S. A. Jafar, I. Maric, and S. Srinivasa, "Breaking Spectrum Gridlock with Cognitive Radios: An Information Theoretic Perspective," *Proceedings of the IEEE*, vol. 97, no. 5, pp. 894–914, May 2009.
- [89] S. Srinivasa and S. A. Jafar, "COGNITIVE RADIOS FOR DYNAMIC SPECTRUM ACCESS - The Throughput Potential of Cognitive Radio: A Theoretical Perspective," *IEEE Communications Magazine*, vol. 45, no. 5, pp. 73–79, May 2007.
- [90] Federal Communications Commission, "Establishment of interference temperature metric to quantify and manage interference and to expand available unlicensed operation in certain fixed mobile and satellite frequency bands," ET Docket 03-289, Notice of Inquiry and Proposed Rulemaking, 2003.
- [91] T. C. Clancy, "Dynamic spectrum access using the interference temperature model," *Annals of Telecommunications, Springer*, vol. 64, no. 7, pp. 573–592, 2009.
- [92] C. Cordeiro, K. Challapali, and M. Ghosh, "Cognitive PHY and MAC layers for dynamic spectrum access and sharing of TV bands," in *Proceedings of the first international workshop on Technology and policy for accessing spectrum (TAPAS'06)*, Boston, MA, USA, August 2006.
- [93] L. Kleinrock and F. Tobagi, "Packet Switching in Radio Channels: Part I—Carrier Sense Multiple-Access Modes and Their Throughput-Delay Characteristics," *IEEE Transactions on Communications*, vol. 23, no. 12, pp. 1400–1416, December 1975.
- [94] T. Chen, H. Zhang, M. Katz, and Z. Zhou, "Swarm Intelligence Based Dynamic Control Channel Assignment in CogMesh," in *Proceedings of the IEEE CoCoNet Workshop in conjunction with IEEE ICC 2008*, Beijing, China, May 2008, pp. 168–178.
- [95] T. C. Clancy, "Achievable capacity under the interference temperature model," in *26th IEEE International Conference on Computer Communications (INFOCOM'07)*, May 2007, pp. 794–802.
- [96] A. Durantini, R. Giuliano, F. Mazzenga, and F. Vatalaro, "Performance evaluation of detect and avoid procedures for improving UWB coexistence with UMTS and WiMAX systems," in *The IEEE 2006 International Conference on Ultra-Wideband*, September 2006, pp. 501–506.
- [97] M. Costa, "Writing on dirty paper," *IEEE Transactions on Information Theory*, vol. 29, no. 3, pp. 439–441, May 1983.

- [98] N. Devroye, P. Mitran, and V. Tarokh, "Achievable rates in cognitive radio channels," *IEEE Transactions on Information Theory*, vol. 52, no. 5, pp. 1813–1827, May 2006.
- [99] L. Giupponi and A. Pérez-Neira, "Fuzzy-based Spectrum Handoff in Cognitive Radio Networks," in *Proceedings of 3rd International Conference on Cognitive Radio Oriented Wireless Networks and Communications (CROWNCOM 2008)*, Singapore, May 2008, pp. 1–6.
- [100] W. Ren, Q. Zhao, and A. Swami, "Power control in cognitive radio networks: how to cross a multi-lane highway," *IEEE Journal on Selected Areas in Communications*, vol. 27, no. 7, pp. 1283–1296, September 2009.
- [101] A.C.V. Gummalla and J.O. Limb, "Wireless medium access control protocols," *IEEE Communications Surveys & Tutorials*, vol. 3, no. 2, pp. 2–15, 2009.
- [102] M.E. Sahin, I. Guvenc, Moo-Ryong Jeong, and H. Arslan, "Handling CCI and ICI in OFDMA femtocell networks through frequency scheduling," *IEEE Transactions on Consumer Electronics*, vol. 55, no. 4, pp. 1936–1944, 2009.
- [103] J. Perez-Romero, O. Salient, R. Agusti, and L. Giupponi, "A Novel On-Demand Cognitive Pilot Channel Enabling Dynamic Spectrum Allocation," in *2nd IEEE International Symposium on New Frontiers in Dynamic Spectrum Access Networks (DySPAN 2007)*, Dublin, Ireland, April 2007, pp. 46–54.
- [104] C. Stevenson, G. Chouinard, Z. Lei, W. Hu, S. Shellhammer, and W. Caldwell, "IEEE 802.22: The first cognitive radio wireless regional area network standard," *IEEE Communications Magazine*, vol. 47, no. 1, pp. 130–138, January 2009.
- [105] J. Xiang, Y. Zhang, T. Skeie, and L. Xie, "Downlink Spectrum Sharing for Cognitive Radio Femtocell Networks," *IEEE Systems Journal*, vol. 4, no. 4, pp. 524–534, 2010.
- [106] S.-Y. Lien, C.-C. Tseng, K.-C. Chen, and C.-W. Su, "Cognitive Radio Resource Management for QoS Guarantees in Autonomous Femtocell Networks," in *IEEE International Conference on Communications (ICC 2010)*, Cape Town, South Africa, May 2010, pp. 1–6.
- [107] S. Barbarossa, S. Sardellitti, A. Carfagna, and P. Vecchiarelli, "Decentralized interference management in femtocells: A game-theoretic approach," in *Proceedings of the Fifth International Cognitive Radio Oriented Wireless Networks Communications (CROWNCOM 2010)*, Cannes, France, June 2010, pp. 1–5.
- [108] 3GPP TSG-RAN1 #62, "R1-105082, Way Forward on eICIC for non-CA based HetNets," August 2010.
- [109] J. Lotze, S.A. Fahmy, B. Özgül, J. Noguera, and L.E. Doyle, "Spectrum sensing on LTE femtocells for GSM spectrum re-farming using Xilinx FPGAs," in *Software-Defined Radio Forum Technical Conference (SDR Forum)*, USA, December 2009.
- [110] P.D. Sutton, J. Lotze, H. Lahlou, S.A. Fahmy, K.E. Nolan, B. Ozgul, T.W. Rondeau, J. Noguera, and L.E. Doyle, "Iris: an architecture for cognitive radio networking testbeds," *IEEE Communications Magazine*, vol. 48, no. 9, pp. 114–122, September 2010.
- [111] 3GPP TSG-RAN4 #52 and NTT DOCOMO, "R4-093244, Downlink Interference Coordination Between eNodeB and Home eNodeB," 24–28 August 2009.

- [112] Z. Bharucha, A. Saul, G. Auer, and H. Haas, "Dynamic Resource Partitioning for Downlink Femto-to-Macro-Cell Interference Avoidance," *EURASIP Journal on Wireless Communications and Networking*, vol. 2010, 2010.
- [113] 3GPP TSG-RAN4 Meeting Ad hoc #2010-01, picoChip Design, and Kyocera, "R4-100193 Victim UE aware Downlink Interference Management," January 2010.
- [114] 3GPP TSG-RAN WG4 #51 and Qualcomm Europe, "R4-091908, Partial Bandwidth Control Channel Performance," May 2009.
- [115] 3GPP TSG-RAN WG4 Meeting #52bis and picoChip Designs, "R4-093668, Victim UE Aware Downlink Interference Management," October 2009.
- [116] M.M. Buddhikot, I. Kennedy, F. Mullany, and H. Viswanathan, "Ultra-broadband femtocells via opportunistic reuse of multi-operator and multi-service spectrum," *Bell Labs Technical Journal*, vol. 13, no. 4, pp. 129–143, 2009.
- [117] S. Kawade and M. Nekovee, "Can cognitive radio access to tv white spaces support future home networks?," in *IEEE Symposium on New Frontiers in Dynamic Spectrum (DySPAN 2010)*, Singapore, April 2010, pp. 1–8.
- [118] R.J. Haines, "Cognitive pilot channels for femto-cell deployment," in *7th International Symposium on Wireless Communication Systems (ISWCS 2010)*, York, UK, September 2010, pp. 631–635.
- [119] M. Mueck, C. Rom, Wen Xu, A. Polydoros, N. Dimitriou, A.S. Diaz, R. Piesiewicz, H. Bogucka, S. Zeisberg, H. Jaekel, T. Renk, F. Jondral, and P. Jung, "Smart femto-cell controller based distributed cognitive pilot channel," in *4th International Conference on Cognitive Radio Oriented Wireless Networks and Communications (CROWNCOM '09)*, Hannover, Germany, June 2009, pp. 1–5.
- [120] I. Guvenc, M. R. Jeong, F. Watanabe, and H. Inamura, "A hybrid frequency assignment for femtocells and coverage area analysis for co-channel operation," *IEEE Communications Letters*, vol. 12, no. 12, pp. 880–882, December 2008.
- [121] Y. Y. Li, M. Macuha, E. S. Sousa, T. Sato, and M. Nanri, "Cognitive interference management in 3G femtocells," in *IEEE International Symposium on Personal, Indoor and Mobile Radio Communications*, September 2009, pp. 1118–1122.
- [122] Y.Y. Li and E.S. Sousa, "Cognitive uplink interference management in 4G cellular femtocells," in *IEEE 21st International Symposium on Personal Indoor and Mobile Radio Communications (PIMRC 2010)*, Istanbul, Turkey, September 2010, pp. 1567–1571.
- [123] Z. Shi, M.C. Reed, and M. Zhao, "On Uplink Interference Scenarios in Two-Tier Macro and Femto Co-Existing UMTS Networks," *EURASIP Journal on Wireless Communications and Networking*, vol. 2010, 2010.
- [124] D.P. Palomar and M. Chiang, "A tutorial on decomposition methods for network utility maximization," *IEEE Journal on Selected Areas in Communications*, vol. 24, no. 8, pp. 1439–1451, August 2006.

- [125] D. Calin, H. Claussen, and H. Uzunalioglu, "On femto deployment architectures and macro-cell offloading benefits in joint macro-femto deployments," *IEEE Communications Magazine*, vol. 48, no. 1, pp. 26–32, 2010.
- [126] J.P.M. Torregoza, R. Enkhbat, and W.J. Hwang, "Joint Power Control, Base Station Assignment, and Channel Assignment in Cognitive Femtocell Networks," *EURASIP Journal on Wireless Communications and Networking*, vol. 2010, 2010.
- [127] J. Jin and B. Li, "Cooperative Resource Management in Cognitive WiMAX with Femto Cells," in *Proceedings of the 29th conference on Information communications (INFOCOM 2010)*, San Diego, CA, USA, March 2010, pp. 1–9.
- [128] I.W. Mustika, K. Yamamoto, H. Murata, and S. Yoshida, "Potential game approach for self-organized interference management in closed access femtocell networks," in *Vehicular Technology Conference (VTC Spring), 2011 IEEE 73rd*, may 2011, pp. 1–5.
- [129] K. Akkarajitsakul, E. Hossain, D. Niyato, and Dong In Kim, "Game theoretic approaches for multiple access in wireless networks: A survey," *IEEE Communications Surveys Tutorials*, vol. 13, no. 3, pp. 372–395, quarter 2011.
- [130] S.M. Cheng, W.C. Ao, and K.C. Chen, "Downlink capacity of two-tier cognitive femto networks," in *IEEE 21st International Symposium on Personal Indoor and Mobile Radio Communications (PIMRC 2010)*, Istanbul, Turkey, September 2010, pp. 1303–1308.
- [131] C.J.C.H. Watkins and P. Dayan, "Q-learning," *Machine learning*, vol. 8, no. 3, pp. 279–292, 1992.
- [132] A. Galindo-Serrano, L. Giupponi, and M. Dohler, "Cognition and doction in ofdma-based femtocell networks," in *IEEE Global Telecommunications Conference (GLOBECOM 2010)*, Miami, FL, USA, December 2010, pp. 1–6.
- [133] V. Chandrasekhar, J.G. Andrews, T. Muharemovic, Zukang Shen, and A. Gatherer, "Power control in two-tier femtocell networks," *IEEE Transactions on Wireless Communications*, vol. 8, no. 8, pp. 4316–4328, August 2009.
- [134] G.W.O. da Costa, A.F. Cattoni, I.Z. Kovacs, and P.E. Mogensen, "A Scalable Spectrum-Sharing Mechanism for Local Area Network Deployment," *IEEE Transactions on Vehicular Technology*, vol. 59, no. 4, pp. 1630–1645, May 2010.
- [135] F. Pantisano, M. Bennis, W. Saad, R. Verdone, and M. Latva-aho, "Coalition formation games for femtocell interference management: A recursive core approach," in *IEEE Wireless Communications and Networking Conference (WCNC 2011)*, March 2011, pp. 1161–1166.
- [136] F. Pantisano, K. Ghaboosi, M. Bennis, and M. Latva-Aho, "Interference avoidance via resource scheduling in tdd underlay femtocells," in *IEEE 21st International Symposium on Personal, Indoor and Mobile Radio Communications Workshops (PIMRC Workshops 2010)*, September 2010, pp. 175–179.
- [137] C.U. Castellanos, D.L. Villa, C. Rosa, K.I. Pedersen, F.D. Calabrese, P.-H. Michaelsen, and J. Michel, "Performance of uplink fractional power control in utran lte," in *IEEE Vehicular Technology Conference (VTC Spring 2008)*, May 2008, pp. 2517–2521.

- [138] R.H. Etkin, D.N.C. Tse, and Hua Wang, "Gaussian interference channel capacity to within one bit," *IEEE Transactions on Information Theory*, vol. 54, no. 12, pp. 5534–5562, December 2008.
- [139] S. Rangan, "Femto-macro cellular interference control with subband scheduling and interference cancelation," in *IEEE GLOBECOM Workshops (GC Workshops 2010)*, December 2010, pp. 695–700.
- [140] I. Widjaja and H. La Roche, "Sizing X2 Bandwidth for Inter-Connected eNBs," in *IEEE 70th Vehicular Technology Conference Fall (VTC 2009-Fall)*, September 2009, pp. 1–5.
- [141] S. Kaimaletu, R. Krishnan, S. Kalyani, N. Akhtar, and B. Ramamurthi, "Cognitive interference management in heterogeneous femto-macro cell networks," in *Communications (ICC), 2011 IEEE International Conference on*, June 2011, pp. 1–6.
- [142] K. Norlund, T. Ottosson, and A. Brunstrom, "Fairness measures for best effort traffic in wireless networks," in *15th IEEE International Symposium on Personal, Indoor and Mobile Radio Communications (PIMRC 2004)*, September 2004, vol. 4, pp. 2953–2957.
- [143] F. Pantisano, M. Bennis, W. Saad, and M. Debbah, "Spectrum Leasing as an Incentive towards Uplink Macrocell and Femtocell Cooperation," *IEEE JSAC Special Issue on Femtocell Networks*, April 2012.
- [144] S.M. Cheng, W.C. Ao, and K.C. Chen, "Efficiency of a cognitive radio link with opportunistic interference mitigation," *IEEE Transactions on Wireless Communications*, vol. 10, no. 6, pp. 1715–1720, June 2011.
- [145] D. López-Pérez, X. Chu, A. V. Vasilakos, and H. Claussen, "Minimising Cell Transmit Power: Towards Self-organized Resource Allocation in OFDMA Femtocells," in *ACM SIGCOMM 2011*, Toronto, Canada, August 2011.
- [146] W. Cheng, H. Zhang, L. Zhao, and Y. Li, "Energy efficient spectrum allocation for green radio in two-tier cellular networks," in *IEEE Global Telecommunications Conference (GLOBECOM 2010)*, December 2010, pp. 1–5.
- [147] Airvana Inc, "How Femtocells Change the Economics of Mobile Service Delivery," <http://www.airvana.com/>.
- [148] M. Heath et al., "Picocells and femtocells: will indoor base stations transform the telecoms industry?," <http://research.analysys.com>, 2007.
- [149] F. Cao and Z. Fan, "The tradeoff between energy efficiency and system performance of femtocell deployment," in *IEEE 7th International Symposium on Wireless Communication Systems (ISWCS 2010)*, September 2010, pp. 315–319.
- [150] I. Ashraf, L.T.W. Ho, and H. Claussen, "Improving Energy Efficiency of Femtocell Base Stations Via User Activity Detection," in *IEEE Wireless Communications and Networking Conference (WCNC 2010)*, April 2010, pp. 1–5.
- [151] Zhisheng Niu, Yiqun Wu, Jie Gong, and Zexi Yang, "Cell zooming for cost-efficient green cellular networks," *IEEE Communications Magazine*, vol. 48, no. 11, pp. 74–79, November 2010.

- [152] R3-110030, “Dynamic H(e)NB Switching by Means of a Low Power Radio Interface for Energy Savings and Interference Reduction,” 3GPP TSG RAN WG3 Meeting, Dublin, Ireland, January 2011.
- [153] G. Miao, N. Himayat, and Y. Li, “Energy-efficient transmission in frequency-selective channels,” in *IEEE Global Telecommunications Conference*, November 2008, pp. 1–5.
- [154] 3GPP TSG RAN, “3GPP TR.25814, Physical Layer Aspects for Evolved UTRA (Release 7),” v7.1.0, September 2006.
- [155] L.H. Ozarow, S. Shamai, and A.D. Wyner, “Information theoretic considerations for cellular mobile radio,” *IEEE Transactions on Vehicular Technology*, vol. 43, no. 2, pp. 359–378, May 1994.
- [156] G. Ungerboeck, “Channel coding with multilevel/phase signals,” *IEEE Transactions on Information Theory*, vol. 28, no. 1, pp. 55–67, January 1982.
- [157] C.E. Shannon, “Communication in the presence of noise,” *Proceedings of the IRE*, vol. 37, no. 1, pp. 10–21, 1949.
- [158] M. J. E. Golay, “Note on the theoretical efficiency of information reception with ppm,” *Proceedings of the IRE*, vol. 37, pp. 1031, 1949.
- [159] S. Verdú, “Spectral efficiency in the wideband regime,” *IEEE Transactions on Information Theory*, vol. 48, no. 6, pp. 1319–1343, 2002.
- [160] F. Meshkati, H.V. Poor, S.C. Schwartz, and N.B. Mandayam, “An energy-efficient approach to power control and receiver design in wireless data networks,” *IEEE Transactions on Communications*, vol. 53, no. 11, pp. 1885–1894, 2005.
- [161] G. Miao, N. Himayat, Y. Li, and D. Bormann, “Energy efficient design in wireless OFDMA,” in *IEEE International Conference on Communications (ICC’08)*, 2008, pp. 3307–3312.
- [162] I. Guvenc and U.C. Kozat, “Impact of spreading on the capacity of neighboring femtocells,” in *IEEE 20th International Symposium on Personal, Indoor and Mobile Radio Communications (PIMRC 2009)*, September 2009, pp. 1814–1818.
- [163] A. De Domenico and E. Calvanese Strinati, “A Radio Resource Management scheduling algorithm for self-organizing femtocells,” in *IEEE 21st International Symposium on Personal, Indoor and Mobile Radio Communications Workshops, PIMRC Workshops 2010*, 2010, pp. 191–196.
- [164] V. Ramachandran, V. Kamble, and S. Kalyanasundaram, “Frequency selective OFDMA scheduler with limited feedback,” in *IEEE Wireless Communications and Networking Conference (WCNC 2008)*, April 2008, pp. 1604–1609.
- [165] 3GPP TSG-RAN WG1 meeting 35 and Ericsson, “R1-031303, System-level evaluation of OFDM-further considerations,” November 2003.
- [166] 3GPP2 and Ericsson, “3GPP2-C30-20030429-010, Effective-SNR Mapping for Modeling Frame Error Rates in Multiple-state Channels,” April 2003.

- [167] E. Dahlman, S. Parkvall, and J. Skold, *4G LTE/LTE-Advanced for Mobile Broadband*, Academic Press, 2011.
- [168] B. Debaillie, A. Giry, M.J. Gonzales, L. Dussop, M. Li, D. Ferling, and V. Giannini, "Opportunities for Energy Savings in Pico/Femto-cell Base-Stations," in *Proceedings of Future Network & Mobile Summit 2011 (FUNEMs 2011)*, June 2011.
- [169] A.J. Fehske, F. Richter, and G.P. Fettweis, "Energy efficiency improvements through micro sites in cellular mobile radio networks," in *2nd IEEE Workshop on Green Communications*, Honolulu, USA, December 2009.
- [170] B. Badic, T. O'Farrell, P. Loskot, and J. He, "Energy efficient radio access architectures for green radio: Large versus small cell size deployment," in *IEEE 70th Vehicular Technology Conference Fall (VTC 2009-Fall)*, September 2009, pp. 1–5.
- [171] Y. Chen, S. Zhang, and S. Xu, "Characterizing Energy Efficiency and Deployment Efficiency Relations for Green Architecture Design," in *IEEE International Conference on Communications Workshops (ICC 2010)*, 2010, pp. 1–5.
- [172] E. Oh, B. Krishnamachari, X. Liu, and Z. Niu, "Towards dynamic energy-efficient operation of cellular network infrastructure," *IEEE Communications Magazine*, pp. 56–61, June 2011.
- [173] K. Son, E. Oh, and B. Krishnamachari, "Energy-aware hierarchical cell configuration: from deployment to operation," in *IEEE INFOCOM 2011 Green Communication and Networking Workshop*, Shanghai, China, April 2011.
- [174] K. Son, H. Kim, Y. Yi, and B. Krishnamachari, "Base station operation and user association mechanisms for energy-delay tradeoffs in green cellular networks," *IEEE Journal on Selected Areas in Communications*, vol. 29, no. 8, pp. 1525–1536, September 2011.
- [175] S. Zhou, J. Gong, Z. Yang, Z. Niu, and P. Yang, "Green mobile access network with dynamic base station energy saving," in *Proc. of ACM MobiCom*, Beijing, China, 2009, vol. September.
- [176] P. Xia, V. Chandrasekhar, and J.G. Andrews, "Open vs. closed access femtocells in the uplink," *IEEE Transactions on Wireless Communications*, vol. 9, no. 12, pp. 3798–3809, 2010.
- [177] H.-S. Jo, P. Xia, and J.G. Andrews, "Downlink Femtocell Networks: Open or Closed," in *IEEE International Conference on Communications (ICC 2011)*, Japan, June 2011.
- [178] C. Han, T. Harrold, S. Armour, I. Krikidis, S. Videv, P.M. Grant, H. Haas, J.S. Thompson, I. Ku, C.X. Wang, T. A. Le, M.R. Nakhai, J. Zhang, and L. Hanzo, "Green radio: radio techniques to enable energy-efficient wireless networks," *IEEE Communications Magazine*, vol. 49, no. 6, pp. 46–54, June 2011.
- [179] E. Calvanese Strinati, A. De Domenico, and A. Duda, "Ghost Femtocells: a Novel Radio Resource Management Scheme for OFDMA Based Networks," in *IEEE Wireless Communications and Networking Conference (WCNC 2011)*, Cancun, Mexico, March 2011.
- [180] E. Calvanese Strinati and P. Greco, "Green resource allocation for ofdma wireless cellular networks," in *IEEE International Symposium on Personal, Indoor and Mobile Radio Communications*, Istanbul, Turkey, September 2010.

-
- [181] R. Gupta and E. Calvanese Strinati, "Base-Station Duty-Cycling and traffic buffering as a means to achieve Green Communications," in *submitted to IEEE Vehicular Technology Conference (VTC Fall-2012)*, Québec City, Canada, September 2012.
- [182] A. Conte, A. Feki, L. Chiaraviglio, D. Ciullo, M. Meo, and MA Marsan, "Cell wilting and blossoming for energy efficiency," *IEEE Wireless Communications*, vol. 18, no. 5, pp. 50–57, 2011.
- [183] 3GPP TR 36.819 v11.0.0, "Coordinated multi-point operation for LTE physical layer aspects (Release 11)," September 2011.
- [184] 3GPP TR 25.892 v2.0.0, "Feasibility Study for OFDM for UTRAN Enhancement (Release 6)," June 2004.
- [185] J. Gong, S. Zhou, Z. Niu, and P. Yang, "Traffic-aware base station sleeping in dense cellular networks," in *18th International Workshop on Quality of Service (IWQoS 2010)*, June 2010, pp. 1–2.
- [186] Z. Niu, "Tango: traffic-aware network planning and green operation," *IEEE Wireless Communications*, vol. 18, no. 5, pp. 25–29, 2011.
- [187] S. Dharmapurikar, P. Krishnamurthy, T. Sproull, and J. Lockwood, "Deep packet inspection using parallel bloom filters," in *Proceedings of the IEEE 11th Symposium on High Performance Interconnects (HOTI'03)*, 2003, pp. 44–51.
- [188] H.M. de Lima Carlos, M. Bennis, K. Ghaboosi, and M. Latva-aho, "On interference analysis of self-organized femtocells in indoor deployment," in *IEEE GLOBECOM Workshops (GC Workshops 2010)*, December 2010, pp. 659–663.
- [189] A. Rabbachin, T.Q.S. Quek, Hyundong Shin, and M.Z. Win, "Cognitive network interference," *IEEE Journal on Selected Areas in Communications*, vol. 29, no. 2, pp. 480–493, February 2011.